Norwegian University of Life Sciences
Faculty of Biosciences

Philosophiae Doctor (PhD)
Thesis 2019:20

The effect of freezing and thawing on water flow and pesticide leaching in partially frozen soil – Soil column experiments and model development

Effekten av frysing og tining på vanntransport og utlekking av plantevernmidler i delvis frossen jord – Kolonnestudier og modellutvikling

Roger Holten

The effect of freezing and thawing on water flow and pesticide leaching in partially frozen soil

Soil column experiments and model development

Effekten av frysing og tining på vanntransport og utlekking av plantevernmidler i delvis frossen jord
Kolonnestudier og modellutvikling

Philosophiae Doctor (PhD) Thesis

Roger Holten

Norwegian University of Life Sciences
Faculty of Biosciences
Department of Plant Sciences

Ås (2019)

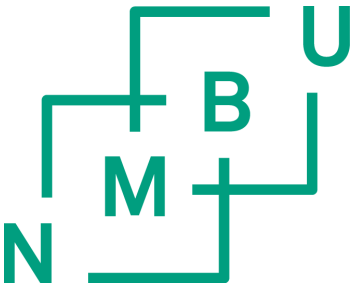

Thesis number 2019:20
ISSN 1894-6402
ISBN 978-82-575-1584-3

Contents

Preface

This thesis is submitted to the Norwegian University of Life Sciences as part of the requirements for the Philosophiae Doctor (PhD) degree. The work has been carried out at the Department of Pesticides and Natural Products Chemistry at the Norwegian Institute of Bioeconomy Research (NIBIO) during the period from August 2015 to January 2019 and in close cooperation with researchers at the Department of Soil and Environment at the Swedish University of Agricultural Sciences (SLU). The work is part of the Bionær project: Innovative approaches and technologies for Integrated Pest Management (IPM) to increase sustainable food production (Smartcrop) funded by The Research Council of Norway (project no.: 244526/E50). The background for Smartcrop was the implementation of EU's directive on sustainable use of pesticides (Directive 2009/128/EC of the European Parliament and of the Council of 21 October 2009 establishing a framework for Community action to achieve the sustainable use of pesticides) in Norwegian legislation in 2014. In the directive, it is stated that one of the goals is to "*achieve a sustainable use of pesticides by reducing the risks and impacts of pesticide use on human health and the environment and promoting the use of integrated pest management and of alternative approaches or techniques such as non-chemical alternatives to pesticides*". This PhD project has been part of Smartcrop's scientific Work Package (WP) 3: "Develop and implement new simulation models for pest-pest-natural enemy interactions and environmental risk of pesticides" and further WP 3.3: "MACRO, a pesticide fate model adapted for winter conditions". The scientific work is presented in three papers which compose the basis of this thesis.

Acknowledgements

I could not have completed this PhD project without the help and support of a number of people who all need to be acknowledged for their valuable contributions. First and foremost, I must thank my girlfriend for her enormous patience with me. Firstly because of my endless talks about experiments, data analysis and article writing, secondly for taking care of home and children in my physically, and very often mentally, absence during the last 3.5 years. She also contributed with some valuable comments during the writing process. I must also thank my children for baring over with a stressed out father and my parents for never saying no when I asked for help with the children or other matters.

A special thanks to Randi Bolli as well for her priceless help on both the planning and execution of the experiments and for valuable discussions and advice concerning data analysis. I would also like to acknowledge Torfinn Torp and his important contribution and help with the statistics.

Further, I must thank Frederik Bøe for his great efforts during most of the experimental work of this project and for his patience and good spirit under the freezing conditions in the lysimeter room. Even through a heavy flu, he kept calm and carried on. Thanks also to Marit Almvik for setting up the methods on the LC/MS-MS, for trusting me with the instrument and contributing to the data analysis and writing.

Finally, I must thank my supervisors, Ole Martin Eklo, Marianne Stenrød, Mats Larsbo, Nickolas Jarvis and Jens Kværner, for having fate in me in the first place and for all the help and support I have received underway. You have impressed me greatly with your knowledge and for being available, either in person or via e-mail, whenever I had questions, big or small. I can easily conclude by saying, as also Sir Isaac Newton did (without any further comparison); "*If I have seen further it is by standing on the sholders [sic] of Giants*".

Thank you all!

Ås, April 9th 2019

Roger Holten

Summary

Increased pesticide concentrations have often been detected in soil leachate, drain discharge and surface runoff during freeze/thaw periods in late winter and early spring, both in Norway and Sweden. Limited knowledge and experimental data exist however on pesticide leaching through partially frozen soil, partly because of the complexity of the processes involved. Climate changes can add to this complexity and influence the use and the fate and behaviour of pesticides. Models that can capture this complexity may help us improve our understanding of the systems and enable more reliable predictions of the transport of pesticides in partially frozen soil and of the potential impacts climate changes may have on water quality.

One of the objectives of this PhD project has been to generate new knowledge and hence be able to increase the understanding of the complex processes of freezing and thawing and the effects these processes have on water flow and on the transport of bromide and pesticides. A second objective has been to develop and evaluate a dual-permeability approach for water flow and heat transport in macroporous soils undergoing freezing and thawing. To achieve these objectives we have conducted a soil column irrigation experiment to quantify the transport of a non-reactive tracer (bromide) and five pesticides (MCPA, clomazone, boscalid, propiconazole, diflufenican) in partially frozen soil. Intact topsoil and subsoil columns (i.d. 9.2 cm, h 20 cm) from two agricultural soils (silt and loam) in South-East Norway were sampled and bromide and pesticides were applied on top of all columns. Half the columns were then frozen (-3 °C) while the other half were left unfrozen (+4 C). Columns were subjected to repeated irrigation events which were followed by periods of freezing or refrigeration. Leachate from the columns was collected and analysed for pesticides and bromide. Parallel to this, physically based equations for soil freezing and thawing was included in the MACRO model. We tested the new model for water flow in the micropore domain against available measured data on the redistribution of water during freezing and illustrative scenario simulations were performed to demonstrate the effects of soil macropores on water flow and heat transport in partially frozen soils.

The column study generated a substantial dataset which showed that pesticide leaching was up to five orders of magnitude larger from frozen than unfrozen columns. Leaching patterns of bromide and pesticides were very similar in most frozen columns with early

breakthrough of high concentrations indicating preferential transport of the pesticides. Only very small amounts of pesticides leached from unfrozen topsoil columns. In the unfrozen columns, bromide showed a more uniform advective-dispersive transport process without clear concentration peaks. The rank order in pesticide leaching observed corresponded to the rank order of mean K_f values for the pesticides suggesting that sorption plays a role in determining leaching losses even in frozen soil. There were indications though that this was most important for pesticides of intermediate mobility.

In the modelling part of the project, several test cases were performed to test the model. Compared to the limited number of existing models and datasets, the new version of MACRO simulated the redistribution of water in the micropore domain during freezing equally well. When comparing the First Order Energy Transfer (FOET) approach with the heat flow equation, energy exchange and average temperatures were reproduced well when running without the freezing model. When running the simulation with the freezing model, similarly good fits was not observed but as the FOET approach is an approximation, a perfect fit was not expected. When looking at the water flow in macropores during freezing, the results of the simulations were in line with both our perception of the processes as well as the limited data that exists on water flow through macropores. In the last test case, the complete model was evaluated by simulating thawing from the soil surface of an initially frozen soil column (h 20 cm) during a constant rainfall of 1.5 mm h^{-1}. This test showed that the model simulated the processes according to our expectations and the theory with regards to the energy transfer between the pore domains and how this affected the freezing and melting of water in macropores and micropores and the infiltration and percolation of water. In several respects the model results were similar to observations made in the soil column studies.

Sammendrag

Høye konsentrasjoner av plantevernmidler er observert i sigevann, drensvann og overflateavrenning fra jord i perioder med frysing/tining sent om vinteren eller tidlig om våren i områder med kaldt klima. Det er begrenset med kunnskap og lite eksperimentelle data på dette med transport av plantevernmidler gjennom frossen jord, noe som bl.a. skyldes at de aktuelle prosessene og mekanismene er veldig komplekse. Klimaendringene kan øke denne kompleksiteten ytterligere og påvirke både bruken av og skjebnen til plantevernmidlene. Datamodeller kan beskrive denne kompleksiteten og hjelpe oss med å forstå det som skjer på en bedre måte slik at vi kan forutsi hvordan plantevernmidler vil transporteres i frossen jord og hvordan klimaendringer kan virke inn på vannkvaliteten.

En av målsetningene med dette PhD-prosjektet har vært å fremskaffe ny kunnskap slik at vi kan forstå mer av de kompliserte fryse-tine prosessene i jord og effektene disse prosessene har på transporten av vann og plantevernmidler. En annen målsetning har vært å utvikle og evaluere en modell for utveksling og transport av vann og varmeenergi i og mellom makro og mikroporer i jord som utsettes for frysing og tining.

For å kunne nå disse målsetningene satte vi i gang et søyleforsøk for å kvantifisere transporten av et ikke-reaktivt sporstoff (bromid) og fem ulike plantevernmidler (MCPA, clomazone, boscalid, propiconazole og diflufenican) i delvis frossen jord. Vi samlet inn intakte jordsøyler av toppjord og undergrunnsjord fra to ulike typer landbruksjord (silt og lettleire) i Sørøst-Norge. Bromid og plantevernmidler ble så tilsatt på overflaten av alle søylene. Halvparten av søylene ble frosset (-3 °C), mens de resterende ble satt på kjølerom (+4 °C). Søylene ble så utsatt for gjentagende vanninger som ble etterfulgt av frysing/kjøling. Sigevann fra søylene ble samlet opp og analysert for bromid og plantevernmidler. Parallelt med dette er matematiske funksjoner for frysing og tining lagt inn i modellen MACRO. Vi har testet og evaluert den nye modellen og undersøkt hvordan den modellerer vanntransporten i mikroporene og sammenlignet dette med tilgjengelige målte data på omfordelingen av vann i jord som fryser. I tillegg har vi utført simuleringer som illustrerer hvordan tilstedeværelsen av makroporer påvirker vann- og varmeenergitransporten i delvis frossen jord.

Resultatene av søyleforsøket viste at opptil 5000 ganger mer plantevernmidler ble transportert ut av de frosne søylene enn fra de ikke-frosne søylene. Transportmønsteret

for bromid og plantevernmidler var ganske likt i de frosne søylene, med høye konsentrasjoner som lekket ut av søylene relativt kort tid etter at vanning ble igangsatt og lite vann hadde gått gjennom søylene. Dette indikerte at transporten foregikk gjennom større kanaler i jorda. Kun små mengder plantevernmidler ble transportert ut av de søylene som ikke var fryste, mens bromid viste en mer enhetlig transport, dvs at transporten skjedde gjennom hele jordprofilet uten å gi de samme konsentrasjonstoppene man så i sigevann fra de fryste søylene. Rekkefølgen mellom de ulike plantevernmidlene i forhold til mengden som lekket ut falt sammen med bindingsegenskapene de enkelte stoffene har i jord. Dette viste at bindingsegenskapene også har en betydning i frossen jord, selv om det var tegn som tydet på at dette betydde mer for plantevernmidler med medium bindingsegenskaper enn for mer mobile stoffer eller stoffer som vanligvis binder seg sterkere i jord.

I modell-delen av prosjektet ble det utført flere tester av den nye modellen. Sammenlignet med det begrensede antall eksisterende modeller og datasett, simulerte den nye versjonen av MACRO omfordeling av vann i mikropore-domenet under frysing veldig bra. Ved sammenligning av FOET-modellen ble energiutveksling og gjennomsnittstemperaturer gjengitt godt når modellen kjørte uten frysing. Ved simulering med frysing var ikke tilpasningen like god, men da FOET-modellen er en tilnærming, var det heller ikke forventet at tilnærmingen skulle bli perfekt. Når vi så på vannstrømmen i makroporene under frysing, var resultatene av simuleringene i tråd med både vår oppfatning av prosessene og de begrensede dataene som eksisterer på området. I den siste testen ble den komplette modellen evaluert ved å simulere tining fra jordoverflaten av en opprinnelig frosset jordkolonne (h 20 cm) med konstant nedbør på 1,5 mm h^{-1}. Denne testen viste at modellen simulerte prosessene i stor grad i henhold til våre forventninger og den generelle teorien, spesielt med hensyn til energioverføringen mellom poredomenene og hvordan dette påvirket frysing og tining av vann i makro- og mikroporer samt infiltrasjon og utlekking av vann. Modellresultatene stemte i flere tilfeller overens med observasjoner gjort i kolonnestudiene og teorien rundt observasjonene.

List of papers

Paper I

HOLTEN, R., BØE, F. N., ALMVIK, M., KATUWAL, S., STENRØD, M., LARSBO, M., JARVIS, N. & EKLO, O. M. 2018. The effect of freezing and thawing on water flow and MCPA leaching in partially frozen soil. Journal of Contaminant Hydrology, 219, 72-85. DOI: 10.1016/j.jconhyd.2018.11.003.

Paper II

HOLTEN, R., LARSBO, M., JARVIS N., STENRØD M., ALMVIK, M. & EKLO, O. M. 2019. Vadose Zone Journal. Leaching of five pesticides of contrasting mobility through frozen and unfrozen soil. Manuscript accepted.

Paper III

LARSBO, M., HOLTEN, R., STENRØD, M., EKLO, O. M. & JARVIS, N. J. Manuscript. A dual permeability approach for modelling soil water flow and heat transport during freezing and thawing. Manuscript.

1 General introduction

1.1 Pesticides in the environment and climate change

Pesticides are widely used in conventional agriculture across the globe to protect crops against damage from pests like insects, fungi and weeds. In a review on the fate of pesticides in the environment, Gavrilescu (2005) states that 4 million tons of pesticides are applied to crops annually around the world to control different pests. These chemicals are often applied directly on bare soil or on plants in the fields in addition to other methods, e.g. as seed dressings. Often pesticides are degraded or transformed, either as a result of biological processes, e.g. aerobic/anaerobic microbial degradation, or as a result of chemical processes, such as hydrolysis or photolysis (Gavrilescu, 2005). On the other hand, it is well-established knowledge that pesticides are transported away from the area they have been applied as documented by studies and monitoring programs around the globe (Stone et al., 2014, Sangchan et al., 2014, Smith et al., 2012, Fadaei et al., 2012, Karlsson et al., 2000, Brûsch et al., 2016, Schummer et al., 2010, Åkesson et al., 2015, Stenrød, 2015). These papers show that transport can be due to e.g. vaporization into the atmosphere, surface run off to nearby water bodies or leaching vertically into the soil. In the last case, the pesticides can reach drainage pipes that transport the pesticides towards surface water or they can reach the groundwater (Sandin et al., 2018, Haarstad and Ludvigsen, 2007). Pesticide residues in the environment is undesirable, both from a soil and water quality perspective, but also because pesticides in the environment can pose a risk to other organisms than the target organisms, both on their own, but also in mixtures (Liess and Ohe, 2005, Tang and Escher, 2014, Grung et al., 2015). To reduce the negative effects of pesticides in the environment, the best possible use and management practices must be applied in addition to in-depth knowledge on the fate and behaviour of pesticides in the environment under different conditions as pointed out by Stenrød et al. (2016). Climate change can also influence the fate and behaviour of pesticides both with regard to their use but also with regard to their persistence and mobility giving rise to new concerns (Bloomfield et al., 2006, Delcour et al., 2015).

The Norwegian Climate Service Centre (NCCS) predicts an increase of 4.5 °C in the annual air temperature and ca. 18 % more precipitation per year in Norway towards year 2100 (Hanssen-Bauer et al., 2015). In support of this, analyses of data from the Norwegian national monitoring programme for pesticides, JOVA, show an increase in the annual

average temperatures of 0.5-2.8 °C in the monitored catchments from 1992 to 2013. This increase corresponds to the average temperature increase observed for bigger areas of the country (Eastern and Western Norway) when compared with the 30 year normal, 1961-1990 (Bechmann and Eggestad, 2016). In addition, more snowmelt episodes during winter and an increase in the frequency of freeze-thaw cycles up to 38 % is expected (Hanssen-Bauer et al., 2015, Mellander et al., 2007, Lundberg et al., 2016). Higher temperatures and more rain can lead to an increased use of pesticides (Delcour et al., 2015, Bloomfield et al., 2006), both due to potentially longer thermal growing seasons but also due to increased pressure from different pests, e.g. weeds, fungi and insects. The average length of the growing season has in fact increased by 6 to 40 days in 7 of 8 catchments in the JOVA program since the start of the program in 1992 (Bechmann and Eggestad, 2016), a trend that supports the prediction. There is also both a weak increase in the area sprayed with fungicides and an increase in the number of detections of fungicides over the last 15 years (Hauken et al., 2017). Increased temperature most probably will enhance degradation while increased precipitation and more intense rainfall episodes can lead to increased leaching and surface run off. Warmer and wetter climate can reduce the residues on the crops, being positive for potential residues in the products, but may also lead to an increased application frequency (Stenrød et al., 2008, Bloomfield et al., 2006, Delcour et al., 2015). As some of these processes may cancel each other out at a regional scale, modelling with MACRO-SE showed that the area with risk of groundwater contamination actually doubled when indirect effects of changes on land-use and pesticide use were considered (Steffens, 2015). All this indicate that climate change can greatly influence soil hydrological processes, pesticide use and transport and the quality of both surface waters and groundwater.

1.2 Macropore flow

1.2.1 Water flow in macropores

Soil is a porous matrix that in addition to solid material (e.g. minerals and organic material), also consists of numerous pores of different sizes that can act as channels for the transport of water, air and solutes. These pores vary in size and shape, but are often divided into two domains, micro- and macropores, at least in modelling (de Vries et al., 2017). In general micropores have a large storage capacity and low flow capacity while

macropores have a low storage capacity and high flow capacity (Larsbo and Jarvis, 2003). The importance of macropores as transport channels for water bypassing the rest of the soil matrix, was recognized already in late 19th century (Jarvis, 2007). These large channels, or macropores, can be defined as pores with diameters of 0.3-0.5 mm and upwards. These pores are characterized by being long and continuous and having low tortuosity. In addition, clay deposits and biofilms along the pore walls have been shown to result in the macropore walls being water repellent. This significantly reduce sideways water movement into the soil matrix (Hallett and Young, 1999), and hence increase downward flow through the macropores. Another important property of macropores is their smaller surface area per volume compared to smaller pores (Luxmoore et al., 1990). Examples of pores that match this definition are biopores made by earthworms and plant roots, planar fissures or cracks formed by freezing/thawing or drying/wetting and irregularly shaped voids between aggregates in cultivated topsoil.

As opposed to general flow through the soil matrix which are governed by several processes, including gravity, capillarity, viscous forces and/or inertial forces, the forces behind water flow in macropores are mostly dominated by gravity alone (Jarvis, 2007). According to Beven and Germann (1982) only a small fraction of the total soil voids may be defined as macropores, but they can dominate vertical flow rates under certain conditions. Dixon and Peterson (1971) referred to extreme cases where opening of one macropore increased the infiltration capacity of a 1.35 m^2 soil plot by about 40 % even though the pore space available for infiltration only increased by 0.002 %. Similarly, the results from a field study where tension infiltrometers were used and water was applied at different capillary potentials, showed that 95 % of the flow occurred in pores larger than 0.25 mm and just 0.32 % of the pore volume (Watson and Luxmoore, 1986). This type of infiltration, which bypasses the soil matrix, is not consistent with theories of uniform soil water flow through a homogenous porous medium as described by Darcy's law or Richard's equation (Beven and Germann, 1982, Beven and Germann, 2013). This is especially true for pores larger than c. 0.15 mm (Jarvis, 2007).

A number of factors influence when flow in macropores are triggered. Intensive rainfall can bring the soil closer to saturation and hence increase the chances for macropore flow to be initiated (Jarvis, 2007). Both a high degree of connectivity and a higher initial soil moisture content have been shown to increase the effectiveness of macropores, both

factors contributing to reduced lateral losses (Beven and Germann, 1982). Flow through macropores starts if the pressure potential of the water in contact with the pore increases sufficiently so that the pore can start filling with water, i.e. the pore's water-entry pressure must be exceeded, normally > -10 cm for macropores (d. 0.3-0.5 mm) (Jarvis, 2007). If this water-entry pressure is not exceeded, e.g. under unsaturated conditions, macropore flow is not triggered. The relationship between infiltration rate and water potential or water entry pressure, is schematically illustrated in Fig. 1 (Jarvis, 2007). At point A in Fig. 1, the macropores are air-filled and water transport is conducted by the matrix with little contribution from macropores. Flow in smaller macropores starts as the water entry pressure reaches about -10 cm (point B in Fig. 1). From this point, only a small increase in water potential results in a significant increase in flow in the macropores (point C in Fig. 1).

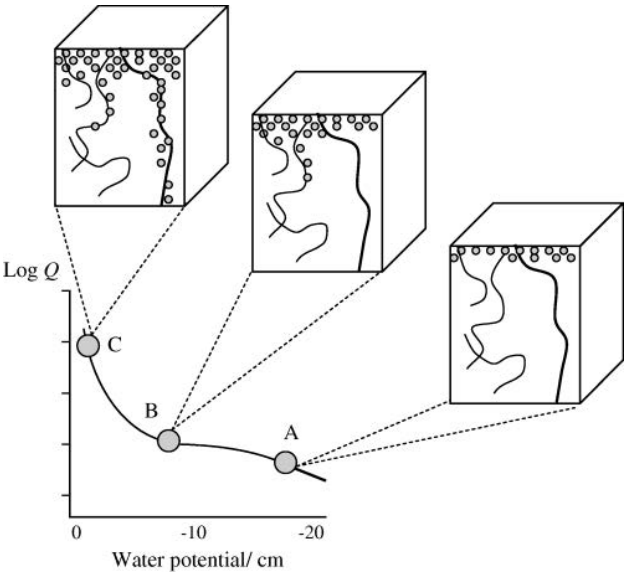

Fig. 1: Illustration of the relationship between water potential and preferential flow (Q) in macropores. At point C the entry pressure is high enough for bigger macropores to be activated and non-equilibrium flow is triggered (The figure has been copied from Jarvis (2007). Reuse granted under Licence number 4486371259054, John Wiley & Sons).

1.2.2 Solute transport and retardation in macropores

Similar to Darcy's law, the advective-dispersive theory was for a long period the leading theory for solute transport in soil (Jarvis, 2007). This theory assumes that solutes are transported dissolved with the water flow (advection) and that solutes are spread either because of mechanical dispersion or diffusion. Dispersion is a mixing process due to local differences in e.g. the water flow in relation to a mean velocity of flow (Schwartz and Zhang, 2003). This type of transport is often uniform and homogenous and occurs trough the soil matrix without involving macropores. In recent years, however, there has been increased experimental evidence and focus on non-uniform/non-equilibrium flow and transport of water and solutes, commonly termed preferential flow, in macropores under unsaturated conditions (Jarvis, 2007). It has been stated though, that the significance and relevance of macropore flow, or preferential flow, is still not recognized enough (Beven and Germann, 2013, Weiler, 2017). When the loss of a solute through advective transport in the macropores is larger than the sum of other processes like sorption to pore walls, diffusion into the matrix or degradation, solutes can be transported quite effective through the soil (Jarvis, 2007). Solute transport can be enhanced due to the before mentioned water repellent biofilms and coatings of the macropores, and it has been shown that diffusion of anionic tracers like bromide and chloride through these coatings was reduced 30 times compared to diffusion in the soil matrix (Köhne et al., 2002).

It is well-established knowledge that increased rainfall increases leaching of surface applied solutes, e.g. pesticides (Flury, 1996, Beulke et al., 2002, Gish et al., 2004, Pot et al., 2005). Intensity and timing of the rainfall is important as more rain shortly after application results in more leaching, but less rain can wash the solutes into the matrix without generating macropore flow, hence reducing the leaching risk (de Jonge et al., 2000) due to e.g. sorption of the solute. Similarly, if a dry period follows an application, the pesticides have time to enter the matrix through diffusion. Sorption is often less in macropores than in the soil matrix (Jarvis, 2007) as shown by e.g. Vanderborght et al. (2002) in a study with two adsorbing dye tracers. The results in that study indicated that the sorption capacity of the macropores was small and that this most likely was due to both the rapid preferential transport of the solutes in addition to the lower concentration of sorption sites in the bigger pores. This lower amount of sorption sites is presumably due to the smaller surface area per volume of the macropores (Jarvis, 2007). It was concluded that the leaching could not be predicted only based on the adsorption

properties of the solute in question (Vanderborght et al., 2002). Sorption to soil particles, which are transported with the water flow in the macropores could also be important, especially for strongly sorbed solutes, e.g. the herbicides glyphosate and pendimethalin, as solutes then bypass potential binding sites in the macropores (de Jonge et al., 2000, Kjær et al., 2011). Compared with a slower and more uniform advective-dispersive transport process through the whole soil matrix, fast flow through macropores also reduces the influence of pesticide properties (e.g. degradation and sorption constants) on leaching (Larsson and Jarvis, 2000, Jarvis, 2007, McGrath et al., 2009). There is also some evidence that preferential flow may have a relatively larger effect on compounds that sorb moderately strongly to soil than either more mobile or more strongly adsorbing compounds (McGrath et al., 2009). Even though the fast macropore transport of solutes may be irrespective of their sorption characteristics, the concentrations that leach are often dependant on sorption as retardation can happen in smaller macropores. This can be seen as a shift in the breakthrough curves of more strongly sorbed solutes compared to the tracers (Jarvis, 2007).

1.3 Transport of water and solutes through partially frozen soil

A rough estimate indicate that about 50 % of the exposed landmass in the Northern Hemisphere is subject to seasonal freezing and thawing (Zhang et al., 2003). Hence, these processes affect considerable land areas. The process of freezing and thawing of soil influence both soil structure as well as chemical and biological processes in the unsaturated zone (Hayashi, 2013, Zhang et al., 2003). Knowledge on water flow and pesticide transport in partially frozen soil has not advanced much in recent years even though some progress have been made (Watanabe et al., 2011, Watanabe and Osada, 2016, Watanabe and Kugisaki, 2017, Moghadas et al., 2016). The complex processes of freezing and thawing of soil and its effect on the fate and behaviour of pesticides are still not well understood (Ireson et al., 2013). As temperatures fall below the freezing point, the higher pressure potential will cause any water present in larger pores to freeze first (Ireson et al., 2013). If the temperature continues to stay below 0 °C, smaller pores will freeze successively. Thawing will thus start at lower temperatures in the smaller pores and as temperature increases water will thaw in the bigger pores. The decreased freezing point in the smaller pores is governed by several factors, e.g. the presence of dissolved

salts and solutes that are translocated and concentrated in the smaller pores. In addition the effect of capillary and absorptive forces attract the water to pore walls and soil particles and add to a lower pressure potential (Ireson et al., 2013, Stähli and Stadler, 1997). Macropores are often air-filled when the soil first freezes and can thus function as effective pathways for preferential flow (van der Kamp et al., 2003) but with subsequent freeze-thaw cycles they can be blocked with ice as well, reducing the soils infiltration capacity and hydraulic conductivity (Ireson et al., 2013). As soil contains a range of pore sizes, there will also be a range in freezing points/temperatures, so water and ice will coexist in the soil. Thus there will be water potential gradients in the soil with lower pressure in the parts with lower temperatures and lower liquid water content (Ireson et al., 2013). This in turn can lead to transport of water towards the freezing front, from areas with high pressure potential to areas with low pressure potential as described for several soil types by Gray and Granger (1986). Frost heave and the formation of ice lenses and subsequent cracking of the soil can be the result as observed in two clayey soils by Hotineanu et al. (2015) leading to increased hydraulic conductivity in the soil.

Even though it has been stated that there are contradictory reports on the effect of the initial moisture content on flow and transport processes in soil (Merdun et al., 2008), the initial water content is a very important factor for the infiltrability when the soil first freezes (Moghadas et al., 2016). Hydraulic conductivity decreases when saturation increases (McCauley et al., 2002). van der Kamp et al. (2003) found that unsaturated macropores was important for the soil infiltrability in frozen macroporous prairie soil during snowmelt. In cultivated soil with less macropores, freezing led to surface ponding during snowmelt, and consequently surface runoff instead of infiltration.

Siimes et al. (2006) discussed that freezing and thawing could be the reason behind increased herbicide concentrations in surface water in spring and stated that the effects of freezing and thawing on herbicide fate should be studied in more detail. Several others, like Larsbo et al. (2016), Bayard et al. (2005) and Niu and Yang (2006) also found pesticides in surface runoff during snowmelt episodes in winter. Results from other studies also indicate that solutes can be transported to deeper soil layers or to drains and subsequent groundwater or surface water respectively. The same studies showed that freezing and thawing was an important factor in releasing solutes, e.g. pesticides and de-

icing chemicals, causing peaks in concentrations (Eklo et al., 1994, French, 1999, Riise et al., 2004, Riise et al., 2006, Ulén et al., 2013).

1.4 Transport processes in partially frozen soil – model development

Water flow and solute transport in partially frozen soil depends on a complex interplay of several factors e.g. air temperature, precipitation as rain or snow, and snow cover depth (Iwata et al., 2011). Models that captures this complexity can help improve the understanding of these processes. This will in turn enable more reliable predictions of the impacts of freezing and thawing on the fate and behaviour of pesticides in general. In addition predictions can be made on the effect climate change might have on the transport mechanisms per se, as well as on groundwater and surface water quality.

Numerical modelling approaches based on Richards' equation for water flow coupled to an equation for the soil heat balance can enable reasonable simulations of the overall hydrology of partially frozen soils (e.g. Stähli et al. (1996) and Kurylyk and Watanabe (2013)). To my knowledge the only existing model that addresses the effect of macropores on water and heat flow is the model presented by Stähli et al. (1996) which is also included in the CoupModel (Jansson, 2012). The concept of Stähli et al. (1996) is that soil often freeze when it is unsaturated and that the smallest pores will stay unfrozen, intermediate sized pores will freeze and the bigger pores will be air-filled. These bigger pores function as high water flow domains, and as water flows through the pores it may freeze because of heat transfer from the high-flow domain to the low-flow domain, i.e., the intermediate sized/smaller pores. Stähli et al. (1996) described only the water and heat exchange in frozen soil but the need to consider non-equilibrium conditions in solute transport models has also been demonstrated for structured soils, but under unfrozen conditions (Köhne et al., 2009a, Köhne et al., 2009b). The process of solute transport under freezing-thawing conditions have so far not been considered in numerical simulation models designed for applications in cold climates. This is quite surprising given that preferential solute transport processes are likely to play a key role in governing surface water and groundwater quality in a changing climate (Hayashi, 2013). Non-equilibrium solute transport may be even more critical in frozen soil for two reasons: i.) the re-distribution of solutes from large to small pores on freezing, and ii.) ice blockage in

intermediate-sized pores, which may significantly limit lateral dispersion during vertical flow in macropores that were air-filled at freezing.

A model has hence been developed to deal with some of the above-mentioned challenges, e.g. to test a dual-permeability approach for water flow and heat transport in macroporous soil undergoing freezing and thawing. This model is based on the MACRO-model (Larsbo et al., 2005, Jarvis and Larsbo, 2012) but with additional physically-based equations for soil freezing and thawing. Measured data from the literature on the redistribution of water during freezing have been used to test the model for the micropore domain and the effect of macropores on water flow and heat transport. This has been illustrated by model simulations (Paper III).

Models should be thoroughly tested against experimental data, hence the need to perform controlled laboratory studies or field studies to generate the appropriate data. During this project, an extensive data set which can be used for later testing of the new version of MACRO was generated.

2 Project justification

Pesticides are applied in different crops in autumn, often as late as October-November in Norway and Sweden, mostly against weeds and fungi (Aarstad and Bjørlo, 2016, Nanos and Kreuger, 2017). Residues of pesticides sprayed earlier during the growing season can also be activated during winter/spring and detected in leachate the year after (Almvik et al., 2011). Winter conditions and their effects on the fate and behaviour of pesticides is hence very relevant but not many publications in peer-reviewed literature has been made on this topic.

It is well documented that pesticides can be transported away from the area they have been applied and that this transport is affected by different climatic factors. Climate change raises additional concerns with regard to both the use of pesticides and their fate and behaviour, especially as one hypothesis is that climate changes can lead to increased use and increased mobility of pesticides. Hence, the necessity to know more about the complex processes in question.

Macropores have been shown to be effective transport pathways for pesticides and solutes vertically through soil. Even though the focus on macropore flow has increased the last two-three decades, it has been stated that this field still is not recognized enough and that e.g. more models should implement processes that generate preferential flow. Compared with a slower and uniform advective-dispersive transport process through the whole soil matrix, fast flow through macropores can reduce the influence of pesticide properties, e.g leaching. It has been indicated that macropore flow has a relatively bigger influence on the transport of intermediately sorbed compounds rather than the most or least mobile compounds. Data on these processes are scarce in general, but even more so for partially frozen soils.

There are also indications from field and laboratory studies that transport of water and solutes occurs through connected and open macropores in partially frozen soil. It has been discussed that that freezing and thawing could be the reason behind increased pesticide concentrations in tile drains and surface water in late winter/early spring and it has been stated that the effects of freezing and thawing on herbicide fate should be studied in more detail. Even though some progress have been made, knowledge on water flow and pesticide transport in partially frozen soil has not advanced much in recent years. The complex processes of freezing and thawing of soil and its effect on the fate and behaviour of pesticides are still not well understood.

A numerical model that describes the effect of non-equilibrium conditions on both water and solute transport would be of great use for both researchers and registration authorities when assessing the fate and behaviour of pesticides under cold climates in general and under climate change especially. So far no numerical simulation model optimized for simulating pesticide transport under cold climate conditions has been validated and published. Models should be tested against empirical data, hence the necessity to perform controlled experiments under the relevant conditions to generate these data.

3 Objectives and hypothesis

The long-term goal for the work initiated in this PhD project is to develop an improved model for transport of pesticides through partially frozen soil and that this model can be

used by authorities for pre-authorization pesticide exposure/risk assessment under Nordic/cold conditions. The short term objective has been to generate high resolution data on water and solute transport through partially frozen soil to be able to test a new version of the numerical model MACRO in which algorithms for freezing and thawing has been included. The main hypothesis is that a new model would give a better description the non-equilibrium transport of water and pesticides in soil macropores under Nordic winter conditions than the models already in use. The main objectives have been divided in three sub-objectives, which corresponds to the objectives of the three included papers.

Paper I: The objective of this study was to better understand the complex processes of freezing and thawing and the effects these processes have on water flow and pesticide transport through soil. We hypothesized that columns subjected to freezing would show a higher degree of preferential transport.

Paper II: The objective of this study was to investigate the effect of freezing and thawing of soil on transport of pesticides with a range of K_f-values. We hypothesized that leaching of pesticides in general would be larger from frozen soil columns with open and connected macropores compared to unfrozen columns and that the effects of freezing on leaching would be largest for moderately strongly sorbing compounds.

Paper III: The objectives of this study was to develop and test a dual-permeability approach for modelling water flow and heat transport in macroporous soils undergoing freezing and thawing. The hypothesis was that a non-equilibrium model concept would be needed to properly capture the dynamics of water flow through partially frozen soil.

4 Materials and methods

In the following a relative short description of the materials and methods used in this project is given. More details can be obtained from Papers I-III.

4.1 Data on water flow and solute transport through partially frozen soil

4.1.1 Soil sampling

Intact soil columns were sampled in May 2016 from two agricultural fields with contrasting soil types in South-East Norway, Kroer loam (59° 38′ 37″ N 10° 49′ 58″ E) and Hov silt (60° 12′ 45″ N 12° 1′ 58″ E). Important soil characteristics have been summarized

in Table 1. At the time of sampling, the fields were under winter wheat. Sampling was done in aluminium cylinders (i.d. 9.2 cm, height 20 cm). Fifty-six columns were sampled, 14 from both the topsoil (0-20 cm) and subsoil (20-40 cm) at each site. The cylinders were forced into the soil using a sledgehammer and dug out by hand, wrapped in black plastic bags and stored at ca. +4 °C.

Table 1: Selected characteristics of the studied soils.

Site	Class.[1]	Horizon, cm depth	Soil texture[2]	Clay (%)	Silt (%)	Sand (%)	pH (H_2O)	Tot. C (%)	Tot. N (%)	CEC
Kroer	Retic Stagnosol	Ap, 0-23 Eg, 23-40	Loam Silt loam	19.1 20.5	43.8 63.0	37.1 16.7	5.5 5.6	2.5 0.4	0.2 0.07	13.3 7.4
Hov	Dystric Fluvic Cambisol	Ap, 0-20 Bw, 28-50	Silt Silt	5.4 4.1	83.8 86.7	10.8 9.2	5.4 6.2	1.2 0.3	0.1 0.02	6.6 3.3

[1]WRB 2014, [2]USDA soil texture classification

4.1.2 Soil X-ray scanning and analyses

The soil columns were scanned at the Department of Soil and Environment at the Swedish University of Agricultural Sciences using a high resolution industrial X-ray CT scanner and the X-ray images were analysed to visualize and quantify soil macropore network characteristics. Details on the processing and analyses of the X-ray images can be viewed in Paper I. Fig. 2 shows a typical image generated from the X-ray scanning.

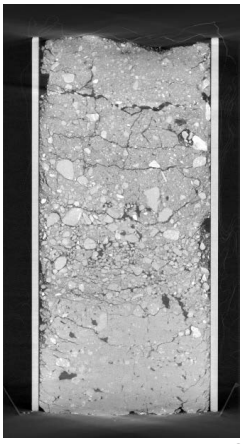

Fig. 2: X-ray image of a vertical section of a Kroer loam sample.

4.1.3 Chemicals

Five pesticides with a range of different properties was investigated in this experiment. In addition, 3 metabolites was included in the analyses. A mix of the five pesticides was prepared to give agricultural relevant application rates (see later). An overview of these pesticides and metabolites and some typical sorption and half-life values, have been summarized in Table 2. Potassium bromide (KBr) was prepared in deionized water.

A solution of artificial rainwater was prepared according to Löv et al. (2017) as described in Paper I.

Table 2: Pesticides and metabolites used in this experiment, and some of their typical sorption coefficients (K_f) and laboratory degradation half-lives (DT_{50}). Values in brackets are mean values.

Compound	Chemical name	K_f, mL g^{-1} (mean)	DT_{50}, 20 °C, days (mean)
MCPA	2-methyl-4-chlorophenoxyacetic acid	0.05-1.99[4] (0.94)	7-41[1] (24)
2-MCP	2-methyl-4-chlorophenol	882[4, 6]	-
Clomazone	2-(2-chlorobenzyl)-4,4-dimethyl-1,2-oxazolidin-3-one	1.54-7.13[4] (4.33)	27-168[2] (68)
Boscalid	2-chloro-N-(4'-chlorobiphenyl-2-yl)nicotinamide	3.3-27.8[4] (12.6)	108-384[3] (232)
Propiconazole	2RS,4RS;2RS,4SR)-1-[2-(2,4-dichlorophenyl)-4-propyl-1,3-dioxolan-2-ylmethyl]-1H-1,2,4-triazole	1.20-59[4] (15)	27-115[4] (72)
Diflufenican	2',4'-difluoro-2-(α,α,α-trifluoro-m-tolyloxy) nicotinanilide	13.5-48.9[4] (31.2)	44-238[5] (128)
AE 0542291	2-[3-(trifluoromethyl) phenoxy] pyridine-3-carboxamide	1.3-4.6[4] (2.99)	13-1000[4] (192)
AE B107137	2-[3-(trifluoromethyl)phenoxy]pyridine-3-carboxylic acid	0.06-0.38[4] (0.22)	2.6-880[4] (20)

[1] European Commission, Review Report for the active substance MCPA, 15 April 2005 (SANCO/4062/2001-final 11 July 2008).
[2] EFSA Scientific report (2007) 109, 1-73, Conclusion on the peer review of clomazone.
[3] European Commission, Review Report for the active substance boscalid (SANCO/3919/2007-rev. 5 21 January 2008).
[4] Pesticide Properties Database (PPDB), 20 September 2018 (https://sitem.herts.ac.uk/aeru/ppdb/en/index.htm).
[5] EFSA Scientific Report (2007) 122, 1-84, Conclusion on the peer review of diflufenican.
[6] Koc

4.1.4 Preparation of soil columns

Twenty of the sampled soil columns from each of the sites Kroer and Hov, in total 40 columns, was included in the experiment. To achieve equal initial conditions the columns were then placed in a box of water with zero pressure potential at the bottom of the soil

for a week to bring the samples close to saturation. The columns were then placed on a sand box (Eijkelkamp) where a pressure potential of -30 cm was applied at the bottom of the soil columns for a week to establish an identical initial condition for all columns, one that also ensured that all continuous macropores would be air-filled. Five columns were randomly chosen from each soil type and depth for the freezing treatment. The remaining five columns were stored unfrozen. Thermistors (ca. 0.2x0.4 cm) were installed in the columns that were subjected to freezing to monitor the temperature during the experiment. These thermistors were installed horizontally into the centre of the columns through holes in the cylinders at 7 and 14 cm depth from the soil surface. The thermistors were then connected to a temperature data logger and temperatures were logged every 10 minutes throughout the experiment. The columns were placed on a 5 cm thick polystyrene insulation board and the column walls were covered with two layers of 2 cm thick polyethylene insulation to ensure freezing from the top and downwards (Fig. 3).

Fig. 3: Insulated soil columns in a Weiss freezing cabinet. The columns were placed on a polystyrene board and thermistors were installed at two depths.

Five mL of the pesticide and potassium bromide solutions were applied as evenly as possible across the surface of each of the columns using a 5 mL pipette, giving rates of 2.1, 0.05, 0.32, 0.15, 0.14 and 59.1 kg ha^{-1} of MCPA, clomazone, boscalid, propiconazole, diflufenican and bromide respectively.

4.1.5 Experimental set up

The insulated columns in the freezing treatment were placed in a $1m^3$ freezing cabinet at -3 °C, while the unfrozen columns were kept at ca +4 °C in a refrigerated room. A temperature of -3 °C was chosen as it was considered low enough to ensure that all water

in the smaller pores would be frozen. The columns were incubated at these temperatures for about four weeks. They were then subjected to repeated irrigation events followed by 14-day periods of freezing (or refrigeration for the unfrozen columns) between irrigations (Fig. 4).

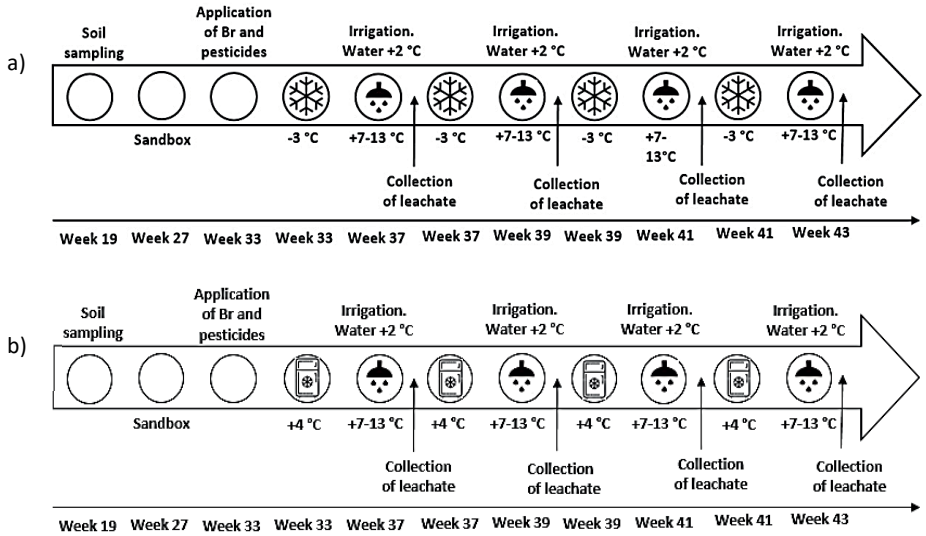

Fig. 4: The timeline and set up of the freeze-thaw-irrigation cycles of the (a) frozen and (b) unfrozen Kroer loam. The set up and timeline for the Hov silt was similar, but with three freeze-thaw cycles instead of four.

The chosen set up allowed free drainage at the base of the soil columns. Irrigation water was distributed to the columns via pvc tubes using peristaltic pumps adjusted to give a rate of 5 mm hr-1 for 5 hours, resulting in a total of about 25 mm of rainwater to each column per irrigation event. Percolate from the soil columns during and after each irrigation was sampled in polycarbonate bottles and sub-samples for chemical analysis were collected manually at approximately every 25 mL until about 24 hours after the start of each irrigation event. From each sub-sample, 3 mL was transferred to a polypropylene centrifuge tube and stored cold (+4 °C) for later analysis of bromide. The remaining volume of leachate for each sample was stored frozen in amber glass bottles for later pesticide analysis. After each irrigation, columns were weighed. Figure 5 shows how the columns were set up in the lysimeter lab.

Fig. 5: Column set up in lysimeter lab during irrigations. Insulated, frozen columns in front, unfrozen columns in the back. Columns were connected to metal sieves and placed on funnels for collection of leachate.

4.1.6 Pesticide and bromide analyses

Bromide analysis was carried out using a Thermo Bromide Ion Selective Electrode coupled to an ion meter while the concentrations of pesticides and metabolites in the leachate samples were measured using LC-MS/MS. All subsamples were analysed for bromide and MCPA, while one single bulk sample per irrigation was prepared for each column for analysis of the remaining four pesticides. This was done to reduce the number of samples mostly due to the costs of the pesticide analyses. For details on the chemical analyses, see Papers I-II.

4.2 A dual-permeability model for coupled water and heat flow in partially frozen soil

4.2.1 Model description – The MACRO model

MACRO is a one-dimensional dual permeability model, which describes variably saturated flow and reactive solute transport in soil. The most important processes in MACRO in this context is only briefly mentioned here. Further details on MACRO can be obtained from Larsbo and Jarvis (2003), Larsbo et al. (2005), Jarvis and Larsbo (2012).

Due to the varying water content in unsaturated soil, water flow in the micropore domain of MACRO (v5.2) is described by Richards' equation with the van Genuchten equation

describing soil water retention and Mualem's model to describe the unsaturated micropore hydraulic conductivity. The water flow is influenced by the degree of saturation and driven by gradients in pressure potentials directly related to the liquid water content. Water flow in the macropore domain on the other hand is dominated by gravity and the fast infiltration in the macropores can be described by kinematic flow theory (Germann et al., 1986, Larsbo and Jarvis, 2003). Flow between the two pore domains, i.e. uptake of water from macropores by micropores, is governed by a first order water diffusion function where the driving force is gradients in water content.

Current versions of MACRO does not account for freezing and the temperatures are calculated with a heat conduction equation assuming that the temperature is the same in both pore domains. This assumption of a temperature equilibrium between pore domains is not valid when parts of the soil are frozen. This is because the water flow in the macropores under these conditions can be so fast that there is no time for this equilibrium to be reached.

4.2.2 Introducing freezing-thawing algorithms in MACRO

The approach for coupling water flow and heat flow in partially frozen soil is very briefly described here, included the most important equations. The detailed model descriptions can be found in Paper III.

Micropore domain

Water flow in variably saturated soil where temperatures can vary on both sides of 0 °C, is described by combining Richard's equation with the one-dimensional (vertical) heat flow equation (without vapour flow) by using the generalized Clapeyron equation as referred in Paper III and described in Hansson et al. (2004). The heat flow equation includes factors like the soil heat capacity in micropores, temperature, thermal conductivity, heat capacity of water, water flux, the latent heat for freezing (energy release as water freezes) and energy exchanges between the macropore and micropore domains (Eq. 1, Eq. 5 in Paper III).

In the model, freezing of the soil is handled as a decrease in liquid water similar to drying, a process assumed analogous to freezing. In other words, water flows are driven by gradients in pressure potentials equivalent to the liquid water content (Paper III). As the

soil freezes, hydraulic conductivity is reduced due to the development if ice, but water can be transported fast from deeper soil layers towards the freezing front and into the frozen soil (Gray and Granger, 1986, Ireson et al., 2013). It has been shown that the water content in the upper, frozen layers of hydraulic models can be overestimated due to these processes (Lundin, 1990) regardless of the formation of ice. In the model, the hydraulic conductivity is further reduced by adding an empirical impedance factor.

The one dimensional vertical heat flow equation used to model soil temperature in micropores:

$$\frac{\partial C_{mic,tot} T_{mic}}{\partial t} - L_f \rho_{liq/ice} \frac{\partial \theta_{mic,ice}}{\partial t} = \frac{\partial}{\partial z}\left[k_h \frac{\partial T_{mic}}{\partial z}\right] - C_{liq} T_{mic} \frac{\partial q_{mic}}{\partial z} - (EX_{cond} + EX_{conv}) \quad \text{Eq. 1.}$$

where $C_{mic,tot}$ (J m^{-3} K^{-1}) is the soil heat capacity of the soil micropore domain, T_{mic} (K) is temperature, k_h (W m^{-1} m^{-3}) is the thermal/heat conductivity, C_{liq} (J m^{-3} K^{-1}) is the heat capacity of liquid water, q_{mic} (m s^{-1}) is the water flux in the micropores, L_f (J kg^{-1}) is the latent heat of freezing, $\rho_{liq/ice}$ (Mg m^{-3}) is the density of water (not accounting for the volume expansion during freezing), EX_{cond} and EX_{conv} [W m^{-3}] are the conductive and convective energy exchanges with the macropore domain, respectively. Finally, t (s) is time and z (m) is the vertical coordinate.

Macropore domain

As the flow in the macropores is assumed to be governed mainly by gravity, water flow velocities can be large and hence conductive heat flow is not accounted for in the macropores. The temperatures in the macropore water are influenced mainly by the movement of energy within the moving water (convection) and the energy exchange with the micropore domain. Thawing of a frozen macropore is hence driven by this exchange of energy with nearby micropores. The smallest macropores will freeze first because the flow is relatively slow and the contact area between the macropores and micropores is large in relation to the water volumes (Paper III).

The heat flow equation for macropores:

$$\frac{dC_{mac,tot} T_{mac}}{dt} - L_f \rho_i \left(\frac{\partial \theta_{mac,ice}}{\partial t}\right) = -C_{liq} T_{mac} \frac{\partial q_{mac}}{\partial z} + (EX_{cond} + EX_{conv}) \quad \text{Eq. 2}$$

where the terms on the left hand side represent changes in the energy content given by the temperature of macropore water and changes in the latent heat content, respectively. The terms on the right hand side represent convection of sensible heat with flowing water and heat exchange between the pore domains. $C_{mac,tot}$ (J m^{-3} $°C^{-1}$) is the volumetric heat capacity for the macropore domain (accounting for both liquid water and ice), q_{mac} (m s^{-1}) is the water flow in the macropores.

Energy exchange between pore domains

The energy exchange between macro- and micropores, EX_{cond} (J s^{-1} m^{-3}), is described by a first order energy transfer function (FOET, eq. 3), where the temperature difference between the pore domains is the driving force:

$$EX_{cond} = \frac{G_f S_{mac,tot} k_h}{d^2} (T_{mic} - T_{mac}) \quad \text{Eq. 3}$$

where G_f (-) is a geometry factor, $S_{mac,\,tot}$ (-) is the degree of saturation in the macropore domain, including both liquid water and ice, which accounts for the contact surface area between the water in the macropores and the soil micropore domain and d (m) is the diffusion pathlength, a parameter related to the geometry of the pore network (aggregate size).

4.2.3 Model testing

The new version of the model have been tested for water flow in the micropore domain against available measured data on the redistribution of water during freezing (Paper III). Some scenario simulations were also performed to demonstrate the effects of soil macropores on water flow and heat transport in partially frozen soils. In total four test cases were performed which are all only briefly described here.

Simulations of the redistribution of micropore water during freezing were run to assess the performance of this approach in MACRO. A soil column (h 20 cm) undergoing freezing from the top was modelled and heat flow through the soil was modelled using a variable heat flux boundary condition. Initial water contents and temperatures were constant with depth. The results were hence compared to measured and modelled data available from literature (Mizoguchi, 1990, Dall'Amico et al., 2011, Hansson et al., 2004).

Further, the First Order Energy Transfer (FOET) model and the heat conduction equation was compared. In this simulation thawing was modelled through lateral energy transfer between the macro- and micropores as water with constant temperature flowed through saturated macropores (Fig. 6). The FOET simulation results were compared to results from a numerical solution of the one dimensional heat conduction equation assuming no convective heat flow. In the FOET simulation, the temperature in the micropore domain, T_{mic}, was represented by one value for the whole domain for each time step, while for the heat flow equation simulation, the temperature was a function of the distance (x) from the boundary. The simulations were run with and without the freezing approach. The temperature in the macropores, T_{mac} was set to +5 °C, and the initial temperature for the micropores, T_{mic}, was set to -5 °C in both approaches.

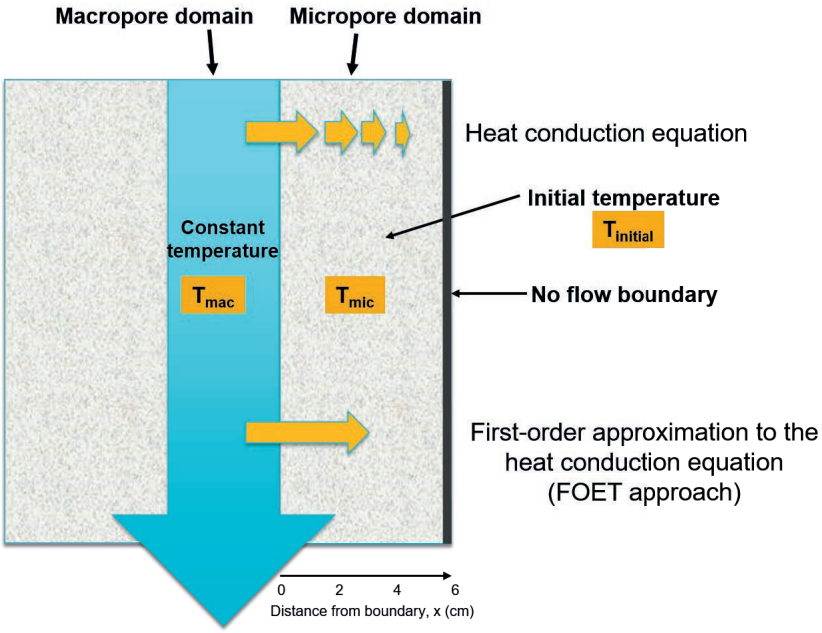

Fig. 6: Conceptual model of the simulation domain for the comparison between the FOET approach and the 1D heat conduction equation. The two approaches are illustrated with different arrows. The boundary temperature is constant at T_{mac}. For the heat flow equation T_{mic} is a function of the distance from the boundary, x (cm).

In a third test case, the goal was to simulate this freezing of the macropores. Hence the model simulation was constricted by the following: (i) the micropore domain was kept saturated at a temperature of -2 °C and no water or heat flow could occur, (ii) the soil was

irrigated with water (+1 °C) at a rate of 1 mm h-1 for 6 minutes every 30 minutes and (iii) the heat exchange between the pore domains could occur through conduction only, i.e. the heat flow rate was a function of the temperature difference between the two domains ("heat diffusion"). The model was parameterized to represent a soil with intermediate potential for non-equilibrium flow with a diffusion pathlength set to 60 mm, hence the heat exchange from the macropore domain towards the micropore domain was also intermediate.

In the last test case, the complete model was tested by simulating thawing of an initially frozen soil column (-2 °C) during constant rainfall (1.5 mm h^{-1}). The air temperature was set to +7 °C and the model was run with two different diffusion pathlength values to simulate intermediate (d=60 mm) and slow (d=300 mm) heat exchange between the pore domains. Otherwise, the micropore domain was parameterised as in the first test case and the macroporosity was set to 0.015 m^3 m^{-3}. For details on the parameterisation, see Paper III.

5 Main results and discussion

5.1 Freeze-thaw effects on water flow and bromide transport

The leaching patterns for bromide were very different between frozen and unfrozen soil columns (Fig. 5-6, A1 and A3 in Paper I). The leaching pattern in the frozen columns indicated preferential flow by the fact that large concentration peaks of bromide were measured in the leachate from frozen columns during the first or second irrigation events, after only a relatively small amount of water had percolated through the columns (<< 1 pore volume). This pattern in the breakthrough curves for bromide was observed for loam topsoil and subsoil and silt topsoil, although the pattern was slightly less pronounced for the silt than the loam. In silt subsoil, no particular signs of preferential flow was observed. The significantly lower mean 5 % arrival volumes for unfrozen loam compared to the silt (Table 3 in Paper I) was an additional indication of preferential flow being present in these columns. In addition, a significant lower mean imaged macroporosity and a lower fraction of connected macroporosity was measured for the silt compared to the loam (Fig. 1 and Table 2 in Paper I). At the early stage, the macropores presumably were still air-filled and being able to conduct relatively large amounts of water, but at later irrigations,

when more water had been applied, larger pores would also become blocked by ice, resulting in reduced hydraulic conductivity and slower thawing (Ireson et al., 2013, Moghadas et al., 2016). Reduced hydraulic conductivity was indicated by the fact that most frozen soil columns started to percolate later than the unfrozen columns, especially at later irrigations (Fig. 3-4 in Paper I). In addition, this was confirmed by ponding building up on top of many of the columns at the first stages of the later irrigations, before the columns started to thaw. When the columns thawed, infiltration of the ponding water could be very fast, indicating the opening of frozen macropores. Flow rates of about 35 mm h^{-1} was observed for frozen columns, while a flow rate of around 7 mm h^{-1} was typical for unfrozen columns. This fast infiltration was observed more often in the loam than in the silt, corresponding to the higher degree of connected macroporosity found for this soil (Table 2 in Paper I). The slower thaw process at later stages was also documented by the temperature curves which showed that for each irrigation event, longer time passed before temperatures started to increase much above 0 °C (Fig. 2 in Paper I). The thawing patterns of the two soil types was quite different with the silt thawing more slowly than the loam, probably due to a higher ice content. The reason for this could be that less pore space was available for infiltration of water and that the infiltration was so slow that the increased exposure to ice caused water to freeze on its way down (Moghadas et al., 2016).

The bromide leaching pattern in the unfrozen columns however, showed a slower, uniform and advective-dispersive pattern with no distinct concentration peaks (Fig. 5-6 and A1-A4 in Paper I). In the unfrozen columns, transport of water and bromide occurred through the whole soil matrix, without the activation of the macropores, resulting in "smoother" breakthrough curves. The calculated 5 % arrival volumes support this, with smaller values found for the frozen soils than unfrozen soils (Table 3 in Paper I) indicating a higher degree of preferential flow in the frozen columns. Statistically significant differences between frozen and unfrozen columns were only found for the silt topsoil though. The breakthrough curves in Fig. 7 below are good examples of the preferential flow observed in frozen soil and the advective-dispersive transport observed in unfrozen soil.

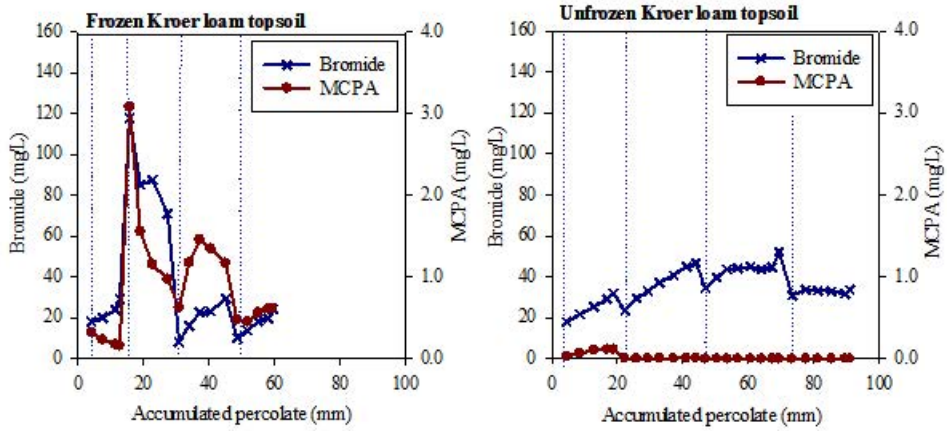

Fig. 7: Bromide and MCPA (mg L^{-1}) concentrations plotted as a function of accumulated amount of percolate (mm) for a representative soil column from frozen and unfrozen topsoil of Kroer loam. Dotted lines indicate the first sampling of leachate after the onset of a new irrigation (Figure copied from Paper I).

Looking at the mean cumulated amount of water that percolated through the columns, and relating it to the applied amount, it was unexpected to see that significantly less water percolated from the frozen columns compared to the unfrozen columns, applying to both soil types and depths (Table 3 in Paper I). We expected that as the frozen columns thawed, the amount of water percolating should be similar to the amount that percolated through the unfrozen columns. The same observation was done for bromide as well, correlating to the amount of water that percolated through the columns. Brown et al. (2000) discussed that that preferential flow rapidly could transport small amounts of bromide to depth, but that over a longer leaching period, preferential flow would give smaller total losses of bromide than matrix flow. This is because preferential flow interacts with only a small part of the soil and associated solute. Since less water percolated from the columns, one should have expected that the frozen columns gained weight during the experiment, but this was not observed. There were different challenges in keeping track of the exact weights of the columns. This was partly due to the balance used, which could only weigh to the nearest 5 gram as well as to challenges with getting correct weights of the frozen columns because of the thermistor wires. Furthermore, the top of the columns had to be adjusted during the course of the experiment to be able to handle the higher levels of ponding water, hence resulting in variable increases in the weights of the columns. Maybe

more importantly, there were indications that the frozen columns had not finished draining after the cessation of irrigation, as a loss of water from the columns was observed while moving them before transportation between the freezing facilities and the lysimeter laboratory. This could also be one explanation to the observations made for water and bromide in this experiment.

5.2 Freeze-thaw effects on pesticide transport and retardation

Brown et al. (2000) argued that preferential flow is the most important process for pesticide transport and that residues can be transported rapidly to deeper soil layers, while slower leaching via matrix flow not will result in larger losses over time because degradation or sorption might reduce the amounts that could leach. The leaching patterns of MCPA shown for frozen and unfrozen soil in this project (Fig. 8, Fig. 5-6, A2, A4 in Paper I) are in line with this. The leaching patterns for MCPA was very similar to the patterns observed for bromide, indicating transport to depth by preferential flow in the frozen soil, being very clear for the loam soil, but not so evident for silt, probably due to the smaller content of connected macropores (Table 2 in Paper I). In total, significantly more MCPA leached from the frozen columns (10-24 % of applied amounts) compared to the unfrozen columns (0.4-10 % of applied amounts), applying to loam topsoil and subsoil as well as the silt topsoil (Table 3 in Paper I). Very little MCPA leached from unfrozen columns. No difference was observed in the leached amounts of MCPA from frozen versus unfrozen silt subsoil with around 10 % leaching (of applied amount).

The results from the analyses of the bulk pesticide samples was in line with the results observed for MCPA, although breakthrough curves could not be generated. The amounts that leached of the four other pesticides included in the experiment (clomazone, boscalid, propiconazole, diflufenican) were in most cases significantly larger from frozen columns than from unfrozen columns with differences ranging up to five orders of magnitude (Table 3 in Paper II), showing that freezing enhanced the transport of these pesticides as well. The measured concentrations in the leachate was in general higher for frozen columns compared to unfrozen columns. With the K_f values reported for these pesticides (Table 2 in Paper II), one would not expect any breakthrough until after a large number of pore volumes had passed through the columns. The relatively rapid breakthrough of the adsorbing pesticides in this case (<< 1 pore volume) added to the evidence that the

leaching processes was dominated by preferential flow through soil macropores that presumably remained open.

The great difference observed in the leached amounts of the pesticides between frozen and unfrozen columns is most probably attributed to processes like sorption and/or degradation as argued by Brown et al. (2000). The slow advective-dispersive transport process observed in the unfrozen columns allowed the pesticides to be exposed to more soil surfaces and binding sites, resulting in stronger sorption and less leaching. In the partially frozen soil, with open and connected macropores fast preferential flow the time was too short for sorption equilibrium to be established. In addition, macropores have a smaller relative surface area compared to smaller pores, hence the number of available binding sites is smaller. Solute transport can be further enhanced due to the water repellent biofilms and coatings of the macropores.

The rank order in pesticide leaching observed in this project (MCPA > clomazone > boscalid > propiconazole > diflufenican), corresponded well to the rank-order of mean K_f values of the pesticides from a range of different soil types, both in frozen and unfrozen soils. The data in this study also showed a strong negative correlation between pesticide sorption properties and leaching (Fig. 7 in Paper II). Hence, is clear that sorption has an effect also in frozen or partially frozen soil but Larsson and Jarvis (2000) argued that the compound sorption properties have a weaker effect when macropore flow is present. Plotting the logarithm of the ratio between the mean amounts of pesticides that leached from frozen columns and unfrozen columns (Fig. 8) indicated that MCPA and diflufenican were less influenced by macropore flow, as the leaching ratios for these substances in general were lower than for substances with more intermediate sorption (clomazone, boscalid, propiconazole). Hence the results indicated, at least indirectly, that macropores played a bigger role for the transport substances of more intermediate mobility, as argued by McGrath et al. (2010). Substances that are more mobile may leach irrespective of the presence of macropores while immobile substances sorb strongly to the soil in any case and are transported either particle-bound through macropores towards drains or via surface run off/erosion. Particulate matter was observed in leachate samples from columns in this experiment. In an extraction test, we did not find any pesticide so particles were not included in the main analyses. This does not rule out that some of the strongly sorbed pesticides, e.g. diflufenican, was lost due to particle bound transport.

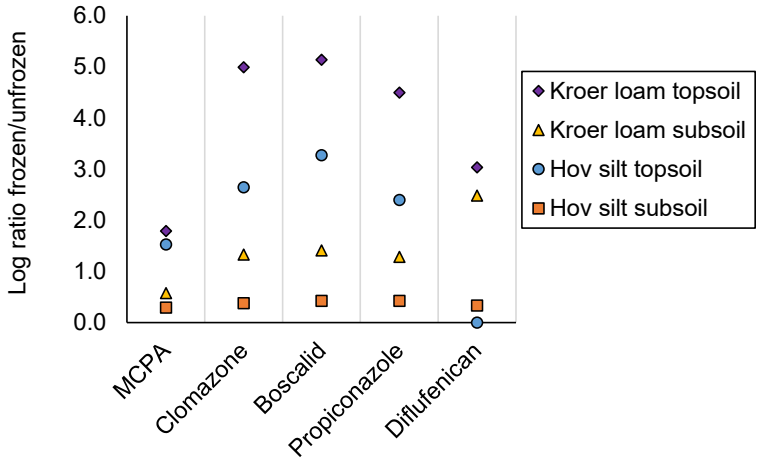

Fig. 8: The logarithm of the ratio of the percentage of the applied amount leached from frozen and unfrozen soil columns of five different pesticides (Figure copied from Paper II).

The metabolites of MCPA (2-MCP) and diflufenican (AE B107137) were included in some of the analyses and 2-MCP was found at a maximum of 0.003 % of the applied amount of MCPA, and in general, the amounts detected of AE B107137 was < 0.04 % of the applied amount of diflufenican. However, in leachate from unfrozen loam subsoil the amount of AE B107137 reached 0.15 % of the applied amount diflufenican. Even though some degree of degradation obviously happened, degradation was not considered an important factor in explaining the big difference between frozen and unfrozen columns.

Freezing of soil can generate cracks in the soil, and one could speculate that these would add to the observed increased leaching compared to unfrozen soil columns. Additionally, for intact soil columns there is often a concern of the bypass of flow along column walls. In our experiment, columns with obvious big gaps along the cylinder walls were not included in the experiment. Any potential gaps in the other cylinders was thought to be a minor problem after wetting and irrigations. It can be mentioned though that during the second irrigation of the Kroer loam, some of the early samples from the frozen subsoil were lost due to leakages/bypass along thermistor wires and through the thermistor holes. The holes were re-sealed before the next irrigation and it was not believed to influence the overall results much. The fact that irrigation water ponded on top of many columns also indicated the lack of significant bypass flow. The results were very

consistent between columns as well, indicating no specific problems with cracks or bypass. Nevertheless, the contribution of cracks or cylinder wall bypass to the big differences observed in this experiment can of course not be completely ruled out.

5.3 Modelling water and heat flow in soil during freezing and thawing

As the three first test cases only focuses on single processes, results from these tests are only briefly discussed here. The results are presented in more detail in Paper III. The focus here is more on the results of the simulations with the complete model. Where applicable, the results of the simulations have been compared to observations made in the experimental column studies.

In the first test case, the redistribution of water in the micropore domain during freezing was simulated well by the model and the depth of the freezing front was accurately reproduced, especially at later time steps.

Without including freezing the FOET approach reproduced both the energy exchange and the average temperature given by the heat conduction model well. When freezing was included, the FOET model was not able to reproduce the energy exchange and average temperature equally well. The FOET model could e.g. not capture the gradual increase in the average temperature simulated by the heat flow equation during thawing. This was probably because the temperature in the soil matrix is only represented by one value in the FOET approach, and the soil thaws at temperatures close to 0 °C.

In the third test case, water flow in macropores during freezing was simulated. Without the freezing model, the simulation showed a kinematic wave moving down through the soil macropores, according to the theory of how water moves through an air-filled macropore. When freezing was included the pattern was different. As soon as water infiltrated the open macropore, it started to freeze. As more water was added through consecutive irrigations larger fractions of the macropores became blocked by ice, and as ice and water coexisted during the earliest irrigations, the macropores became completely blocked by ice after the last irrigation and no further infiltration was possible.

When running the complete model, the scenario was the thawing of an initially frozen 20 cm soil high column during a constant rainfall of 1.5 mm h^{-1}. The results show that the temperature increases fast towards the air temperature at the soil surface (Fig. 9a and b)

but with increasing depth a plateau just below 0 °C develops. This is a similar temperature pattern as the one observed in the thawing soil columns described in Paper I and as the one discussed in test case 2 in Paper III. Freezing and thawing processes in the macropores are governed by the energy exchange between the macropores and the adjacent micropores. Initially, the infiltration of the frozen matrix is limited and water at an initial temperature of 7 °C enters the macropore domain. Energy is then transferred from the water in the macropore to the micropore domain. As this exchange continues, the temperature in the macropore decreases and macropore water begins to freeze when the temperature reaches 0 °C. When the energy transfer is intermediate (diffusion pathlength 60 mm), the negative energy exchange stops after only a few hours (Fig. 9c) as the macropore domain becomes blocked by ice down to a depth of 10 cm (Fig. 9e). The temperatures in the two domains are then at equilibrium and no further energy exchange occurs. At deeper soil layers, water still exists as both liquid water and ice (Fig. 9e).

The temperature in the soil matrix, or micropore domain, continues to increase mainly due to conductive heat transfer from the soil surface and downwards. At a depth of 10 cm this can be seen at ca. 27 h as the next step of increase in the temperature curve (Fig. 9a). In the energy exchange curve this can be seen as a peak at the same time point (Fig. 9c) illustrating the energy transfer from the micropore domain to the macropore, which at this point is completely frozen (Fig. 9e) but which then thaws quite fast as the temperature reaches 0 °C. Temperature equilibrium is then established when all the ice in the macropore has melted.

As soon as the ice in the macropores start to melt, water starts to flow downwards. It can then reach deeper layers where water still is frozen and hence refreeze due to the energy transfer to the adjacent soil matrix/micropore domain. Hence, the degree of ice saturation increases. At a depth of 20 cm this happens at about time point 70 h (Fig. 9e).

Looking at the intermediate energy exchange simulation, the water infiltrates the initially air-filled macropores and percolation increases rapidly to begin with until it reaches the level of the irrigation rate (Fig. 9g). As the temperature of the infiltrating water reaches 0 °C the macropore gets completely blocked by ice and the percolation stops. At time point 80 h, the whole soil matrix is thawed and percolation proceeds and reaches a peak value of ca. 5 mm h^{-1} before settling at the irrigation rate of 1.5 mm h^{-1} (Fig. 9g). This is analogous to what was observed at later irrigations of the frozen columns in the column experiment

(Paper I), where infiltration was prevented most probably due to ice blocking of the macropores. Ponding on top of the columns were strong indications of this, and as the energy from the irrigation water transferred to the ice in the soil, the ice in the macropores melted and allowed for a very quick infiltration of the water. In contrast to the simulation though, the frozen soil columns thawed much quicker during the column experiments. During the last irrigation event, the silt was completely thawed after approx. 30 hours in the column experiment (Fig. 2 in Paper I). This much quicker thawing was most probably caused by the high room temperature (10 °C) and that the columns could thaw from the bottom as well as from the top.

In contrast to this, the slow energy exchange simulation, with the 300 mm diffusion pathlength, shows that the macropore domain never becomes completely frozen (Fig. 9f) due to a continuous energy transfer from the irrigation water to the soil. Since no ice blocking occurs, the infiltration and percolation quickly equals the irrigation rate (Fig. 9h).

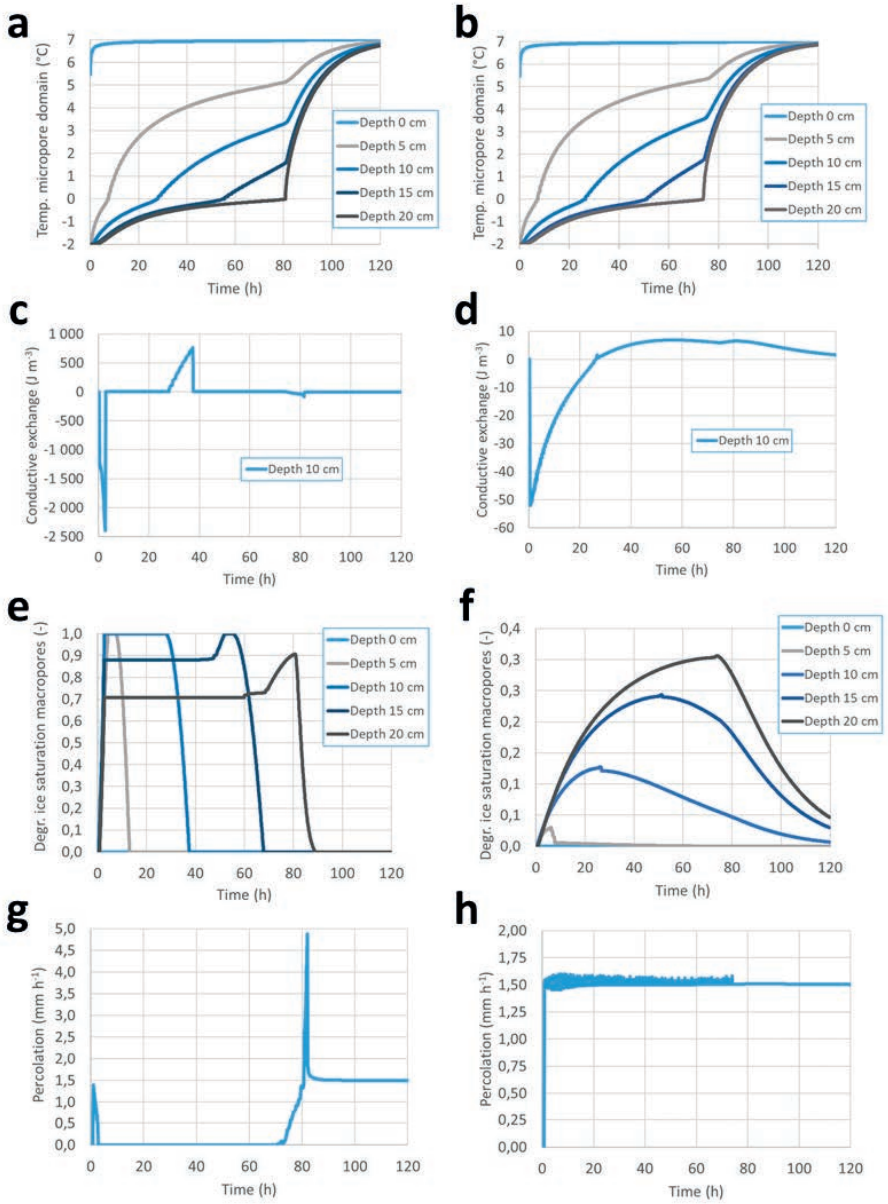

Fig. 9: Simulation results for thawing during constant rainfall (test case 4). Panels to the left (a, c, e and g) and to the right (b, d, f and h) show results from simulations with intermediate (d=60 mm) and slow (d=300 mm) energy transfer between pore domains, respectively. Panels a and b show soil temperatures at five depth below the soil surface. Panels c and d show the conductive energy transfer at 10-cm depth. Panels e and f show the degree of ice saturation in the macropores. Panels g and h show the percolation at the bottom of the soil column. Note the different scales on the vertical axes (Figure copied from Paper III).

5.4 Validity of results

5.4.1 Experimental data on water, bromide and pesticide transport

Even though the investigated processes themselves are relevant also for a field situation, the column experiment was not designed to mimic a realistic field situation. Hence, there are several reasons why we cannot directly extrapolate from these quantitative results to realistic field conditions. Despite these limitations, the results of the column study were very consistent across soil types, depths and treatments and the differences observed were in most cases statistical significant at a 5 % significance level (Table 3 in Paper I, Table 3 in Paper II) and should be assessed as reliable and valid.

The performed column study represents a worst-case scenario for pesticide leaching as it was conducted with pesticides stored on or close to the soil surface, macropores were initially air-filled and long-range connectivity of macropore networks were not accounted for. The columns were e.g. only 20 cm in length, whereas field leaching would be measured at the depth of drain pipes, e.g. at 1 m. Due to the lack of long range connectivity, this would naturally apply to the subsoil columns as well as they were not connected to topsoil, resulting in an even more worst-case leaching situation as the columns were exposed to the entire applied amount of pesticides and not a reduced amount after travelling through a topsoil layer.

The column study was also performed under cold conditions, were the temperatures in the lysimeter room of the irrigation water was held as low as possible. This was to ensure that the conditions was optimal to investigate the processes of interest. Temperatures in both the room and the irrigation water increased during the irrigation events, and were higher than what one could expect in a field situation during winter/early spring (LandbruksMeteorologisk Tjeneste (NIBIO), 2018). As a result, the process of heat transfer from the irrigation water to the soil, occurred at a faster rate than it would do in the field (Moghadas et al., 2016). In general, air temperature, precipitation, snow cover and soil frost are factors that can vary greatly from area to area and from year to year. Covering these variations is of course not possible in a single column study.

The pesticides used in our experiments are not necessarily used in late autumn, but they serve as examples of how substances with different properties behave under freeze-thaw conditions. Furthermore, the column experiment included only two soil types, limiting the conclusions to these two soils. Nevertheless, Cambisols and Stagnisols are representative

for agricultural areas in Norway accounting for 21 and 28 % of the classified agricultural area respectively (Lågbu et al., 2018) and hence serve as good model soils.

Even though the investigated processes themselves are relevant also for a field situation, the column experiment was not designed to mimic a realistic field situation. Hence, there are several reasons why we cannot directly extrapolate from these quantitative results to realistic field conditions. Despite these limitations, the results of the column study were very consistent across soil types, depths and treatments and the differences observed were in most cases statistical significant at a 5 % significance level (Table 3 in Paper I, Table 3 in Paper II) and should be assessed as reliable and valid.

5.4.2 Model simulations of water and heat flow

Modelling approaches are always based on numerous approximations and are in its nature more or less uncertain with regard to estimations of real world processes. There is a need to evaluate the model quantitatively against measured data to ensure realistic estimations of water flow and solute transport through partially frozen soil. Nevertheless, the results of the modelling performed so far, show that the model reproduces available data well and that it behaves according to expectations and current knowledge of the processes involved.

6 Conclusions

The extensive data set generated documents that pesticides and bromide are preferentially transported through soil macropores at relatively high concentrations in partially frozen soil. Little pesticides leached through unfrozen soil while bromide was transported uniformly through the soil following an advective-dispersive infiltration pattern. Our hypothesis that columns subjected to freezing would show a higher degree of preferential transport was hence confirmed. In unfrozen soil, pesticides were probably exposed to binding sites, and were sorbed to soil, reducing the leached amounts. The pesticides had a range of K_f values and the results suggest that sorption plays a role in determining leaching losses even in frozen soil but that preferential flow is more important for intermediately sorbed compounds, confirming our hypothesis. These relationships have to our knowledge not been investigated in detail before, at least not in

partially frozen soils. This study therefore contributes to filling an important knowledge gap. However, the findings here also show that there are aspects that may be worthwhile investigating further. The interactions observed are complex and modelling with an appropriate model could help interpreting some of the results. The data collected in this study should prove useful for testing models of water flow and solute transport in partially frozen and structured soil. In addition, these relationships are worth considering when assessing the fate and behaviour of pesticides during the cold period of year and may be worth taking into account in pesticide monitoring programs and include sampling in winter and early spring during thawing of the soil.

Even though only a first attempt to include soil freezing-thawing algorithms in a dual permeability model for water flow and heat transport, the model simulations performed so far showed a good reproduction of limited available quantitative data and that the model behaved according to current knowledge and understanding of water flow and heat transport in macroporous soil.

7 Implications and recommendations for further research

The data on the transport of water and bromide and the leaching of pesticides generated here cannot be used to extrapolate a field situation directly. They point in a direction though that confirms other field and laboratory studies referred in this thesis in that freezing and thawing processes during winter and late spring can increase the leaching of pesticides in soil. This knowledge points towards a need to revise the current use of pesticides late in the growing season. The results presented in this thesis may e.g. indicate that the properties of the pesticides perhaps should not be the most important factor when deciding which pesticides to use in the autumn, but rather mitigate a potential risk of leaching by e.g. reducing the application rates (Larsson and Jarvis, 2000). Further, climate change models predict longer growing seasons and increased pest pressure due to warmer and wetter climate, perhaps leading to an increase in the use of pesticides. In addition, the same models predict an increase in the number of freeze-thaw cycles. All this emphasize the importance of increasing the knowledge of how these processes affect the fate and behaviour of pesticides and other contaminants in the environment. Even though the experiments presented in this thesis have generated maybe the most extensive dataset ever presented on freezing/thawing and the effect on transport of pesticides in

soil, there is still a need for more knowledge to fully understand the processes involved. A similar study performed under field conditions should be performed to verify whether the same processes observed in the laboratory also occur under field conditions. As mentioned earlier, these processes are highly complex, and models of water flow and solute transport can be a good way to capture this complexity. The modelling presented in this thesis represents the first attempt to describe these processes, but more work is needed and the plan is to use the data generated in the column studies to do further evaluations of the new version of the MACRO model. A complementary set of field data would be valuable for validation purposes. In the long run, the development of an environmental exposure model for the estimation of water flow and solute transport in partially frozen soil could e.g. be very useful to regulatory authorities in the registration of pesticides in areas that are exposed to freezing of soil.

References

AARSTAD, P. A. & BJØRLO, B. 2016. Bruk av plantevernmidler i jordbruket i 2014. 2016/02. Oslo-Kongsvinger.Statistisk sentralbyrå (SSB). In Norwegian.

BAYARD, D., STÄHLI, M., PARRIAUX, A. & FLÜHLER, H. 2005. The influence of seasonally frozen soil on the snowmelt runoff at two Alpine sites in southern Switzerland. *Journal of Hydrology,* 309**,** 66-84. https://doi.org/10.1016/j.jhydrol.2004.11.012

BECHMANN, M. & EGGESTAD, H. O. 2016. Temperaturendringer, plantevekst og avrenning. NIBIO POP 2 (2). Norwegian Institute of Bioeconomy Research (NIBIO). In Norwegian.

BEULKE, S., BROWN, C. D., FRYER, C. J. & WALKER, A. 2002. Lysimeter study to investigate the effect of rainfall patterns on leaching of isoproturon. *Pest Management Science,* 58**,** 45-53. doi:10.1002/ps.419

BEVEN, K. & GERMANN, P. 1982. Macropores and water flow in soils. *Water Resources Research,* 18**,** 1311-1325. DOI: 10.1029/WR018i005p01311

BEVEN, K. & GERMANN, P. 2013. Macropores and water flow in soils revisited. *Water Resources Research,* 49**,** 3071-3092. doi:10.1002/wrcr.20156

BLOOMFIELD, J. P., WILLIAMS, R. J., GOODDY, D. C., CAPE, J. N. & GUHA, P. 2006. Impacts of climate change on the fate and behaviour of pesticides in surface and groundwater—a UK perspective. *Science of The Total Environment,* 369**,** 163-177. DOI: https://doi.org/10.1016/j.scitotenv.2006.05.019

BROWN, C. D., HOLLIS, J. M., BETTINSON, R. J. & WALKER, A. 2000. Leaching of pesticides and a bromide tracer through lysimeters from five contrasting soils. *Pest Management Science,* 56**,** 83-93. DOI: 10.1002/(SICI)1526-4998(200001)56:1<83::AID-PS98>3.0.CO;2-8

BRÛSCH, W., ROSENBOM, A. E., BADAWI, N., GUDMUNDSSON, L., V., P.-H. F., HANSEN, C. H., NIELSEN, C. B., PLAUBORG, F. & OLSEN, P. 2016. The Danish Pesticide Leaching Assessment Programme. Monitoring Results May 1999-June 2014. ISBN 978-87-

7871-426-8. Geological Survey of Denmark and Greenland, Danish Ministry of Energy, Utilities and Climate, Department of Agroecology and Department of Bioscience, Aarhus University. www.pesticidvarsling.dk.

DALL'AMICO, M., ENDRIZZI, S., GRUBER, S. & RIGON, R. 2011. A robust and energy-conserving model of freezing variably-saturated soil. *The Cryosphere,* 5**,** 469-484. 10.5194/tc-5-469-2011

DE JONGE, H., DE JONGE, L. W. & JACOBSEN, O. H. 2000. [14C]Glyphosate transport in undisturbed topsoil columns. *Pest Management Science,* 56**,** 909-915. doi:10.1002/1526-4998(200010)56:10<909::AID-PS227>3.0.CO;2-5

DE VRIES, E. T., RAOOF, A. & VAN GENUCHTEN, M. T. 2017. Multiscale modelling of dual-porosity porous media; a computational pore-scale study for flow and solute transport. *Advances in Water Resources,* 105**,** 82-95. https://doi.org/10.1016/j.advwatres.2017.04.013

DELCOUR, I., SPANOGHE, P. & UYTTENDAELE, M. 2015. Literature review: Impact of climate change on pesticide use. *Food Research International,* 68**,** 7-15. https://doi.org/10.1016/j.foodres.2014.09.030

DIXON, R. M. & PETERSON, A. E. 1971. Water Infiltration Control: a Channel System Concept1. *Soil Science Society of America Journal,* 35**,** 968-973. 10.2136/sssaj1971.03615995003500060033x

EKLO, O. M., ASPMO, R. & LODE, O. 1994. Runoff and leaching experiments of dichlorprop, MCPA, propiconazole, dimethoate and chlorosulfuron in outdorr lysimeters and filed catchment areas. *Norwegian Journal of Agricultural Sciences,* 13**,** 7-212.

FADAEI, A., DEHGHANI, M. H., NASSERI, S., MAHVI, A. H., RASTKARI, N. & SHAYEGHI, M. 2012. Organophosphorous Pesticides in Surface Water of Iran. *Bulletin of Environmental Contamination and Toxicology,* 88**,** 867-869. DOI: 10.1007/s00128-012-0568-0

FLURY, M. 1996. Experimental Evidence of Transport of Pesticides through Field Soils—A Review. *Journal of Environmental Quality,* 25**,** 25-45. DOI: 10.2134/jeq1996.00472425002500010005x

FRENCH, H. K. 1999. *Transport and degradation of deicing chemicals in a heterogenous unsaturated soil.* Doctor Scientiarum Thesis Doctor Scientiarum Thesis, Agricultural University of Norway. 8257503940

GAVRILESCU, M. 2005. Fate of Pesticides in the Environment and its Bioremediation. *Engineering in Life Sciences,* 5**,** 497-526. 10.1002/elsc.200520098

GERMANN, P. F., PIERCE, R. S. & BEVEN, K. 1986. Kinematic wave approximation to the initiation of subsurface storm flow in a sloping forest soil. *Advances in Water Resources,* 9**,** 70-76. https://doi.org/10.1016/0309-1708(86)90012-6

GISH, T. J., KUNG, K.-J. S., PERRY, D. C., POSNER, J., BUBENZER, G., HELLING, C. S., KLADIVKO, E. J. & STEENHUIS, T. S. 2004. Impact of Preferential Flow at Varying Irrigation Rates by Quantifying Mass Fluxes Trade names are included for the benefit of the reader and imply no endorsement or preferential treatment of the product listed by the U.S. Department of Agriculture. *Journal of Environmental Quality,* 33**,** 1033-1040. 10.2134/jeq2004.1033

GRAY, D. M. & GRANGER, R. J. 1986. In situ measurements of moisture and salt movement in freezing soils. *Canadian Journal of Earth Sciences,* 23**,** 696-704. 10.1139/e86-069

GRUNG, M., LIN, Y., ZHANG, H., STEEN, A. O., HUANG, J., ZHANG, G. & LARSSEN, T. 2015. Pesticide levels and environmental risk in aquatic environments in China — A review. *Environment International,* 81**,** 87-97. DOI: https://doi.org/10.1016/j.envint.2015.04.013

HAARSTAD, K. & LUDVIGSEN, G. H. 2007. Ten Years of Pesticide Monitoring in Norwegian Ground Water. *Groundwater Monitoring & Remediation,* 27**,** 75-89. DOI: 10.1111/j.1745-6592.2007.00153.x

HALLETT, P. D. & YOUNG, I. M. 1999. Changes to water repellence of soil aggregates caused by substrate-induced microbial activity. *European Journal of Soil Science,* 50**,** 35-40. doi:10.1046/j.1365-2389.1999.00214.x

HANSSEN-BAUER, I., FØRLAND, E., HADDELAND, I., HISDAL, H., MAYER, S., NESJE, A., NILSEN, J., SANDVEN, S., SANDØ, A. & SORTEBERG, A. 2015. Klima i Norge 2100. NCCS report 2, Oslo, Norway 1-203.ISSN: 2387-3027.

HANSSON, K., ŠIMŮNEK, J., MIZOGUCHI, M., LUNDIN, L.-C. & VAN GENUCHTEN, M. T. 2004. Water Flow and Heat Transport in Frozen Soil. *Vadose Zone Journal,* 3**,** 693-704. 10.2136/vzj2004.0693

HAUKEN, M., STENRØD, M., SKAALSVEEN, K., DEELSTRA, J., EGGESTAD, H. O., BECHMANN, M., RILEY, H., SELNES, S., LUNNAN, T., KVITVÆR, A., STUBHAUG, E., MOLVERSMYR, Å., DREYER, L.-I. & PAULSEN, L. I. 2017. Jord- og vannovervåking i landbruket (JOVA). Feltrapporter fra programmet i 2015. NIBIO Report vol. 3 nr. 44. Norsk institutt for bioøkonomi (NIBIO). In Norwegian. http://hdl.handle.net/11250/2459978.

HAYASHI, M. 2013. The Cold Vadose Zone: Hydrological and Ecological Significance of Frozen-Soil Processes. *Vadose Zone Journal,* 12. DOI: 10.2136/vzj2013.03.0064

HOTINEANU, A., BOUASKER, M., ALDAOOD, A. & AL-MUKHTAR, M. 2015. Effect of freeze–thaw cycling on the mechanical properties of lime-stabilized expansive clays. *Cold Regions Science and Technology,* 119**,** 151-157. DOI: https://doi.org/10.1016/j.coldregions.2015.08.008

IRESON, A. M., VAN DER KAMP, G., FERGUSON, G., NACHSHON, U. & WEATHER, H. S. 2013. Hydrogeological processes in seasonally frozen northern latitudes: understanding, gaps and challenges. *Hydrogeology Journal***,** 53-66. DOI: 10.1007/s10040-012-0916-5

IWATA, Y., NEMOTO, M., HASEGAWA, S., YANAI, Y., KUWAO, K. & HIROTA, T. 2011. Influence of rain, air temperature, and snow cover on subsequent spring-snowmelt infiltration into thin frozen soil layer in northern Japan. *Journal of Hydrology***,** 165-176.

JANSSON, P. E. 2012. CoupModel: Model Use, Calibration, and Validation. *Transactions of the ASABE,* 55**,** 1337. https://doi.org/10.13031/2013.42245

JARVIS, N. & LARSBO, M. 2012. MACRO (v5.2): Model Use, Calibration, and Validation. *Transactions of the American Society of Agricultural and Biological Engineers,* 55**,** 10.

JARVIS, N. J. 2007. A review of non-equilibrium water flow and solute transport in soil macropores: principles, controlling factors and consequences for water quality. *European Journal of Soil Science,* 58**,** 523-546. DOI: 10.1111/j.1365-2389.2007.00915.x

KARLSSON, H., MUIR, D. C. G., TEIXIERA, C. F., BURNISTON, D. A., STRACHAN, W. M. J., HECKY, R. E., MWITA, J., BOOTSMA, H. A., GRIFT, N. P., KIDD, K. A. & ROSENBERG, B. 2000. Persistent Chlorinated Pesticides in Air, Water, and Precipitation from the Lake Malawi Area, Southern Africa. *Environmental Science & Technology,* 34**,** 4490-4495. DOI: 10.1021/es001053j

KJÆR, J., ERNSTSEN, V., JACOBSEN, O. H., HANSEN, N., DE JONGE, L. W. & OLSEN, P. 2011. Transport modes and pathways of the strongly sorbing pesticides glyphosate and

pendimethalin through structured drained soils. *Chemosphere,* 84**,** 471-479. DOI: https://doi.org/10.1016/j.chemosphere.2011.03.029

KURYLYK, B. L. & WATANABE, K. 2013. The mathematical representation of freezing and thawing processes in variably-saturated, non-deformable soils. *Advances in Water Resources,* 60**,** 160-177. https://doi.org/10.1016/j.advwatres.2013.07.016

KÖHNE, J. M., GERKE, H. H. & KÖHNE, S. 2002. Effective Diffusion Coefficients of Soil Aggregates with Surface Skins. *Soil Science Society of America Journal,* 66**,** 1430-1438. 10.2136/sssaj2002.1430

KÖHNE, J. M., KÖHNE, S. & ŠIMŮNEK, J. 2009a. A review of model applications for structured soils: a) Water flow and tracer transport. *Journal of Contaminant Hydrology,* 104**,** 4-35. https://doi.org/10.1016/j.jconhyd.2008.10.002

KÖHNE, J. M., KÖHNE, S. & ŠIMŮNEK, J. 2009b. A review of model applications for structured soils: b) Pesticide transport. *Journal of Contaminant Hydrology,* 104**,** 36-60. https://doi.org/10.1016/j.jconhyd.2008.10.003

LANDBRUKSMETEOROLOGISK TJENESTE (NIBIO). 17.12.2018. http://lmt.nibio.no/.

LARSBO, M. & JARVIS, N. 2003. MACRO 5.0. A model of water flow and solute transport in macroporous soil. Technical description. Emergo 6. 49.Swedish University of Agricultural Sciences.

LARSBO, M., ROULIER, S., STENEMO, F., KASTEEL, R. & JARVIS, N. 2005. An Improved Dual-Permeability Model of Water Flow and Solute Transport in the Vadose Zone. *Vadose Zone Journal,* 4**,** 8. 10.2136/vzj2004.0137

LARSBO, M., SANDIN, M., JARVIS, N., ETANA, A. & KREUGER, J. 2016. Surface Runoff of Pesticides from a Clay Loam Field in Sweden. *Journal of Environmental Quality,* 45**,** 1367-1374. DOI: 10.2134/jeq2015.10.0528

LARSSON, M. H. & JARVIS, N. J. 2000. Quantifying interactions between compound properties and macropore flow effects on pesticide leaching. *Pest Management Science,* 56**,** 133-141. DOI:10.1002/(SICI)1526-4998(200002)56:2<133::AID-PS103>3.0.CO;2-N

LIESS, M. & OHE, P. C. V. D. 2005. Analyzing effects of pesticides on invertebrate communities in streams. *Environmental Toxicology and Chemistry,* 24**,** 954-965. doi:10.1897/03-652.1

LUNDBERG, A., GUSTAFSSON, D., STUMPP, C., KLØVE, B. & FEICCABRINO, J. 2016. Spatiotemporal Variations in Snow and Soil Frost—A Review of Measurement Techniques. *Hydrology,* 3**,** 28. DOI: https://doi.org/10.3390/hydrology3030028

LUNDIN, L.-C. 1990. Hydraulic properties in an operational model of frozen soil. *Journal of Hydrology,* 118**,** 289-310. https://doi.org/10.1016/0022-1694(90)90264-X

LUXMOORE, R. J., JARDINE, P. M., WILSON, G. V., JONES, J. R. & ZELAZNY, L. W. 1990. Physical and chemical controls of preferred path flow through a forested hillslope. *Geoderma,* 46**,** 139-154. DOI: https://doi.org/10.1016/0016-7061(90)90012-X

LÖV, Å., SJÖSTEDT, C., LARSBO, M., PERSSON, I., GUSTAFSSON, J. P., CORNELIS, G. & KLEJA, D. B. 2017. Solubility and transport of Cr(III) in a historically contaminated soil – Evidence of a rapidly reacting dimeric Cr(III) organic matter complex. *Chemosphere,* 189**,** 709-716. DOI: https://doi.org/10.1016/j.chemosphere.2017.09.088

LÅGBU, R., NYBORG, Å. & SVENDGÅRD-STOKKE, S. 2018. Jordsmonnstatistikk Norge (Soil statistics Norway). Nr. 13. Vol. 4. Ås.NIBIO. In Norwegian.

MCCAULEY, C. A., WHITE, D. M., LILLY, M. R. & NYMAN, D. M. 2002. A comparison of hydraulic conductivities, permeabilities and infiltration rates in frozen and

unfrozen soils. *Cold Regions Science and Technology,* 34**,** 117-125. https://doi.org/10.1016/S0165-232X(01)00064-7

MCGRATH, G., HINZ, C. & SIVAPALAN, M. 2010. Assessing the impact of regional rainfall variability on rapid pesticide leaching potential. *Journal of Contaminant Hydrology,* 113**,** 56-65. DOI: https://doi.org/10.1016/j.jconhyd.2009.12.007

MCGRATH, G. S., HINZ, C. & SIVAPALAN, M. 2009. A preferential flow leaching index. *Water Resources Research,* 45. DOI: 10.1029/2008WR007265

MELLANDER, P.-E., LÖFVENIUS, M. O. & LAUDON, H. 2007. Climate change impact on snow and soil temperature in boreal Scots pine stands. *Climatic Change,* 85**,** 179-193. DOI: 10.1007/s10584-007-9254-3

MERDUN, H., MERAL, R. & RIZA DEMIRKIRAN, A. 2008. Effect of the initial soil moisture content on the spatial distribution of the water retention. *Eurasian Soil Science,* 41**,** 1098-1106. 10.1134/s1064229308100128

MIZOGUCHI, M. 1990. *Water, heat and salt transport in freezing soil.* PhD Thesis (In Japanese), University of Tokyo.

MOGHADAS, S., GUSTAFSSON, A. M., VIKLANDER, P., MARSALEK, J. & VIKLANDER, M. 2016. Laboratory study of infiltration into two frozen engineered (sandy) soils recommended for bioretention. *Hydrological Processes,* 30**,** 1251-1264. DOI: 10.1002/hyp.10711

NANOS, T. & KREUGER, J. 2017. Resultat från milöövervakningen av bekämpningsmedel (växtskyddsmedel). Årssammanställning 2014. Sveriges lantbruksuniversitet (SLU), Institutionen för vatten och miljö. Rapport 2015:19. In Swedish. http://www.slu.se/vatten-miljo

NIU, G.-Y. & YANG, Z.-L. 2006. Effects of frozen soil on snowmelt runoff and soil water storage at a continental scale. *Journal of Hydrometeorology,* 7**,** 937-952.

POT, V., ŠIMŮNEK, J., BENOIT, P., COQUET, Y., YRA, A. & MARTÍNEZ-CORDÓN, M. J. 2005. Impact of rainfall intensity on the transport of two herbicides in undisturbed grassed filter strip soil cores. *Journal of Contaminant Hydrology,* 81**,** 63-88. https://doi.org/10.1016/j.jconhyd.2005.06.013

RIISE, G., LUNDEKVAM, H., HAUGEN, L. E. & MULDER, J. 2006. Suspended sediments as carriers for the fungicide propiconazole in agricultural runoff. *Verhandlungen des Internationalen Verein Limnologie***,** 1296–1300. DOI: https://doi.org/10.1080/03680770.2005.11902891

RIISE, G., LUNDEKVAM, H., WU, Q. L., HAUGEN, L. E. & MULDER, J. 2004. Loss of Pesticides from Agricultural Fields in SE Norway – Runoff Through Surface and Drainage Water. *Environmental Geochemistry and Health,* 26**,** 269-276. DOI: 10.1023/B:EGAH.0000039590.84335.d6

SANDIN, M., PIIKKI, K., JARVIS, N., LARSBO, M., BISHOP, K. & KREUGER, J. 2018. Spatial and temporal patterns of pesticide concentrations in streamflow, drainage and runoff in a small Swedish agricultural catchment. *Science of The Total Environment,* 610-611**,** 623-634. DOI: https://doi.org/10.1016/j.scitotenv.2017.08.068

SANGCHAN, W., BANNWARTH, M., INGWERSEN, J., HUGENSCHMIDT, C., SCHWADORF, K., THAVORNYUTIKARN, P., PANSOMBAT, K. & STRECK, T. 2014. Monitoring and risk assessment of pesticides in a tropical river of an agricultural watershed in northern Thailand. *Environmental Monitoring and Assessment,* 186**,** 1083-1099. 10.1007/s10661-013-3440-8

SCHUMMER, C., MOTHIRON, E., APPENZELLER, B. M. R., RIZET, A.-L., WENNIG, R. & MILLET, M. 2010. Temporal variations of concentrations of currently used

pesticides in the atmosphere of Strasbourg, France. *Environmental Pollution,* 158**,** 576-584. DOI: https://doi.org/10.1016/j.envpol.2009.08.019

SCHWARTZ, F. W. & ZHANG, H. 2003. *Fundamentals of Groundwater*, John Wiley & Sons, Inc., New York

SIIMES, K., RÄMÖ, S., WELLING, L., NIKUNEN, U. & LAITINEN, P. 2006. Comparison of the behaviour of three herbicides in a field experiment under bare soil conditions. *Agricultural water management,* 84**,** 53-64. DOI: https://doi.org/10.1016/j.agwat.2006.01.007

SMITH, R., MIDDLEBROOK, R., TURNER, R., HUGGINS, R., VARDY, S. & WARNE, M. 2012. Large-scale pesticide monitoring across Great Barrier Reef catchments – Paddock to Reef Integrated Monitoring, Modelling and Reporting Program. *Marine Pollution Bulletin,* 65**,** 117-127. https://doi.org/10.1016/j.marpolbul.2011.08.010

STEFFENS, K. 2015. *Modelling Climate Change Impacts on Pesticide Leaching.* PhD, Swedish University of Agricultural Sciences. 978-91-576-8269-7

STENRØD, M. 2015. Long-term trends of pesticides in Norwegian agricultural streams and potential future challenges in northern climate. *Acta Agriculturae Scandinavica, Section B — Soil & Plant Science,* 65**,** 199-216. DOI: 10.1080/09064710.2014.977339

STENRØD, M., ALMVIK, M., EKLO, O. M., GIMSING, A. L., HOLTEN, R., KÜNNIS-BERES, K., LARSBO, M., PUTELIS, L., SIIMES, K., TURKA, I. & UUSI-KÄMPPÄ, J. 2016. Pesticide regulatory risk assessment, monitoring, and fate studies in the northern zone: recommendations from a Nordic-Baltic workshop. *Environmental Science and Pollution Research,* 23**,** 15779-15788. DOI: 10.1007/s11356-016-7087-1

STENRØD, M., PERCEVAL, J., BENOIT, P., ALMVIK, M., BOLLI, R. I., EKLO, O. M., SVEISTRUP, T. E. & KVÆRNER, J. 2008. Cold climatic conditions: Effects on bioavailability and leaching of the mobile pesticide metribuzin in a silt loam soil in Norway. *Cold Regions Science and Technology,* 53**,** 4-15. DOI: http://dx.doi.org/10.1016/j.coldregions.2007.06.007

STONE, W. W., GILLION, R. J. & MARTIN, J. D. 2014. An Overview Comparing Results from Two Decades of Monitoring for Pesticides in the Nation's Streams and Rivers, 1992–2001 and 2002–2011. Scientific Investigations Report 2014-5154. U.S. Department of the Interior and U.S. Geological Survey (USGS). DOI: http://dx.doi.org/10.3133/sir20145154.

STÄHLI, M., JANSSON, P.-E. & LUNDIN, L.-C. 1996. Preferential Water Flow in a Frozen Soil — a Two-Domain Model Approach. *Hydrological Processes,* 10**,** 1305-1316. 10.1002/(sici)1099-1085(199610)10:10<1305::Aid-hyp462>3.0.Co;2-f

STÄHLI, M. & STADLER, D. 1997. Measurement of water and solute dynamics in freezing soil columns with time domain reflectometry. *Journal of Hydrology***,** 352-369. DOI: https://doi.org/10.1016/S0022-1694(96)03227-1

TANG, J. Y. M. & ESCHER, B. I. 2014. Realistic environmental mixtures of micropollutants in surface, drinking, and recycled water: Herbicides dominate the mixture toxicity toward algae. *Environmental Toxicology and Chemistry,* 33**,** 1427-1436. doi:10.1002/etc.2580

ULÉN, B. M., LARSBO, M., KREUGER, J. K. & SVANBÄCK, A. 2013. Spatial variation in herbicide leaching from a marine clay soil via subsurface drains. *Pest Management Science,* 70**,** 405-414. DOI: 10.1002/ps.3574

VAN DER KAMP, G., HAYASHI, M. & GALLÉN, D. 2003. Comparing the hydrology of grassed and cultivated catchments in the semi-arid Canadian prairies. *Hydrological processes***,** 559-575. DOI: 10.1002/hyp.1157

VANDERBORGHT, J., GÄHWILLER, P. & FLÜHLER, H. 2002. Identification of Transport Processes in Soil Cores Using Fluorescent Tracers. *Soil Science Society of America Journal,* 66**,** 774-787. 10.2136/sssaj2002.7740

WATANABE, K., KITO, T., WAKE, T. & SAKAI, M. 2011. Freezing experiments on unsaturated sand, loam and silt loam. *Annals of Glaciology,* 52**,** 37-43.

WATANABE, K. & KUGISAKI, Y. 2017. Effect of macropores on soil freezing and thawing with infiltration. *Hydrological Processes,* 31**,** 270-278. 10.1002/hyp.10939

WATANABE, K. & OSADA, Y. 2016. Comparison of Hydraulic Conductivity in Frozen Saturated and Unfrozen Unsaturated Soils. *Vadose Zone Journal,* 15. 10.2136/vzj2015.11.0154

WATSON, K. W. & LUXMOORE, R. J. 1986. Estimating Macroporosity in a Forest Watershed by use of a Tension Infiltrometer1. *Soil Science Society of America Journal,* 50**,** 578-582. 10.2136/sssaj1986.03615995005000030007x

WEILER, M. 2017. Macropores and preferential flow—a love-hate relationship. *Hydrological Processes,* 31**,** 15-19. doi:10.1002/hyp.11074

ZHANG, T., BARRY, R., KNOWLES, K., LING, F. & ARMSTRONG, R. Distribution of seasonally and perennially frozen ground in the Northern Hemisphere. Proceedings of the 8th International Conference on Permafrost, 2003. AA Balkema Publishers, 1289-1294.

ÅKESSON, M., SPARRENBOM, C. J., DAHLQVIST, P. & FRASER, S. J. 2015. On the scope and management of pesticide pollution of Swedish groundwater resources: The Scanian example. *AMBIO,* 44**,** 226-238. DOI: 10.1007/s13280-014-0548-1

Paper I

Journal of Contaminant Hydrology 219 (2018) 72–85

Contents lists available at ScienceDirect

Journal of Contaminant Hydrology

journal homepage: www.elsevier.com/locate/jconhyd

The effect of freezing and thawing on water flow and MCPA leaching in partially frozen soil

Roger Holten [a,b,*], Frederik Norheim Bøe [c], Marit Almvik[a], Sheela Katuwal[d], Marianne Stenrød[a], Mats Larsbo[e], Nicholas Jarvis[e], Ole Martin Eklo[a,b]

[a] Norwegian Institute of Bioeconomy Research (NIBIO), Division of Biotechnology and Plant Health, Department of Pesticides and Natural Products Chemistry, P.O. Box 115, NO-1431 Ås, Norway
[b] Norwegian University of Life Sciences, Faculty of Bio Sciences, Department of Plant Sciences, P.O. Box 5003, N-1432 Ås, Norway
[c] Norwegian Institute of Bioeconomy Research (NIBIO), Division of Environment and Natural Resources, Department of Soil and Land Use, P.O. Box 115, NO-1431 Ås, Norway
[d] Aarhus University, Department of Agroecology, Blichers Allé 20, P.O. Box 50, DK-8830 Tjele, Denmark
[e] Swedish Agricultural University, Department of Soil and Environment, P.O. Box 7014 75007, Uppsala, Sweden

ARTICLE INFO

Keywords:
Freeze-thaw effects
Preferential flow
Macropores
Solute transport
MCPA

ABSTRACT

Limited knowledge and experimental data exist on pesticide leaching through partially frozen soil. The objective of this study was to better understand the complex processes of freezing and thawing and the effects these processes have on water flow and pesticide transport through soil. To achieve this we conducted a soil column irrigation experiment to quantify the transport of a non-reactive tracer and the herbicide MCPA in partially frozen soil. In total 40 intact topsoil and subsoil columns from two agricultural fields with contrasting soil types (silt and loam) in South-East Norway were used in this experiment. MCPA and bromide were applied on top of all columns. Half the columns were then frozen at −3 °C while the other half of the columns were stored at +4 °C. Columns were then subjected to repeated irrigation events at a rate of 5 mm artificial rainwater for 5 h at each event. Each irrigation was followed by 14-day periods of freezing or refrigeration. Percolate was collected and analysed for MCPA and bromide. The results show that nearly 100% more MCPA leached from frozen than unfrozen topsoil columns of Hov silt and Kroer loam soils. Leaching patterns of bromide and MCPA were very similar in frozen columns with high concentrations and clear peaks early in the irrigation process, and with lower concentrations leaching at later stages. Hardly any MCPA leached from unfrozen topsoil columns (0.4–0.5% of applied amount) and concentrations were very low. Bromide showed a different flow pattern indicating a more uniform advective-dispersive transport process in the unfrozen columns with higher concentrations leaching but without clear concentration peaks. This study documents that pesticides can be preferentially transported through soil macropores at relatively high concentrations in partially frozen soil. These findings indicate, that monitoring programs should include sampling during snow melt or early spring in areas were soil frost is common as this period could imply exposure peaks in groundwater or surface water.

1. Introduction

In cold climates, increased pesticide concentrations are often detected in soil leachate, drain discharge, surface runoff, and surface water bodies during freeze/thaw periods in late winter and early spring (Eklo et al., 1994; French, 1999; Riise et al., 2004; Riise et al., 2006; Siimes et al., 2006; Ulén et al., 2013). With climate change, this may become an increasingly relevant issue. For example, in the Nordic countries, climate models predict higher temperatures and more snowmelt episodes during winter and an increase in the frequency of freeze-thaw cycles of up to 38% (Hanssen-Bauer et al., 2015; Mellander et al., 2007; Lundberg et al., 2016).

However, the effects of freezing and thawing on the fate and behaviour of pesticides in soil are complex and still not well understood,

* Corresponding author at: Norwegian Institute of Bioeconomy Research (NIBIO), Division of Biotechnology and Plant Health, Department of Pesticides and Natural Products Chemistry, P.O. Box 115, NO-1431 Ås, Norway.
E-mail addresses: roger.holten@nibio.no (R. Holten), frederik.boe@nibio.no (F.N. Bøe), marit.almvik@nibio.no (M. Almvik), sheela.katuwaSl@agro.au.dk (S. Katuwal), marianne.stenrod@nibio.no (M. Stenrød), mats.larsbo@slu.se (M. Larsbo), nicholas.jarvis@slu.se (N. Jarvis), olemartin.eklo@nibio.no (O.M. Eklo).

https://doi.org/10.1016/j.jconhyd.2018.11.003
Received 23 May 2018; Received in revised form 2 November 2018; Accepted 11 November 2018
Available online 13 November 2018

so the mechanisms underlying these field observations are unclear. Soil freezing and thawing potentially influences the pathways of water flow and solute transport through soils, as well as chemical and biological processes affecting pesticide fate in the soil (Hayashi, 2013; Ireson et al., 2013).

The importance of macropores as non-equilibrium or preferential flow paths for rapid water flow and solute transport has long since been recognized (Jarvis et al., 2016; Beven and Germann, 1982). The occurrence of macropore flow can result in dramatic increases in the leaching of pesticides to groundwater and to surface water via subsurface drainage pipes (Jarvis, 2007; Flury, 1996). Macropores can be defined as pores with diameters of 0.3–0.5 mm and larger (Jarvis et al., 2017; Jarvis, 2007). These large pores have a smaller relative surface area than smaller pores and in cases where macropores dominate flow processes, solutes in flowing water can bypass bulk soil and any potential binding sites (Luxmoore et al., 1990). Examples of macropores are biopores made by earthworms and plant roots and planar fissures formed by freezing/thawing or drying/wetting. Any water present in such large pores will freeze first. As the temperature continue to decrease, water in successively smaller pores will freeze (Ireson et al., 2013). However, large macropores will often be air-filled when the soil freezes and can therefore function as effective pathways for preferential flow on thawing or if rain falls on frozen ground (Van Der Kamp et al., 2003). With subsequent freeze-thaw cycles they can become blocked with ice, which reduces the hydraulic conductivity (Ireson et al., 2013).

Models currently used in risk assessment and management do not account for the effects of freezing and thawing on pesticide leaching. Models should be tested against experimental data, hence the need to perform controlled laboratory studies or field studies to generate the data required to support the development of such a model. To date, only relatively few studies have investigated experimentally the significance of freezing and thawing for preferential transport of solutes through soil (Stadler et al., 2000; Gentry et al., 2000; Barnes and Wolfe, 2008; Wang et al., 2016; Hafsteinsdóttir et al., 2013; Wei et al., 2015). These referred studies focused mainly on the transport of tracers, nitrogen, petroleum or heavy metals. In a laboratory study, Stenrød et al. (2008) reported higher mobility of metribuzin and transport to greater depths in frozen soil compared to unfrozen soil but this study did not focus on preferential flow per se, and the results were not statistically significant. To our knowledge, no other studies of this type have been carried out specifically for pesticides.The objective of the present study was therefore to increase understanding of the effects of freezing and thawing on water flow and pesticide transport through soil. To achieve this we conducted a soil column irrigation experiment to quantify the transport of a non-reactive tracer and the herbicide MCPA in partially frozen soil. We hypothesize that columns subjected to freezing will show a higher degree of preferential transport.

2. Materials and methods

2.1. Soil sampling and characterization

Intact soil columns were sampled in May 2016 from two agricultural fields with contrasting soil types (Table 1) in South-East Norway (Kroer, 59° 38′ 37″ N 10° 49′ 58″ E; Hov 60° 12′ 45″ N 12° 1′ 58″ E). The Kroer loam have been characterized earlier by Greve et al. (1998), so no additional characterization was performed in this study. Soil characterization of the Hov silt had also been carried out earlier by the division of Survey and Statistics at NIBIO. This characterization was done according to the World Reference Base for Soil Resources, WRB (IUSS Working Group WRB, 2014). Additional information on the chemical characterization of the soils are summarized in Fig. A1 in Appendix C.

The water content of the sampled soils was neither t measured in the columns at sampling nor in the laboratory before the experiment started. This was to avoid disturbing the intact soil columns. Sampling was done in aluminium cylinders (i.d. 9.2 cm, height 20 cm). Fifty-six columns were sampled, 14 from both the topsoil (0–20 cm) and subsoil (20–40 cm) at each site. The cylinders were forced into the soil using a sledgehammer and dug out by hand, wrapped in black plastic bags and stored at ca. +4 °C. At the time of sampling, the fields were under winter wheat. Information about the use of pesticides on the sampled fields was obtained from the farmers and indicated no use of the herbicide MCPA during the last 2–3 years prior to sampling.

The soil columns were first scanned at the Department of Soil and Environment at the Swedish University of Agricultural Sciences using a high resolution industrial X-ray CT scanner (GE Phoenix v/tome/×m). The X-ray scanner had a 240 kV X-ray tube, a tungsten target (beryllium window) and a GE 16″ flat panel detector. The spatial resolution of the reconstructed 3-D images was 115 µm, with an actual resolution for feature recognition estimated to be double the pixel size (i.e. 230 µm). Radiographs collected for each soil column, in total 2000 per column, were reconstructed to 3-D images using the GE phoenix datos|x image reconstruction software. The reconstructed images were exported as 16-bit TIFF.

The X-ray images were analysed to visualize and quantify soil macropore network characteristics. The processing and analysis of the x-ray images were performed with an open source software ImageJ 1.51u (Schneider et al., 2012). Details of the image processing procedure are provided in Appendix B. Briefly, X-ray images were preprocessed for alignment, illumination correction, contrast enhancement and noise removal before applying the local adaptive thresholding method of Phansalkar et al. (2011). Using the segmented images the macroporosity ($mm^3\,mm^{-3}$), specific surface area ($mm^2\,mm^{-3}$) and the average pore thickness (mm) of the total macropore networks or the macropores pores connected throughout the soil depth, also referred to as connected macropore network, were quantified.

2.2. Chemicals

A solution of the phenoxy-acid herbicide MCPA (2-methyl-4-chlorophenoxyacetic acid, Dr. Ehrensdorfer GmbH, purity 99.5%) at a concentration of 282.6 mg L^{-1} was prepared by dissolving 70.65 mg MCPA in 250 mL acetone (VWR, Purity 99.4%). Potassium bromide (KBr) at a concentration of 11.7 g L^{-1} (7.9 g Br L^{-1}) was prepared in deionized water (Milli-Q™). MCPA is, according to the pesticide properties database (PPDB), classified as a mobile substance with typical sorption coefficients (K_f) in different soils of 0.05–1.99 mL g^{-1} (mean 0.94 mL g^{-1}). PPDB also classifies MCPA as non-persistent with a range of DT_{50} values of 7–41 days (mean 24 days) under laboratory conditions

Table 1
Selected characteristics of the studied soils.

Site	Class.[1]	Horizon, cm depth	Soil texture[2]	Clay (%)	Silt (%)	Sand (%)	pH (H_2O)	Tot. C (%)	Tot. N (%)	CEC
Kroer	Retic Stagnosol	Ap, 0–23	Loam	19.1	43.8	37.1	5.5	2.5	0.2	13.3
		Eg, 23–40	Silt loam	20.5	63.0	16.7	5.6	0.4	0.07	7.4
Hov	Dystric Fluvic Cambisol	Ap, 0–20	Silt	5.4	83.8	10.8	5.4	1.2	0.1	6.6
		Bw, 28–50	Silt	4.1	86.7	9.2	6.2	0.3	0.02	3.3

[1] WRB, 2014.
[2] USDA soil texture classification.

at 20 °C. MCPA also degrades rapidly by aqueous photolysis at pH 7 and 20 °C with a DT_{50} of 0.05 days, and even more rapidly (DT_{50} 1 h) at test conditions of pH 5–9 and 25 °C. In natural sunlight at pH 5 the DT_{50} of MCPA is 25.4 days (Lewis et al., 2016).

The MCPA metabolite 2-methyl-4-chlorophenol (2-MCP, Sigma-Aldrich, purity 99.4%) were also included in the analyses. This metabolite has been classified as slightly mobile according to PPDB, with a Koc of 882 mL g^{-1}.

A solution of artificial rainwater (Löv et al., 2017) was prepared (0.58 mg L^{-1} NaCl, 0.70 mg L^{-1} $(NH_4)_2SO_4$, 0.50 mg L^{-1} $NaNO_3$, 0.57 mg L^{-1} $CaCl_2$) and HCl (0.95 mL L^{-1} 37%) was added to obtain a pH of about 5. The rainwater was stored at about +4 °C in 20 L plastic containers.

2.3. Experimental set up

Twenty of the sampled soil columns from each of the sites Kroer and Hov, in total 40 columns, was included in the experiment. The rest of the sampled columns were excluded due to their bad condition (e.g. high content of straw in the bottom, soil was too loose and crumbled out of the columns or due to big gaps between soil and cylinder walls). The top of the soil columns was levelled to 2 cm below the rim of the top of the aluminium cylinders to ensure sufficient room for ponding during irrigation. The columns were also carefully levelled at the bottom. To achieve equal initial conditions the columns were then placed in a box of water with zero pressure potential at the bottom of the soil for a week to bring the samples close to saturation. The columns were then placed on a sand box (Eijkelkamp) where a pressure potential of −30 cm was applied at the bottom of the soil columns for a week to establish an identical initial condition for all columns, one that also ensured that all continuous macropores would be air-filled.

Five columns were randomly chosen from each soil type and depth for the freezing treatment. The remaining five columns were stored unfrozen. Analysis of Variance (ANOVA) tests performed using All Pairwise Multiple Comparison Procedures (Student-Newman-Keuls Method) in SigmaPLot (SigmaPlot for Windows Version 13.0, Systat Software, Inc.) showed no significant differences for either of the soils or depths in any of the measured pore network characteristics between the columns that underwent the freezing treatment and the unfrozen columns. All columns were then placed on fine-meshed metal sieves filled with glass beads to allow for free drainage. Thermistors were installed in the columns that were subjected to freezing to monitor the temperature during the experiment. These thermistors were installed horizontally into the center of the columns through holes in the cylinders at 7 and 14 cm depth from the soil surface The thermistors were then connected to a temperature data logger (Delta-T, Burwell - Cambridge - U.K. Accuracy ± 0.5 °C). Temperature was logged every 10 min throughout the experiment. The columns were placed on a 5 cm thick polystyrene insulation board and the column walls were covered with two layers of 2 cm thick polyethylene insulation to ensure freezing from the top and downwards.

Five mL of both the MCPA and potassium bromide (KBr) solutions were applied at the surface of each column as evenly as possible by hand using a 5 mL pipette (Finnpipette), giving rates of 2.1 kg ha^{-1} of MCPA and 59.1 kg Br^- ha^{-1}. The application rate of MCPA is an agricultural relevant rate in Norway. The insulated columns in the freezing treatment were then placed in a 1 m^3 freezing cabinet (Weisstechnik 1000SB, Weiss Technik GMBH, D-6301 Reiskirchen, Germany. Accuracy ± 0.5 °C) at −3 °C, while the unfrozen columns were kept at ca +4 °C in a refrigerated room. A temperature of −3 °C was chosen as it was considered low enough to ensure that all water in mesopores and macropores would be frozen. The top of the columns were sealed with a plastic lid and incubated at these temperatures for about four weeks. They were then subjected to repeated irrigation events with the prepared artificial rainwater, followed by 14-day periods of freezing (or refrigeration for the control columns) between irrigations. The experiment lasted for a total of 8 weeks for the silt soil (3 irrigations) and 10 weeks for the loam (4 irrigations).

The frozen columns and the unfrozen columns were transported to the irrigation room in the morning of each irrigation event. The irrigation room was at a temperature of about 5–8 °C at the start of the irrigations, but this increased to a maximum of ca. 12 °C during the day. The artificial rain water was at a temperature of about 2–4 °C at the start of each irrigation, but this increased to a maximum of about 6 °C at the end of the irrigations.

The columns were placed on top of funnels with collector flasks beneath. This setup allowed free drainage at the base of the soil columns. Irrigation water was distributed to the columns using peristaltic pumps (Autoclude model VL) adjusted to give a rate of 5 mm hr^{-1} for 5 h, resulting in a total of about 25 mm of rainwater to each column per irrigation event. Water was transferred through PVC-tubes (VWR, 4 × 6 mm) and dripped onto filter paper (Whatman Grade 1 85 mm, GE Healthcare Life Sciences) placed on the surface of the columns to ensure uniform distribution. The actual irrigation rates varied slightly between columns but there were no systematic differences between treatments, soils or depths. Preliminary tests indicated that on average the columns received 5 to 9% less water than the nominal rate. Rough calculations suggest that the total amount of irrigation water supplied to the columns during the experiment would be equivalent to ca. one pore volume.

Percolate from the soil columns during and after each irrigation was sampled in 150 mL polycarbonate bottles (Corning®, VWR) and subsamples for chemical analysis were collected manually at approximately every 25 mL until about 24 h after the start of each irrigation event. From each sub-sample, 3 mL was transferred to a 15 mL polypropylene centrifuge tube (Corning®, VWR) and stored cold (+4 °C) for later analysis of bromide. The remaining volume of leachate for each sample was stored frozen (−20 °C) in amber 60 mL glass bottles for later pesticide analysis.

Results of water and pesticides are reported as total amounts/volumes transported through the soil columns during the irrigation events (as % of the applied amounts) and as measured concentrations.

The term 5% arrival time is frequently used as an indicator of the degree of preferential flow (Koestel et al., 2011). It is usually defined as the normalized time at which 5% of the applied amount of a solute has passed through a soil column. Small values indicate a high degree of preferential transport (Larsbo et al., 2016). In our case, as the outflows are not the same for all columns even if the boundary condition is the same (a non-steady-state flow experiment), we used the 5% arrival volume for bromide to assess whether there were any differences in the strength of preferential flow between the frozen and unfrozen columns. The first 5% of the tracer mass in this instance is based on the initial applied bromide mass.

2.4. Chemical analysis

Bromide analysis was carried out using a Thermo Bromide Ion Selective Electrode (Thermo Fisher Scientific, Orion 9635BNWP) coupled to an ion meter (Mettler Toledo Seven Compact pH/Ion Meter S220) that was placed directly in the 3 mL leachate samples after addition of ionic strength adjuster (ISA, Thermo Fisher Scientific).

The concentrations of MCPA and the metabolite 2-MCP in the leachate samples were measured using LC-MS/MS (Waters Alliance 2695 LC-system coupled to a Quattro Ultima Pt triple quadropole mass spectrometer from Micromass, Manchester, UK). Leachates were filtrated with a syringe filter (PTFE 0.2 µm filter, 13 mm diameter, VWR) into vials. Leachates from the unfrozen soil columns were analysed directly, whereas the samples from the frozen columns were diluted

1 + 9 in water before analysis due to high MCPA-concentrations. 50 µL 2,4-D (Dr. Ehrensdorfer GmbH, purity 99%) was added as an internal standard to all samples at a final level of 10 ng/mL, to adjust for any variability during analysis. A 5 µL sample volume was injected, and the analytes separated on a Phenomenex Gemini C18 column (100 × 2 mm, particle diameter 3 µm) using 5 mM formic acid and methanol as mobile phases. The analytes were detected in the negative electrospray mode, with transitions *m/z* 199 > 141 and m/z 200 > 142 for MCPA and the pseudo-transition m/z 141 > 141 for 2-MCP. The MCPA metabolite 2-MCP was not detected in any of the samples. Concentrations were measured using a 5-point internal standard calibration range from 0.5–500 ng MCPA/mL. The limits of quantification were 0.125 ng MCPA/mL and 5 ng 2-MCP/mL.

After removing water for MCPA analysis, the remaining leachate was combined to make one bulk sample per column and irrigation. As 2-MCP was not detected by the method used to analyse for MCPA, selected bulk samples were concentrated and analysed for the metabolite 2-MCP.

2.5. Statistical analysis

Statistical analysis of the differences in macropore characteristics, water, bromide and MCPA transport were carried out with an analysis of variance (ANOVA) Type III test and a post-hoc pairwise Tukey test (Tukey's 'Honest Significant Difference' method) in R Commander (R Core Team, 2016). The mean total amounts of water, bromide and MCPA leached were used as response variables and soil type and treatment (frozen or unfrozen) as predictor variables (factors). Statistically significant results are reported at the 5% significance level unless otherwise stated.

3. Results

3.1. Image analysis and soil characteristics

The characteristics of the imaged macropore networks are summarized in Table 2. As was also demonstrated by Jarvis et al. (2017), the results showed that the connectivity of the macropore networks depends strongly on imaged macroporosity, with a threshold value for continuity (percolation) of ca. 4% (Fig. 1). In general, the topsoils had larger imaged porosities than the subsoils, while the loam soil at Kroer was found to have a larger imaged porosity and better connected macropore network than the silt soil at Hov (Fig. 1). In particular, the subsoil at Hov appeared to have no connected macroporosity.

3.2. Temperatures

Temperatures in the initially frozen soil columns increased quickly towards 0 °C after the start of the irrigations, but then stabilized before starting to increase again (Fig. 2). It generally took several hours before the temperatures continued to increase above 0 °C and this lag phase was longer at each irrigation. At the third irrigation of the silt, soil temperatures did not increase much above 0 °C until 27–30 h after the start of the irrigation. Another observation made, was that loam subsoil started thawing before the loam topsoil. Measurements from all thermistors at both depths (7 and 14 cm) were included in the figure but no clear difference between the two depths could be observed and the two thermistor depths have not been indicated in the figure. The data logger stopped working under the third irrigation of the Kroer loam soil columns, so no temperature curve could be obtained from this irrigation event. It took some time before the first irrigation of the Kroer loam started, hence the temperatures in the columns had risen to near 0 °C at the beginning of the irrigation.

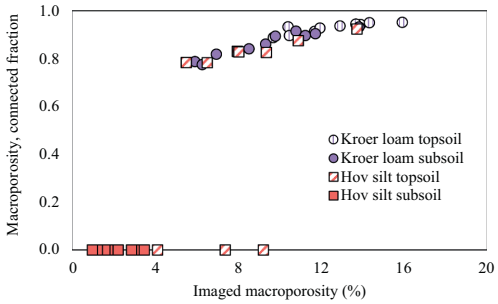

Fig. 1. The connected fraction of the macroporosity plotted as a function of imaged porosity for the Kroer loam and Hov silt topsoil and subsoil.

3.3. Infiltration and drainage

ANOVA for percolated volumes of water show that significantly larger amounts of percolation were collected from the unfrozen loam soil columns than from the frozen columns ($p < .001$) and significantly more from frozen topsoil columns than from frozen subsoil columns ($p < .05$). No significant differences were observed between the unfrozen topsoil and subsoil columns. Similar observations were made for the silt soil (Table 3).

Due to the different number of irrigations the two soils received, a direct statistical comparison of the two soil types was not performed. Nevertheless, some differences worth mentioning were observed. For example, ponding was observed on frozen columns already during the first irrigation and to a greater extent for the silt than for the loam soil. In the silt soil, ponding was even observed on unfrozen subsoil columns. In general, the extent of ponding increased in both soils for the later irrigations. In the silt, swelling or frost heave of the soil was also observed in addition to freezing of the irrigation water along the edges at the top of the soil columns, especially during the later irrigations.

Another observation made for both soil types was that when the frozen soil columns started to thaw during the irrigation, the ponded water infiltrated quickly and percolated through the columns. After thawing, 25 mL samples were collected at ca. 6–7 min intervals,

Table 2
Mean values of measured macropore network characteristics for Hov silt ($n = 20$) and Kroer loam (n = 20) soil columns. Different superscript letters denote statistically significant different results ($p < .05$), based on pairwise comparison of the samples.

Site, depth	Total macropore network			Connected macropore network		
	Mean macropor. (± SD)	Mean spec. Surface area, mm^2/mm^{-3} (± SD)	Mean thickness, mm (± SD)	Mean macropor. (± SD)	Mean spec. Surface area, mm^2/mm^{-3} (± SD)	Mean thickness, mm (± SD)
Hov silt, 0–20 cm	0.08 (0.03)^{b}	0.3 (0.09)^{b}	1.0 (0.2)^{ab}	0.05 (0.04)^{bc}	0.2 (0.2)^{bc}	0.8 (0.6)^{ab}
Hov silt, 20–40 cm	0.02 (0.01)^{c}	0.1 (0.04)^{c}	0. 9 (0.2)^{b}	0.0 (0.0)^{c}	0.0 (0.0)^{c}	0.0 (0.0)^{b}
Kroer loam, 0–20 cm	0.1 (0.02)^{a}	0.5 (0.05)^{a}	1.1 (0.1)^{a}	0.1 (0.02)^{a}	0.4 (0.06)^{a}	1.1 (0.1)^{a}
Kroer loam, 20–40 cm	0.09 (0.03)^{b}	0.4 (0.09)^{b}	1.2 (0.1)^{a}	0.08 (0.03)^{ab}	0.3 (0.1)^{ab}	1.3 (0.1)^{a}

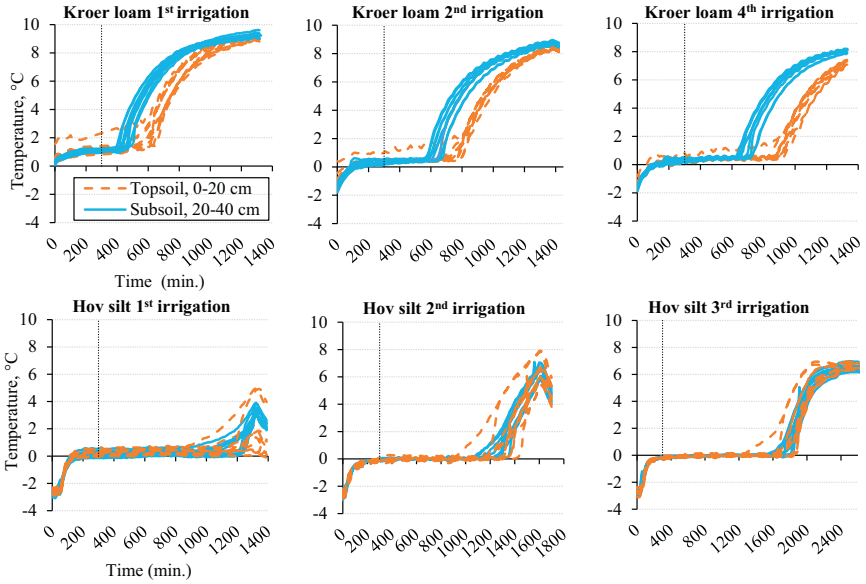

Fig. 2. Temperatures measured at 7 and 14 cm in frozen Kroer loam and Hov silt columns during three irrigation events. For the loam the curves stops at the time the columns were put back in the freezing cabinet (temperatures then started to decrease). For the silt, the temperatures continued to increase even after the columns were put back into the freezing room (around 1400 min). The end of each irrigation event (at 300 min) is symbolized with a dotted line. The same legend applies to all plots.

equivalent to flow rates of ca. 35 mm h^{-1}. This sudden infiltration was observed more often in the loam than in the silt. In contrast, the interval between each sampling in unfrozen soil was typically ca. 30 min, equivalent to a flow rate of ca. 7 mm h^{-1}.

Figs. 3 and 4 show the accumulated amount of water that percolated from frozen and unfrozen Kroer loam and Hov silt soil columns plotted against time. These figures show the constant outflow rate during irrigations of the unfrozen columns (almost equal to the inflow rate) and the rapid cessation when the irrigations stopped. This was very clear for both the loam topsoil and subsoil as well as the silt topsoil, whereas this difference was smaller for the unfrozen silt subsoil. In the frozen columns the outflow started later, especially for the later irrigations, and many of the frozen columns continued to percolate slowly a long time after irrigation ceased. During the second irrigation of the Kroer loam, some of the early samples from the frozen subsoil were lost due to leakages through the thermistor holes. The holes were re-sealed before the next irrigation. This was not believed to influence the overall results.

3.4. Bromide leaching

Following the pattern observed for the percolation of water, significantly ($p < .001$) more bromide leached from the unfrozen loam columns than from the frozen loam columns in both topsoil and subsoil (Table 3). On average, significantly more bromide leached from the unfrozen loam subsoil than the unfrozen loam topsoil ($p < .05$). In the case of the silt soil, there were no statistically significant differences between the amounts of bromide leached from frozen and unfrozen topsoil columns ($p > .05$). For subsoil on the other hand, the results were similar to what was observed for the loam.

Table 3
Total amount of water, bromide and MCPA percolated from Kroer loam soil columns during four irrigations and Hov silt soil columns during three irrigations. Different superscript letters denote statistically significant different results, based on pairwise comparison of samples from the same soil.

Soil	Soil depth (cm)	Temp. treatm. (°C)	Water		Bromide		Bromide	MCPA	
			(mm) mean (SD)	(% of applied[1])	(mg) mean (SD)	(% of applied)	5% arrival vol. mean (SD)	(µg) mean (SD)	(% of applied[2])
Kroer, loam	0–20	-3	60.2 (4.9)^{b}	60.2	14.7 (1.3)^{c}	37.4	7.5 (5.0)^{de}	346.5 (96.9)^{a}	24.5
	0–20	+4	91.2 (3.4)^{a}	91.2	22.6 (4.0)^{b}	57.5	18.0 (6.6)^{bcd}	5.0 (3.9)^{b}	0.4
	20–40	-3	47.1 (6.5)^{c}	47.1	11.1 (3.6)^{c}	28.2	3.6 (3.4)^{e}	327.9 (51.4)^{a}	23.2
	20–40	+4	87.1 (4.4)^{a}	87.1	28.3 (1.7)^{a}	72.1	7.8 (2.2)^{cde}	121.1 (97.2)^{b}	8.6
Hov, silt	0–20	-3	56.8 (6.0)^{B}	75.7	9.9 (3.5)^{AB}	25.2	5.6 (3.3)^{de}	232.2 (47.7)^{A}	16.4
	0–20	+4	70.5 (2.1)^{A}	94.0	12.3 (3.8)^{A}	31.5	35.8 (6.6)^{a}	7.5 (2.6)^{B}	0.5
	20–40	-3	39.5 (4.4)^{C}	52.7	5.1 (1.7)^{B}	13.1	20.9 (6.9)^{bc}	145.3 (58.7)^{A}	10.3
	20–40	+4	61.5 (9.0)^{AB}	82.0	11.9 (3.5)^{A}	30.4	26.2 (11.5)^{ab}	149.8 (100.4)^{A}	10.6

[1] % of nominal amount of water added.
[2] % of nominal (measured amounts in the applied pesticide solution were 102% of nominal).

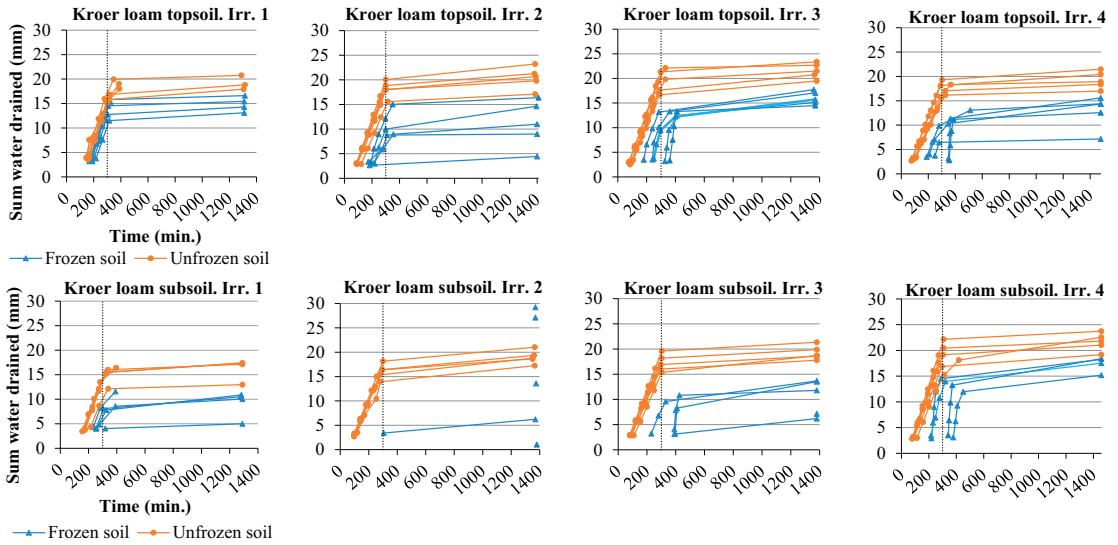

Fig. 3. The accumulated amount of water that drained from frozen and unfrozen soil columns during four irrigation events of the Kroer loam topsoil and subsoil, plotted against time. The vertical dotted line illustrates the end of the irrigations. During the second irrigation, some of the early samples from the subsoil were lost due to leakages through the thermistor holes. The same legend apply to all plots.

The leaching patterns of bromide are illustrated in Figs. 5 and 6 for typical columns from each soil and treatment combination. It was difficult to pick representative columns but the purpose was to illustrate that, for these soils and treatments, preferential flow occurred, although manifested slightly differently for different columns. Figs. 5 show evidence of strong preferential flow through the frozen topsoils of the loam columns, with the highest bromide concentrations found in the first sample of the second irrigation. Results from the other loam topsoil columns showed the same pattern albeit with some variations in the timing of the peak bromide concentrations (Fig. A1 in Appendix A). The evidence of strong preferential flow was weaker for the frozen silt topsoil columns (Fig. 6), though clearer for two of the columns (Fig. A3

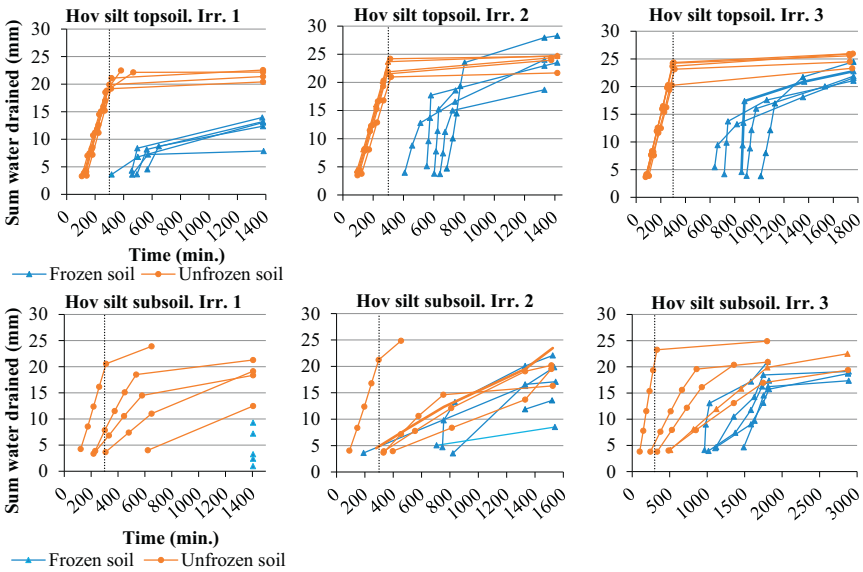

Fig. 4. The accumulated amount of water that drained from frozen and unfrozen soil columns during three irrigation events of the Hov silt topsoil and subsoil, plotted against time. The vertical dotted line illustrates the end of the irrigations. Different time scales are due to large variations in infiltration times. Only one sample was collected for each frozen subsoil column at the first irrigation due to very little percolation. The same legend apply to all plots.

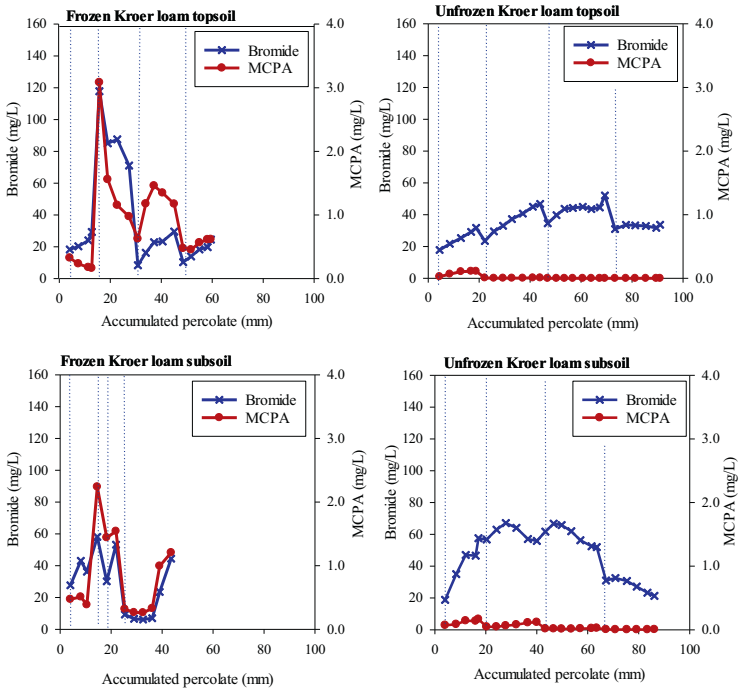

Fig. 5. Bromide and MCPA (mg L^{-1}) concentrations plotted as a function of accumulated amount of percolate (mm) for a representative soil column from frozen and unfrozen topsoil and subsoil of Kroer loam and Hov silt. Dotted lines indicate the first sampling of leachate after the onset of a new irrigation.

in Appendix A) where an early breakthrough of relatively high concentrations of bromide was observed in the first collected samples. This pattern was not equally clear for the frozen silt subsoil (Fig. 6 and Fig. A3 in Appendix A).

Contrary to the frozen soils, the leaching patterns were quite different in the unfrozen soils with smoother breakthrough curves without distinct early concentration peaks, especially evident in the loam soil (Fig. 5). Data for the other columns show the same pattern (see Appendix A).

The calculated 5% arrival volumes support the results shown above, with smaller values found for the frozen soils than unfrozen soils (Table 3). However, statistically significant differences between frozen and unfrozen columns were only found for the silt topsoil ($p < .001$). Furthermore, a statistically significant difference was found between unfrozen silt and loam columns for both topsoil and subsoil ($p < .01$), which confirms that preferential flow was generally stronger in the loam soil.

3.5. MCPA leaching

In contrast to water and bromide, significantly more MCPA leached from frozen topsoil and subsoil loam columns than from the unfrozen soils ($p < .001$, Table 3). Similar results were found for the silt topsoil, where the mean amount of MCPA leached from frozen columns was significantly larger ($p < .01$) than from the unfrozen columns. For the unfrozen silt soil, MCPA leaching was significantly larger ($p < .05$) from the subsoil than from the topsoil (Table 3).

In the frozen loam columns, the shapes of the breakthrough curves for MCPA were strikingly similar to those of bromide with peak concentrations of MCPA of ca. 2 to 3 mg L^{-1} measured in leachate by the end of the first irrigation (Fig. 5). MCPA concentrations also peaked early in the unfrozen loam columns (peaks hidden because of the scale of the plots), but the concentrations were much smaller and significantly less MCPA leached from unfrozen columns during the experiment (Fig. 5, Table 3). MCPA breakthrough curves for all loam columns are collected in Appendix A (Fig. A2).

Similar to the loam soil, most of the frozen silt topsoil columns showed early concentration peaks for MCPA, although the measured concentrations in the percolate were much smaller and the pattern was less clear than for the loam (Fig. 6, Fig. A4 in Appendix A). MCPA concentrations in leachate from the unfrozen silt topsoil columns were much smaller than for the frozen columns (Fig. 6) and hardly any MCPA leached from these columns (Table 3). Leaching losses of MCPA were similar for frozen and unfrozen silt subsoil (Table 3). The breakthrough curves of the frozen silt subsoil columns peaked at different irrigations (Fig. A 4 in Appendix A), but four of the unfrozen silt subsoil columns showed a pattern closer to the one observed for bromide leaching, i.e. smoother breakthrough curves without clear concentration peaks. One of the unfrozen silt subsoil columns differed from the others though, by showing an early concentration peak (Fig. 6). MCPA breakthrough curves for all silt columns are collected in Appendix A (Fig. A4).

A general observation made for many of the columns was the smaller concentrations of MCPA and bromide in the first sample after the start of a new irrigation. This applied especially to bromide (Fig. 5) but was also observed for MCPA (Fig. 6).

The metabolite 2-MCP was detected in some of the bulk samples

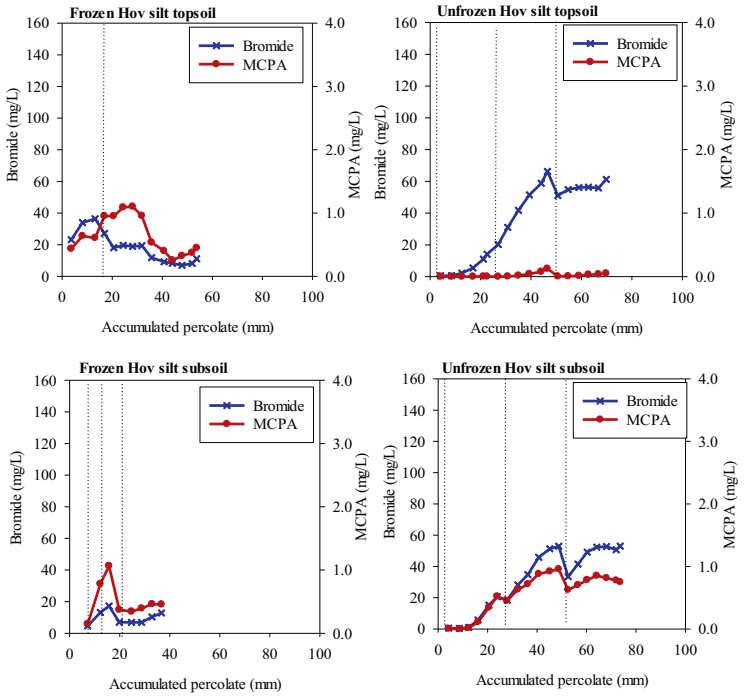

Fig. 6. Bromide and MCPA (mg L^{-1}) concentrations plotted as a function of accumulated amount of percolate (mm) for a representative soil column from from frozen and unfrozen topsoil and subsoil of Kroer loam and Hov silt. Dotted lines indicate the first sampling of leachate after the onset of a new irrigation.

from both frozen and unfrozen soil columns, both from loam and silt soils. In leachate from frozen Kroer loam topsoil columns, 2-MCP was only detected in the samples from the last irrigation at concentrations of about 0.3 µg L^{-1}. The metabolite was not detected in leachate from unfrozen loam topsoil or frozen loam subsoil. In unfrozen loam subsoil the metabolite was found in all samples from three columns at concentrations between 0.04 and 0.49 µg L^{-1} (mean 0.16 µg L^{-1}). The maximum amounts detected of the metabolite was in unfrozen Kroer loam subsoil and equalled to about 0.02% of the applied amount of MCPA. The metabolite was not detected in leachate samples from the Hov silt soil.

4. Discussion

4.1. Freeze-thaw effects on water flow and tracer transport

The observed differences in leaching patterns for bromide between frozen and unfrozen columns suggest that preferential flow through continuous macropores occurred largely in the frozen soils. The calculated lower 5% arrival volumes for frozen columns also support this conclusion (Table 3). Contrary to this, the bromide breakthrough curves from the unfrozen columns indicate a slower and more uniform advective-dispersive transport process through the whole soil matrix. The bromide breakthrough curves follow the same pattern in many of the frozen columns (Figs. 5, 6 and Appendix A), with large concentrations peaking after relatively small amounts of water had percolated through the columns followed by tailing to smaller concentrations. This applied to both loam and silt soils, although the silt did not show the same clear preferential flow pattern as the loam, especially in the subsoil, presumably because it was limited by the lack of continuity of the macropore network (Fig. 1 and Jarvis et al. (2016)). However, even for the silt soil, the 5% arrival volumes indicated stronger preferential flow for frozen soils than unfrozen soils (Table 3). The differences observed in 5% arrival volume were only statistically significant in topsoil, although the breakthrough curves indicated the same tendency for both soils.

Smaller concentrations of bromide were detected in the first percolate samples after the onset of a new irrigation than in the final samples of the previous irrigation. This could be partly explained by the fact that as soil water freezes, solutes may become concentrated in the unfrozen water in the smaller pores and as temperatures increase again, solutes may only slowly diffuse back into the mobile water in larger pores (Stähli and Stadler, 1997; Ireson et al., 2013). Thus, when the soil thaws again, the first water draining from the macropores may be relatively clean (Larsson et al., 1999).

In general, the transport patterns indicating preferential flow through macropores occurred during the earliest irrigations, when the macropores presumably were still air-filled. Later, when more water had been applied, the larger pores also became blocked by ice, resulting in reduced hydraulic conductivity and slower thawing (Ireson et al., 2013; Moghadas et al., 2016). The ponding observed on top of many columns at the initial stages of the later irrigations supports this assumption. For the frozen loam soil, ponding was first observed during the second irrigation, but some of the silt columns exhibited ponding already during the first irrigation. Hence, water content is important for how fast the thawing process occurs. In addition to the ponding, this was observed as the frozen columns both started to thaw (Fig. 2) and drain (Figs. 2-3) later at later irrigations in this experiment. These

observations were more evident for the silt than the loam. This could be explained by less pore space being available for infiltration of water and that infiltration was so slow that the increased exposure to ice caused its freezing on the way down (Moghadas et al., 2016). This could also be the reason why it took so long for the water to infiltrate the silt subsoil during and after the last irrigation (Fig. 4).

When the frozen soil columns started to thaw during the irrigations, the ponded water infiltrated quickly and percolated through the columns. After thawing, 25 mL samples were collected at ca. 6–7 min intervals, equivalent to flow rates of ca. 35 mm $h^{-}1$ being a lot faster than the fastest flow rates observed for unfrozen columns (ca. 7 mm h^{-1}). This fast infiltration was not observed for silt subsoil, being in line with the estimations of relatively high 5% arrival volume values (Table 3), indicating a little degree of preferential flow, and the smaller content of connected macropores in this soil (Fig. 1).

In addition to the different leaching patterns observed for bromide between the two treatments, significantly less amounts of bromide leached from frozen columns compared to unfrozen columns (Table 3). Brown et al. (2000) discussed that preferential flow rapidly can transport small amounts of bromide to depth, but that over a longer leaching period, preferential flow will give smaller total losses of bromide than matrix flow. This is because preferential flow interacts with only a small part of the soil and associated solute. In our case the difference observed in bromide leaching could also be due to the fact that significantly less water was collected from the frozen soil columns than the unfrozen columns. As the frozen columns thawed, one would not expect any difference in the total amount of water percolating. There were indications that the frozen columns had not finished draining after the cessation of irrigation, as a loss of water from the columns was observed while moving them before transportation between the freezing facilities and the lysimeter laboratory. Furthermore, ice was observed under the frozen columns in the freezing cabinet. Continued sampling beyond 24 h after the start of irrigation would have been desirable to sample more water from the frozen columns, but due to time constraints, this was not possible.

4.2. Freeze-thaw effects on MCPA leaching

Brown et al. (2000) argues that preferential flow seems to be the most important process for pesticide transport and that residues can be transported rapidly to deeper soil layers, while slower leaching via matrix flow not will result in larger losses over time because degradation or sorption might reduce the amounts that could leach. In this study, very little MCPA leached through the unfrozen loam and silt topsoil columns and it is possible that this could be due to faster degradation in these columns, which were maintained at higher temperatures (+4 °C compared with −3 °C). The amount of MCPA retained in the soil was not measured, so the extent of degradation (and thus a complete mass balance) cannot be determined with certainty. However, the metabolite 2-MCP was detected in low amounts in some bulk leachate samples, both from frozen Kroer loam topsoil and unfrozen Kroer loam subsoil implying that some degradation did occur during the experiment. This could be due to aerobic soil degradation or more probable, due to aqueous photolysis during sampling and sample preparation since 2-MCP is a major aqueous photolysis metabolite. It is highly unlikely though that differences in degradation rates between frozen and unfrozen columns could explain the large differences observed in the leached amounts of MCPA.

The markedly larger leaching losses of MCPA from frozen topsoil columns was therefore most probably a result of much weaker sorption during transport. Sorption has been shown to be a temperature dependent process and for most compounds sorption decreases with increasing temperature (Ten Hulscher and Cornelissen, 1996; Shariff and Shareef, 2011). It could then be hypothesized that sorption would be stronger at lower temperatures. Stenrød et al. (2008) on the other hand found smaller K_d values and increased pore water concentrations for metribuzin upon release of frost in packed columns stored at −5 °C indicating that this might not always be the case. Nevertheless, the effect of freezing on the water flow pathways is probably the most important reason for the differences observed in our experiment. Due to the fast transport through macropores, the time for adsorption of MCPA would be limited in the frozen soil columns, where flow would have been mostly restricted to the larger pores that were either initially air-filled or which drained quickly on thawing. In addition, compared to smaller pores, macropores have a small ratio of surface area to pore volume, reducing the number of available binding sites for passing solutes (Jarvis, 2007). In contrast, in the unfrozen soil with a slower and more uniform flow pattern, MCPA, although a relatively mobile substance, would be exposed to more soil surfaces and binding sites resulting in a higher degree of sorption and less MCPA being transported through the columns.

Freezing of soil can lead to frost heave, formation of ice lenses and subsequent cracking of the soil and hence an increased hydraulic conductivity (Hotineanu et al., 2015). In our case, this could have explained some of the differences observed between frozen and unfrozen columns with regards to MCPA leaching. However, less water percolated through the frozen soil columns and less bromide leached, so this was probably not a major factor. The fact that the results were quite consistent across all columns supports this conclusion. The similarity between the replicatet columns and consistent differences between the treatments also indicates that bypass of water along the side column walls was a minor problem.

Compared with the unfrozen topsoil columns, considerably more MCPA leached through the unfrozen subsoil columns (Table 3) This could have been due to significantly weaker sorption in subsoils because of smaller organic carbon contents (Hiller et al., 2010). Slower degradation in the subsoil columns during the experiment may also have been a contributing factor.

5. Conclusions

This study documents the preferential transport of MCPA and a bromide tracer through soil macropores at relatively high concentrations in partially frozen soil. Very little MCPA leached from unfrozen columns, while for bromide a more uniform advective-dispersive transport process was found. To our knowledge, these contrasting solute transport processes in frozen and unfrozen soil columns have not previously been documented experimentally.This study therefor contributes to filling an important knowledge gap. The experiment was carried out under high flow conditions in the laboratory. Nevertheless, the data collected in this study should prove useful for testing models of water flow and solute transport in partially frozen and structured soil. Our findings, together with those from other studies (Eklo et al., 1994; French, 1999; Riise et al., 2004; Riise et al., 2006; Ulén et al., 2013), also suggest that monitoring programs in climates where soil freezing is common should include sampling during snowmelt or rainfall in early spring.

Acknowledgements

This work is a part of the BIONÆR project: Innovative approaches and technologies for Integrated Pest Management (IPM) to increase sustainable food production (Smartcrop) funded by The Research Council of Norway (project no.: 244526/E50). We are grateful for the help given by Randi Bolli on the set up of the expermient and for helpful discussion of the results. I would also like to thank Jens Kværner for valuble comments during the writing process.

Appendix A

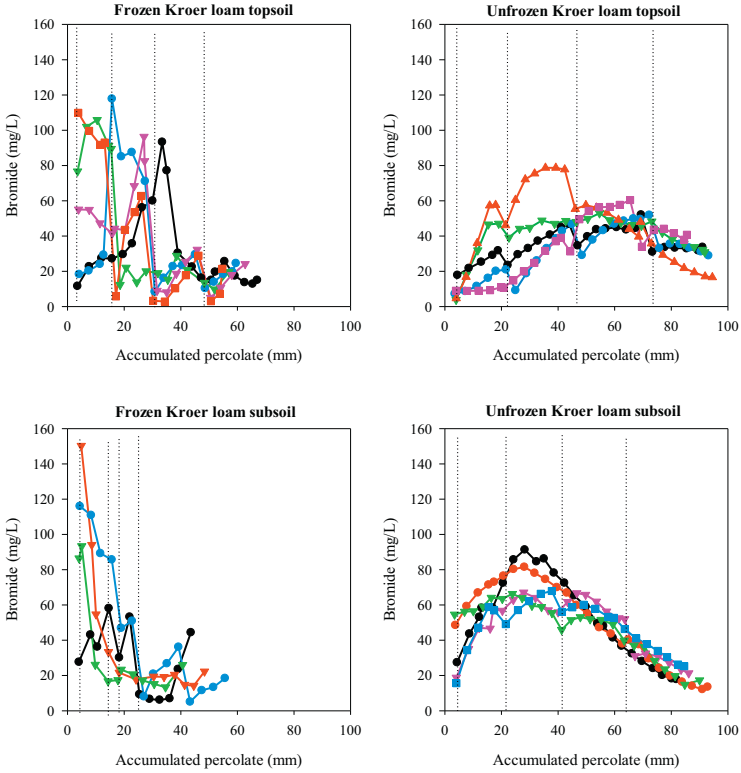

Fig. A1. Bromide (mg L^{-1}) concentrations plotted as a function of accumulated amount of percolate (mm) for all soil columns from the Kroer loam soil. Dotted lines indicate the first sampling of leachate after the start of a new irrigation. For frozen loam subsoil one of the five columns was excluded due to leakages through thermistor holes.

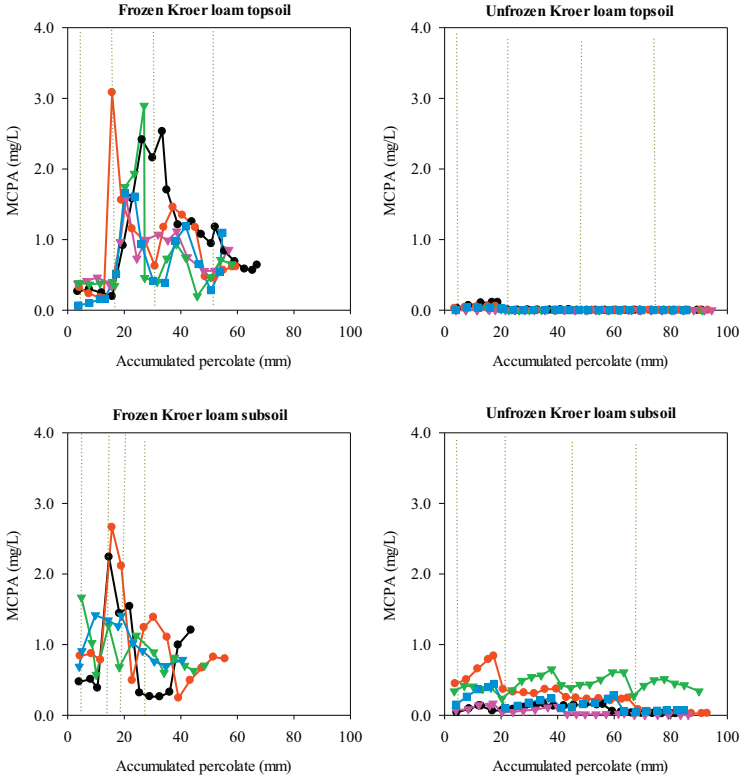

Fig. A2. MCPA ($\mu g\,L^{-1}$) concentrations plotted as a function of accumulated amount of percolate (mm) for all soil columns from the Kroer loam soil. Dotted lines indicate the first sampling of leachate after the start of a new irrigation. For frozen loam subsoil one of the five columns was excluded due to leakages through thermistor holes.

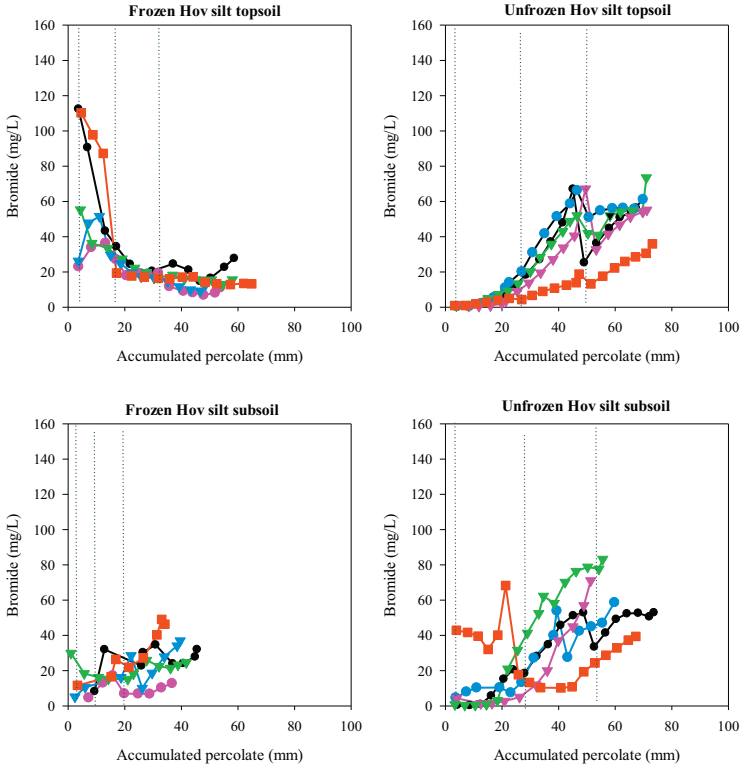

Fig. A3. Bromide (mg L^{-1}) concentrations plotted as a function of accumulated amount of percolate (mm) for all soil columns from the Hov silt soil. Dotted lines indicate the first sampling of leachate after the onset of a new irrigation.

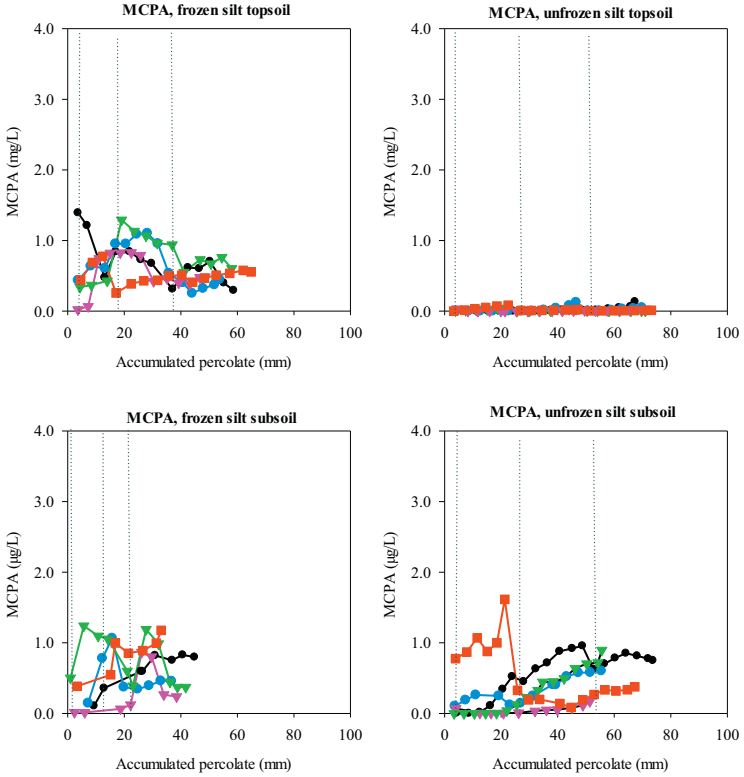

Fig. A4. MCPA (µg L^{-1}) concentrations plotted as a function of accumulated amount of percolate (mm) for all soil columns from frozen silt soil. Dotted lines indicate the first sampling of leachate after the onset of a new irrigation.

Appendix B

The reconstructed images were first corrected for the alignment to ensure that the z-axis of the soil column in the images was vertical, using the 'Untilt Stack' plugin (Cooper, 2015). Differences in illumination were observed along the z-axis of the image stack resulting possibly from the slight changes in the X-ray beam cone with scanning time. A pixel-based mathematical operation was performed for illumination correction using the mean grey value of all pixels in the 3-D image and the mean grey value of the slice containing the pixel for illumination correction. Noise in the image and poor contrast between the background and the feature of interest often interfere with the segmentation process. A 3-D median filter with a radius of 2 voxels was used for reducing the noise. The contrast between the background soil matrix and pore features was improved by normalizing the image histogram using the 'enhance contrast' algorithm (saturated pixels = 0.4%) in ImageJ. The 3-D image was cropped on the sides using a circular section to exclude the column wall, and on the top and bottom to remove the uneven and/or smeared soil surface. Segmentation of the pore features was performed using the local adaptive thresholding method of Phansalkar et al. (2011). Briefly explained, the algorithm calculates threshold value for each pixel in a slice based on the mean and standard deviation of the grey values of the neighboring pixels within a circular window specified by the user. A pixel is classified as a pore if its grey value is smaller than the calculated threshold value for that pixel. Isolated features with one pixel width in the segmented images were removed by performing an erosion operation

The segmented images were analysed for quantification of macropore properties using the 'Particle Analyzer' plugin within the 'BoneJ' plugin in ImageJ (Doube et al., 2010). The plugin labels the individual pores (set of pore voxels connected to form one cluster) and returns the measurements of various properties, selected by the user, of the labelled pores. Total macroporosity ($mm^3\ mm^{-3}$) was calculated as the volume of macropores per unit volume of soil. Macroporosity of those pores connected throughout the soil depth were referred to as connected macroporosity ($mm^3\ mm^{-3}$). The average pore thickness (mm) was calculated as the volume weighted average of the thickness of all the macropores in the analysed images.

Table A1
Cation distribution of Kroer loam and Hov silt. Data for the Kroer loam soil has been reported in Greve et al. (1998). The Hov silt has been characterized by the Division of Survey and Statistics at NIBIO according to the World Reference Base for Soil Resources, WRB (IUSS Working Group WRB, 2014).

Site	Horizon, cm depth	cmol kg^{-1}					CEC	Base sat.
		H^+	Ca	Mg	K	Na		(%)
Kroer	Ap, 0–23	4.8	7.14	0.66	0.61	0.04	13.25	64
	Eg, 23–40	2.9	3.04	0.96	0.47	0.04	7.41	61
Hov	Ap, 0–20	3.5	2.43	0.32	0.33	0.058	6.64	47
	Bw, 28–50	2.0	0.87	0.12	0.27	0.051	3.31	40

References

Barnes, D.L., Wolfe, S.M., 2008. Influence of ice on the infiltration of petroleum into frozen coarse-grained soil. Pet. Sci. Technol. 26, 856–867. https://doi.org/10.1080/10916460701824508.

Beven, K., Germann, P., 1982. Macropores and water flow in soils. Water Resour. Res. 18, 1311–1325. https://doi.org/10.1029/WR018i005p01311.

Brown, C.D., Hollis, J.M., Bettinson, R.J., Walker, A., 2000. Leaching of pesticides and a bromide tracer through lysimeters from five contrasting soils. Pest Manag. Sci. 56, 83–93. https://doi.org/10.1002/(SICI)1526-4998(200001)56:1<83::AID-PS98>3.0.CO;2-8.

Cooper, J., 2015. Untilt Stack. https://imagej.nih.gov/ij/plugins/untilt-stack/index.html.

Doube, M., Kłosowski, M.M., Arganda-Carreras, I., Cordelières, F.P., Dougherty, R.P., Jackson, J.S., Schmid, B., Hutchinson, J.R., Shefelbine, S.J., 2010. BoneJ: Free and extensible bone image analysis in ImageJ. Bone 47, 1076–1079. https://doi.org/10.1016/j.bone.2010.08.023.

Eklo, O.M., Aspmo, R., Lode, O., 1994. Runoff and leaching experiments of dichlorprop, MCPA, propiconazole, dimethoate and chlorosulfuron in outdorr lysimeters and filed catchment areas. Nor. J. Agric. Sci. 13, 7–212.

Flury, M., 1996. Experimental evidence of Transport of Pesticides through Field Soils—a Review. J. Environ. Qual. 25, 25–45. https://doi.org/10.2134/jeq1996.00472425002500010005x.

French, H.K., 1999. Transport *and degradation of deicing chemicals in a heterogenous unsaturated soil*. Doctor Scientiarum Thesis. Agricultural University of Norway ISBN: 8257503940.

Gentry, L.E., David, M.B., Smith-Starks, K.M., Kovacic, D.A., 2000. Nitrogen fertilizer and herbicide transport from tile drained fields. J. Environ. Qual. 29, 232–240. https://doi.org/10.2134/jeq2000.00472425002900010030x.

Greve, M., Helweg, A., Yli-Halla, M., Eklo, O.M., Nyborg, Å.A., Solbakken, E., Öborn, I., Stenström, J., 1998. Nordic Reference Soils. Nordic Council of Ministers 537.

Hafsteinsdóttir, E.G., White, D.A., Gore, D.B., 2013. Effects of freeze–thaw cycling on metal-phosphate formation and stability in single and multi-metal systems. Environ. Pollut. 175, 168–177. https://doi.org/10.1016/j.envpol.2013.01.007.

Hanssen-Bauer, I., Førland, E., Haddeland, I., Hisdal, H., Mayer, S., Nesje, A., Nilsen, J., Sandven, S., Sandø, A., Sorteberg, A., 2015. Klima i Norge 2100. NCCS report, Oslo, Norway. 2. pp. 1–203 (ISSN: 2387-3027).

Hayashi, M., 2013. The cold vadose zone: hydrological and ecological significance of frozen-soil processes. Vadose Zone J. 12. https://doi.org/10.2136/vzj2013.03.0064.

Hiller, E., Cernansky, S., Zemanova, L., 2010. Sorption, degradation and leaching of the phenoxyacid herbicide MCPA in two agricultural soils. Pol. J. Environ. Stud. 19, 315–321.

Hotineanu, A., Bouasker, M., Aldaood, A., Al-Mukhtar, M., 2015. Effect of freeze–thaw cycling on the mechanical properties of lime-stabilized expansive clays. Cold Reg. Sci. Technol. 119, 151–157. https://doi.org/10.1016/j.coldregions.2015.08.008.

Ireson, A.M., Van Der Kamp, G., Ferguson, G., Nachshon, U., Weather, H.S., 2013. Hydrogeological processes in seasonally frozen northern latitudes: understanding, gaps and challenges. Hydrogeol. J. 53–66. https://doi.org/10.1007/s10040-012-0916-5.

IUSS WORKING GROUP WRB, 2014. World Reference Base for Soil Resources 2014. International soil classification system for naming soils and creating legends for soil maps. In: World Soil Resources Reports No.106. FAO, Rome.

Jarvis, N.J., 2007. A review of non-equilibrium water flow and solute transport in soil macropores: principles, controlling factors and consequences for water quality. Eur. J. Soil Sci. 58, 523–546. https://doi.org/10.1111/j.1365-2389.2007.00915.x.

Jarvis, N., Koestel, J., Larsbo, M., 2016. Understanding Preferential Flow in the Vadose Zone: recent advances and Future prospects. Vadose Zone J. 15. https://doi.org/10.2136/vzj2016.09.0075.

Jarvis, N., Larsbo, M., Koestel, J., 2017. Connectivity and percolation of structural pore networks in a cultivated silt loam soil quantified by X-ray tomography. Geoderma 287, 71–79. https://doi.org/10.1016/j.geoderma.2016.06.026.

Koestel, J.K., Moeys, J., Jarvis, N.J., 2011. Evaluation of nonparametric shape measures for solute breakthrough curves. Vadose Zone J. 10, 1261–1275. https://doi.org/10.2136/vzj2011.0010.

Larsbo, M., Sandin, M., Jarvis, N., Etana, A., Kreuger, J., 2016. Surface Runoff of Pesticides from a Clay Loam Field in Sweden. J. Environ. Qual. 45, 1367–1374.

Larsson, M.H., Jarvis, N., Torstensson, G., Kasteel, R., 1999. Quantifying the impact of preferential flow on solute transport to tile drains in a sandy field soil. J. Hydrol. 215 (18). https://doi.org/10.1016/S0022-1694(98)00265-0.

Lewis, K.A., Tzilivakis, J., Warner, D.J., Green, A., 2016. An international database for pesticide risk assessments and management. Human and Ecological Risk Assessment: An International Journal 22, 1050–1064. https://doi.org/10.1080/10807039.2015.1133242.

Löv, Å., Sjöstedt, C., Larsbo, M., Persson, I., Gustafsson, J.P., Cornelis, G., Kleja, D.B., 2017. Solubility and transport of Cr(III) in a historically contaminated soil – evidence of a rapidly reacting dimeric Cr(III) organic matter complex. Chemosphere 189, 709–716. https://doi.org/10.1016/j.chemosphere.2017.09.088.

Lundberg, A., Gustafsson, D., Stumpp, C., Kløve, B., Feiccabrino, J., 2016. Spatiotemporal variations in snow and soil frost—a review of measurement techniques. Hydrology 3, 28. https://doi.org/10.3390/hydrology3030028.

Luxmoore, R.J., Jardine, P.M., Wilson, G.V., Jones, J.R., Zelazny, L.W., 1990. Physical and chemical controls of preferred path flow through a forested hillslope. Geoderma 46, 139–154. https://doi.org/10.1016/0016-7061(90)90012-X.

Mellander, P.-E., Löfvenius, M.O., Laudon, H., 2007. Climate change impact on snow and soil temperature in boreal Scots pine stands. Clim. Chang. 85, 179–193. https://doi.org/10.1007/s10584-007-9254-3.

Moghadas, S., Gustafsson, A.M., Viklander, P., Marsalek, J., Viklander, M., 2016. Laboratory study of infiltration into two frozen engineered (sandy) soils recommended for bioretention. Hydrol. Process. 30, 1251–1264. https://doi.org/10.1002/hyp.10711.

Phansalkar, N., More, S., Sabale, A., Joshi, M., 2011. Adaptive local thresholding for detection of nuclei in diversity stained cytology images. In: International Conference on Communications and Signal Processing, 10–12 Feb. 2011 2011, pp. 218–220.

R CORE TEAM, 2016. R: A Language and Environment for statistical Computing. https://www.R-project.org.

Riise, G., Lundekvam, H., Wu, Q.L., Haugen, L.E., Mulder, J., 2004. Loss of Pesticides from Agricultural Fields in SE Norway – Runoff through Surface and Drainage Water. Environ. Geochem. Health 26, 269–276. https://doi.org/10.1023/B:EGAH.0000039590.84335.d6.

Riise, G., Lundekvam, H., Haugen, L.E., Mulder, J., 2006. Suspended sediments as carriers for the fungicide propiconazole in agricultural runoff. Verhandlungen des Internationalen Verein Limnologie 1296–1300. https://doi.org/10.1080/03680770.2005.11902891.

Schneider, C.A., Rasband, W.S., Eliceiri, K.W., 2012. NIH image to ImageJ: 25 years of image analysis. Nat Meth 9, 671–675. https://doi.org/10.1038/nmeth.2089.

Shariff, R.M., Shareef, K.M., 2011. Thermodynamic adsorption of herbicides on eight agricultural soils. Int. J. Sci. Eng. Res. 2.

Siimes, K., Rämö, S., Welling, L., Nikunen, U., Laitinen, P., 2006. Comparison of the behaviour of three herbicides in a field experiment under bare soil conditions. Agric. Water Manag. 84, 53–64. https://doi.org/10.1016/j.agwat.2006.01.007.

Stadler, D., Stähli, M., Aeby, P. & Flühler, H. 2000. Dye Tracing and Image Analysis for Quantifying Water Infiltration into Frozen Soils. 64, 505–516. DOI: https://doi.org/10.2136/sssaj2000.642505x.

Stähli, M., Stadler, D., 1997. Measurement of water and solute dynamics in freezing soil columns with time domain reflectometry. J. Hydrol. 352–369. https://doi.org/10.1016/S0022-1694(96)03227-1.

Stenrød, M., Perceval, J., Benoit, P., Almvik, M., Bolli, R.I., Eklo, O.M., Sveistrup, T.E., Kværner, J., 2008. Cold climatic conditions: Effects on bioavailability and leaching of the mobile pesticide metribuzin in a silt loam soil in Norway. Cold Reg. Sci. Technol. 53, 4–15. https://doi.org/10.1016/j.coldregions.2007.06.007.

Ten Hulscher, T.E.M., Cornelissen, G., 1996. Effect of temperature on sorption equilibrium and sorption kinetics of organic micropollutants - a review. Chemosphere 32, 609–626. https://doi.org/10.1016/0045-6535(95)00345-2.

Ulén, B.M., Larsbo, M., Kreuger, J.K., Svanbäck, A., 2013. Spatial variation in herbicide leaching from a marine clay soil via subsurface drains. Pest Manag. Sci. 70, 405–414. https://doi.org/10.1002/ps.3574.

Van Der Kamp, G., Hayashi, M., Gallén, D., 2003. Comparing the hydrology of grassed and cultivated catchments in the semi-arid Canadian prairies. Hydrol. Process. 559–575. https://doi.org/10.1002/hyp.1157.

Wang, F., Ouyang, W., Hao, F., Jiao, W., Shan, Y., Lin, C., 2016. Role of freeze-thaw cycles and chlorpyrifos insecticide use on diffuse Cd loss and sediment accumulation. Sci. Rep. 6, 1–10. https://doi.org/10.1038/srep27302.

Wei, M.-L., Du, Y.-J., Reddy, K.R., Wu, H.-L., 2015. Effects of freeze-thaw on characteristics of new KMP binder stabilized Zn- and Pb-contaminated soils. Environ. Sci. Pollut. Res. 22, 19473–19484. https://doi.org/10.1007/s11356-015-5133-z.

Paper II

Leaching of five pesticides of contrasting mobility through frozen and unfrozen soil

Roger Holten[a,b,*], Mats Larsbo[c], Nicholas Jarvis[c], Marianne Stenrød[a], Marit Almvik[a], Ole Martin Eklo[a, b]

[a] Norwegian Institute of Bioeconomy Research (NIBIO), Division of Biotechnology and Plant Health, Department of Pesticides and Natural Products Chemistry, P.O. Box 115, NO-1431 Ås, Norway.

E-mail addresses: roger.holten@nibio.no, marianne.stenrod@nibio.no, marit.almvik@nibio.no, olemartin.eklo@nibio.no

[b] Norwegian University of Life Sciences, Faculty of Biosciences, Department of Plant Sciences, P.O. Box 5003, N-1432 Ås, Norway.

[c] Swedish Agricultural University, Department of Soil and Environment, P.O. Box 7014 75007 Uppsala, Sweden. *E-mail addresses:* mats.larsbo@slu.se, nicholas.jarvis@slu.se

*Corresponding Author.

Abstract

Field and laboratory studies show increased leaching of pesticides through macropores in frozen soil. Fast macropore flow has been shown to reduce the influence of pesticide properties on leaching, but data on these processes are scarce. The objective of this study was to investigate the effect of soil freezing and thawing on transport of pesticides with a range of soil sorption coefficients (K_f). To do this we conducted a soil column study to quantify the transport of bromide and five pesticides (MCPA, clomazone, boscalid, propiconazole and diflufenican). Intact topsoil and subsoil columns from two agricultural soils (silt and loam) in South-East Norway were used in this experiment and pesticides were applied to the soil surface in all columns. Half the columns were then frozen (-3 °C) while the other half were left unfrozen (+4 °C). Columns were subjected to repeated irrigation events where 25 mm rainwater were applied during 5 hours at each event. Irrigations were followed by 14-day periods of freezing or refrigeration. Percolate was collected and analysed for pesticides and bromide. Pesticide leaching was up to five orders of magnitude larger from frozen than unfrozen columns. Early breakthrough (<< 1 pore volume) of high concentrations were observed for pesticides in frozen columns indicating that leaching was dominated by preferential flow. The rank order in pesticide leaching observed in this study corresponded to the rank order of mean K_f values for the pesticides and the results suggests that sorption plays a role in determining leaching losses even in frozen soil.

Key words: Freeze-thaw effects, Preferential flow, Macropores, Pesticide leaching,

Sorption

1. Introduction

There is evidence that pesticides can leach through partially frozen soil during winter and early spring. Several field studies have shown large pesticide concentrations in leachate and drain water during freeze/thaw periods in Norway, Finland and Sweden (Riise et al., 2004, Riise et al., 2006, Siimes et al., 2006, Ulén et al., 2013). Preferential flow is a non-equilibrium process (Jarvis et al., 2016), which is frequently triggered in soils containing large vertically continuous structural pores, termed macropores generally having diameters of c. 0.3 mm and larger (Beven and Germann, 1982, Jarvis, 2007). This includes biopores made by earthworms and plant roots and planar fissures caused by freeze/thaw and desiccation. Macropore flow can lead to increased leaching of pesticides to deeper soil layers or drainage systems and consequently result in higher concentrations of pesticides in groundwater or surface water (Jarvis, 2007, Flury, 1996, Kjær et al., 2011). Compared with a slower and more uniform advective-dispersive transport process through the soil matrix, fast flow through macropores also reduces the influence of pesticide properties (e.g. degradation and sorption constants) on leaching (Larsson and Jarvis, 2000, Jarvis, 2007, McGrath et al., 2009). There is also some evidence that preferential flow may have a relatively larger effect on compounds that sorb moderately to soil than either more mobile or more strongly adsorbing compounds (McGrath et al., 2009).

Although soil freezing and thawing have been shown to influence the transport of solutes through soil, these processes are complex and their effects on the fate and behaviour of pesticides are not well understood (Hayashi, 2013, Ireson et al., 2013). In a soil column study that generated high resolution data of leached concentrations during artificial irrigation events, it was found that the non-reactive tracer bromide and the mobile herbicide MCPA were transported in large concentrations through macropores in partially frozen soil (Holten et al., 2018). The study showed that significantly more MCPA leached from frozen than unfrozen columns and that very little MCPA leached from unfrozen columns. The leaching patterns of

bromide and MCPA were very consistent in frozen columns. A non-uniform pattern with concentrations peaking in the early leachate samples after the start of the first or second irrigation and decreasing concentrations later indicated preferential flow in open and connected macropores in the early stages of the experiment. Macropores are often air-filled when the soil first freezes (van der Kamp et al., 2003) and can hence have high infiltration capacities when the matrix is frozen. In unfrozen columns, the leaching pattern of bromide was much more uniform with no distinct concentration peaks in the leachate, suggesting a slower advective-dispersive transport process through the soil matrix. In the same experiment, the leaching of the pesticides clomazone, boscalid, propiconazole and diflufenican were also measured. In contrast to the high resolution data reported for MCPA (Holten et al., 2018) with 25 mL subsamples of leachate analysed during the course of several consecutive irrigation events, these pesticides were analysed in bulk leachate samples each representing one irrigation event. The effect of freezing and thawing on the transport of pesticides with different sorption properties has to our knowledge not been investigated before. In this paper we report the results from the analysis of the bulk leachate samples from the experiment described in Holten et al. (2018). We hypothesize that leaching of pesticides in general will be larger from frozen soil columns with open and connected macropores compared to unfrozen columns and that the effects of freezing on leaching will be largest for moderately sorbing compounds.

2. Materials and methods

2.1 Soil sampling and characterization

Intact soil columns were sampled in mid- to late May 2016 from two agricultural fields with different soil types in South-East Norway (Kroer, 59° 38′ 37″ N 10° 49′ 58″ E; Hov 60° 12′ 45″ N 12° 1′ 58″ E) using aluminium cylinders (i.d. 9.2 cm, height 20 cm). Fifty-six columns were sampled, 14 from both the topsoil (0-20 cm) and subsoil (20-40 cm) at each site. The

cylinders were forced into the soil using a sledgehammer and dug out by hand, and stored at ca. +4 °C. At the time of sampling the fields were under winter wheat. According to the farmers at Kroer and Hov, none of the pesticides included in our study had been applied during the last 2-3 years prior to sampling.

The Kroer loam has been characterized earlier (Greve et al., 1998), so no additional characterization was performed in this study. A simple soil characterization of the Hov silt was carried out at the Division of Survey and Statistics at NIBIO. Soil characteristics are summarized in Table 1. This characterization was done according to the World Reference Base for Soil Resources, WRB (IUSS Working Group WRB, 2014).

The water content of the soils was neither measured at sampling nor in the laboratory before the experiment started. This was to avoid disturbing the intact soil columns.

Table 1. Selected characteristics of the studied soils.

Site	Classification†	Horizon, cm depth	Soil texture‡	Clay (%)	Silt (%)	Sand (%)	Tot. C (%)	pH (H_2O)
Kroer	Retic Stagnosol	Ap, 0-23	Loam	19.1	43.8	37.1	2.5	5.5
		Eg, 23-40	Silt loam	20.5	63.0	16.7	0.5	5.6
Hov	Dystric Fluvic Cambisol	Ap, 0-20	Silt	5.4	83.8	10.8	1.2	5.4
		Bw, 28-50	Silt	4.1	86.7	9.2	0.3	6.2

†WRB 2014, ‡USDA Soil Texture Calculator

2.2 Chemicals

The pesticides MCPA (2-methyl-4-chlorophenoxyacetic acid, purity 99.5 %), clomazone (2-(2-chlorobenzyl)-4,4-dimethyl-1,2-oxazolidin-3-one, purity 97.5 %), boscalid (2-chloro-N-(4'-chlorobiphenyl-2-yl)nicotinamide, purity 98.4 %) and propiconazole ((2RS,4RS;2RS,4SR)-1-[2-(2,4-dichlorophenyl)-4-propyl-1,3-dioxolan-2-ylmethyl]-1H-1,2,4-triazole, purity 98 %) were all supplied from Dr. Ehrenstorfer GmbH, whereas diflufenican (2',4'-difluoro-2-(α,α,α-trifluoro-m-tolyloxy)nicotinanilide purity > 99 %) was supplied from Chiron AS. Two diflufenican metabolites were also included in the analyses, AE 0542291 (2-[3-

(trifluoromethyl)phenoxy]pyridine-3-carboxamide, purity 99 %) and AE B107137 (2-[3-(trifluoromethyl)phenoxy]pyridine-3-carboxylic acid, purity 98 %), both supplied by Bayer CropScience. In addition, the MCPA metabolite 2-MCP (2-methyl-4-chlorophenol, Sigma, purity 96.0 %) was included. A mix of the five pesticides was prepared at concentrations of 282.6 (MCPA), 7.1 (clomazone), 41.9 (boscalid), 19.6 (propiconazole) and 18.8 (diflufenican) mg L^{-1} in acetone (VWR Chemicals, purity 99.7 %). These concentrations resulted in agricultural relevant application rates. Ranges and mean values of degradation half-lives (DT_{50}) and soil sorption coefficients (K_f) for the studied pesticides are summarized in Table 2. The pesticides cover a wide range of degradation and sorption properties; from mobile and non-persistent (MCPA) to slightly mobile and persistent (diflufenican).

A solution of artificial rainwater (Löv et al., 2017) was prepared (0.58 mg L^{-1} NaCl, 0.70 mg L^{-1} $(NH_4)_2SO_4$, 0.50 mg L^{-1} $NaNO_3$, 0.57 mg L^{-1} $CaCl_2$) and acidified with HCl (0.95 mL L^{-1} 37 %) to a pH of about 5. The rainwater was stored at about +4 °C in 20 L plastic containers.

Table 2: Ranges of sorption coefficients (K_f) and laboratory degradation half-lives (DT_{50}) for MCPA, clomazone, boscalid, propiconazole and diflufenican. Values in brackets are mean values.

Compound	K_f, mL g^{-1} (mean)	DT_{50}, 20 °C, days (mean)
MCPA	0.05-1.99¶ (0.94)	7-41† (24)
Clomazone	1.54-7.13¶ (4.33)	27-168‡ (68)
Boscalid	3.3-27.8¶ (12.6)	108-384§ (232)
Propiconazole	1.20-59¶ (15)	27-115¶ (72)
Diflufenican	13.5-48.9¶ (31.2)	44-238# (128)

† European Commission, Review Report for the active substance MCPA, 15 April 2005 (SANCO/4062/2001-final 11 July 2008).

‡ EFSA Scientific report (2007) 109, 1-73, Conclusion on the peer review of clomazone.

§ European Commission, Review Report for the active substance boscalid (SANCO/3919/2007-rev. 5 21 January 2008).

¶ Pesticide Properties Database (PPDB), 20 September 2018 (https://sitem.herts.ac.uk/aeru/ppdb/en/index.htm).

EFSA Scientific Report (2007) 122, 1-84, Conclusion on the peer review of diflufenican.

2.3 Experimental set up and sampling

Twenty of the sampled soil columns from each of the sites Kroer and Hov, in total 40 columns, were included in the experiment. To ensure uniform initial conditions, the columns were placed in a box of water letting them absorb water until they were close to saturation. They were then placed on a sand box (Eikjelkamp) at -30 cm pressure potential at the bottom to ensure that macropores were initially air-filled.

Five columns were randomly chosen from each soil type and depth for the freezing treatment. Likewise, five columns were chosen from each soil type and depth for the non-freezing treatment. More details on the preparation and selection of columns can be found in Holten et al. (2018). Thermistors were installed horizontally into the middle of the columns at 7 and 14 cm depth from the soil surface in the columns that were subjected to freezing and temperature was logged every 10 minutes throughout the experiment. The columns were insulated both at the bottom and around the column walls to ensure freezing from the top and downwards (Fig. 1).

Fig. 1: Insulated soil columns in a Weiss freezing cabinet. The columns were placed on a polystyrene board. Thermistors were installed at two depths.

Five mL of the pesticide solution was applied as evenly as possible across the surface of each of the columns using a 5 mL pipette, giving rates of 2.1, 0.05, 0.32, 0.15 and 0.14 kg ha^{-1} of

MCPA, clomazone, boscalid, propiconazole and diflufenican respectively. The insulated columns in the freezing treatment were placed in a 1 m^3 freezing cabinet at -3 °C, while the unfrozen columns were kept at ca +4 °C in a refrigerated room. Plastic lids were put on top of all the columns to reduce evaporation. The columns were incubated at these temperatures for about four weeks. They were then subjected to repeated irrigation events in a separate room with the prepared artificial rainwater, followed by 14-day periods of freezing (or refrigeration for the unfrozen columns) between irrigations. The experiment lasted for a total of 8 weeks for the silt soil (3 irrigations) and 10 weeks for the loam (4 irrigations).The columns were transported to the irrigation room in the morning of each irrigation event. The irrigation room and the artificial rain water was at temperatures of about 5-8 °C and 2-4 °C at the start of the irrigation respectively. Temperatures increased to ca. 12 and 6 °C in the room and water respectively during the day as it was difficult to obtain completely stable temperatures when working in the room. A temperature of -3 °C was chosen for the freezing cabinet as it was considered low enough to ensure that any water present in macropores after the irrigations would be frozen.

As described in Holten et al. (2018), the column setup allowed free drainage at the base of the soil columns. Irrigation water was distributed on the top of the columns using peristaltic pumps (Autoclude model VL) adjusted to give a rate of 5 mm hr^{-1} for 5 hours, resulting in a total of about 25 mm of rainwater to each column per irrigation event. Water was dripped onto filter paper placed on the surface of the columns to ensure that it was distributed as uniformly as possible. The actual irrigation rates varied somewhat between columns but there were no systematic differences between treatments, soils or depths. Rough calculations suggested that the total amount of irrigation water supplied to the columns during the experiment would be equivalent to ca. one pore volume (Holten et al., 2018).

Leachate from the soil columns was sampled in polycarbonate bottles (Corning®, VWR) at approximately every 25 mL (as reported in Holten et al. (2018) and stored frozen (-20°C) in amber 60 mL glass bottles for later analysis. All subsamples were combined to one single bulk sample per irrigation for each column for further pesticide analysis (total volumes from 20 to 140 mL).

2.4 Pesticide analysis

The bulk water samples were preconcentrated and analysed for the content of clomazone, boscalid, propiconazole, diflufenican and the diflufenican metabolites AE 0542291 and AE B107137. The MCPA metabolite 2-MCP was also analysed for in selected leachate samples. The contribution from any particle-bound pesticides was not generally measured throughout the experiment, but a preliminary test was performed to analyse potential residues on leached particles.

Each bulk leachate sample was preconcentrated using solid phase extraction sorbents. In short, the water samples were thawed and centrifuged (5000 rpm, 15 min.) in Teflon tubes to remove particles, and then internal standards (propiconazole-d_5, Dr. Ehrenstorfer GmbH purity 99.4 %, and diflufenican-d_3, Chiron AS purity 98 %, 10 µL of a 1 µg mL^{-1} mix) was added to each water sample. The samples were passed through preconditioned Oasis HLB columns (Waters, USA. Sorbent mass 60 mg). 2-mL water was added to wash the sorbent and then the analytes were eluted from the sorbent with 2-mL acetone. The eluate was evaporated to dryness under a stream of nitrogen and dissolved in 1-mL acetone. Samples were filtrated with RC 0.45 µm syringe filters (Phenomenex, regenerated cellulose membrane) into LC vials. The concentration of internal standards corresponded to 10 ng mL^{-1} in the final extracts. Blank and control samples was prepared from MilliQ-deionized water and preconcentrated simultaneously with each batch of samples. Control samples were spiked with 5 µL of a 1 µg mL^{-1} acetone mix of all the

analytes, giving a concentration of 5 ng mL^{-1} in the final extract. The recovery of the analytes with this extraction method was 79-116 %, as measured from eight control samples.

Pesticide analyses was performed by LC-MS/MS (Waters Alliance 2695 LC-system coupled to a Quattro Ultima Pt triple quadropole mass spectrometer from Micromass, Manchester, UK). A sample volume of 5 µl was injected and the analytes were separated on a Phenomenex Gemini C18 column (100x2 mm, particle diameter 3 µm) with 5 mM formic acid (A) og methanol (B) as mobile phase.

The analytes were detected in the positive ESI mode, with quantifier ion transitions 240>125 (clomazone), 343>307 (boscalid), 342>159 (propiconazole), 395>266 (diflufenican), 283>266 (AE 0542291) and 284>266 (AE B107137). All analytes were verified with a qualifier ion transition as well (not listed). Quantification was based on the peak area of the quantifier ion. Internal standard (propiconazole-d_5 and diflufenican-d_3) calibration was performed using quadratic regression analysis of the peak area ratios (quantifier ion/internal standard) versus the concentration ratios. Bracketed calibration standards were set up in the range 0.2-300 ng mL^{-1} in acetone. The limit of quantification (LOQ) for the analytes was 0.5 ng mL^{-1} in the final extract. A LOQ of 0.5 ng mL^{-1} in the extract corresponds to 0.005 µg L^{-1} in a 100-mL bulk water sample.

Mean measured concentrations of the pesticides are reported for each soil, soil depth, treatment and irrigation event. For samples were no detections above the limit of quantification (LOQ) were made, concentrations were set to 0.001 µg L^{-1}, one fifth of the LOQ. In addition, the total mass transported through the soil columns is reported as a percentage of the applied amount.

2.5 Statistical analysis

Statistical analysis of the differences in pesticide transport were carried out with an ANOVA Type III test and a post-hoc pairwise Tukey test (Tukey's 'Honest Significant Difference'

method) in R Commander (R Core Team, 2016). Correlation analyses (Spearman's rho) were performed with Minitab v. 17.1.0. In the analysis of variance for the effect of freezing on the amount of pesticides leached, log-transformed values (Ln+2) of mean total amounts of pesticides leached were used as response variables. This was done to get more homogeneous variances and hence comply with the prerequisite of normally distributed data. Soil type and treatment (frozen, unfrozen) were used as predictor variables (factors). Statistically significant results are reported at the 5 % significance level unless otherwise stated.

3. Results

3.1 Temperatures

As presented in Holten et al. (2018), the temperatures in the frozen soil columns started to increase quickly towards 0 °C when taken from the freezing cabinets, stabilized for a period before quickly increasing towards room temperature (Fig. 2). The period of stable temperatures around 0 °C was longer during later irrigations. For the silt soil, this period increased from about 16 to about 26 hours between the first and third irrigations for both topsoil and subsoil. It took some time before the first irrigation of the Kroer loam started, hence the temperatures in the columns had risen to about 0 °C at the beginning of the irrigation.

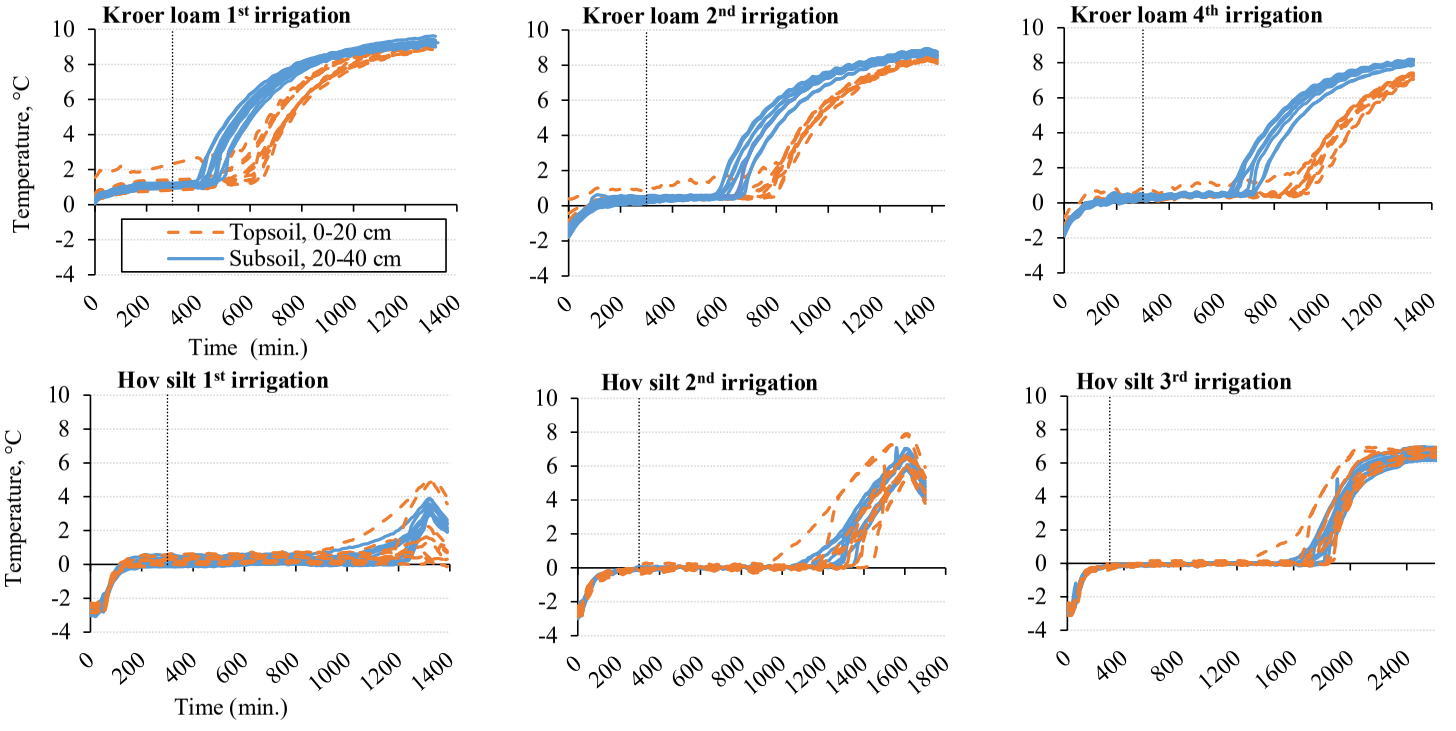

Fig. 2: Temperatures measured at 7 and 14 cm in frozen Kroer loam and Hov silt columns during three irrigation events. For the loam the curves stops at the time the columns were put back in the freezing cabinet (temperatures then started to decrease). For the silt, the temperatures continued to increase even after the columns were put back into the freezing room (around 1400 min). The end of each irrigation event (at 300 minutes) is symbolized with a dotted line. The same legend applies to all plots. (Fig. copied from Holten et al. (2018)).

3.2 Infiltration, drainage and bromide leaching

The measurements of drainage and leaching of bromide in this experiment have been discussed in detail in Holten et al. (2018), but some of these data have also been included in Table 3 to help interpret the other results presented in this paper. These data show that contrary to the pesticide masses, significantly more water drained and more bromide leached from the unfrozen columns than from the frozen columns. This result applied to the loam topsoil and subsoil as well as to the silt subsoil.

In Holten et al. (2018) breakthrough curves of bromide in frozen columns showed high concentration peaks of bromide in leachate from columns during either the first or second irrigation, after only very little water had percolated through the columns (<< 1 pore volume). In contrast, the leaching patterns in unfrozen columns were slower and more uniform without clear concentration peaks.

Another observation discussed in Holten et al. (2018) was a fast infiltration of ponding water in frozen soil columns as temperatures increased above 0 °C. After thawing, 25 mL samples were collected at ca. 6-7 minute intervals, equal to flow rates of ca. 35 mm h^{-1}. In contrast, the interval between each sampling in unfrozen soil was typically about 30 minutes, equal to a flow rate of approximately 7 mm h^{-1}. As presented and discussed in detail in Holten et al. (2018), the data on the drainage of the columns showed that the outflow rates were quite constant during irrigation of the unfrozen columns (almost equal to the inflow rate) and that the outflow ceased rapidly when the irrigation stopped. This was clear for both the loam topsoil and subsoil as well as the silt topsoil, but this difference was smaller for the unfrozen silt subsoil. In the frozen columns, the outflow started later, especially for the later irrigations, and many of the frozen columns continued to percolate slowly a long time after irrigation ceased. Data on the accumulated amount of percolated water plotted against time has been included in Appendix A to this paper.

3.3 Pesticide leaching

Figures 3-7 shows the mean concentrations of the five different pesticides in leachate from all columns and irrigations (y-axis on log scale). Concentrations of all the pesticides were in most cases much larger (but not necessarily significantly larger) in leachate from frozen columns than from unfrozen columns with differences ranging up to five orders of magnitude. Concentrations in leachate from frozen columns increased from the first irrigation to the second before levelling out at a high level through the subsequent irrigations. In leachate from unfrozen soil columns, concentrations were lower (often ≤ LOQ), more constant or decreased throughout the experiment. In many cases, pesticides were detected in fewer samples from unfrozen than from frozen soil columns. These observations generally apply to both Kroer loam topsoil and subsoil and Hov silt topsoil (Figures 3-6).

Concentrations varied between pesticides: for example, clomazone and boscalid leached at ca. 10 times larger concentrations than propiconazole and diflufenican in Kroer loam topsoil (Fig. 3). The results for the loam subsoil were similar, although the differences between the unfrozen columns were less clear (Fig. 4). Diflufenican was not detected in any leachate samples from the unfrozen loam subsoil columns. Many of the same trends as discussed above were also observed for the Hov silt topsoil (Fig. 5), but the differences were even less clear in the silt subsoil (Fig. 6) than in the loam subsoil, with no significant differences between the concentrations of the pesticides from frozen and unfrozen columns. Mean concentrations of MCPA sub-samples weighted by volume (data from Holten et al. (2018)) have been added for comparison (Fig. 7). These results show that much larger concentrations of MCPA leached (ca. 2 orders of magnitude) compared to the other four pesticides (note the different scale of Fig. 7 compared to Fig. 3-6). With respect to the effects of treatment and soil type/depth, the results for MCPA were similar to the results for the other pesticides.

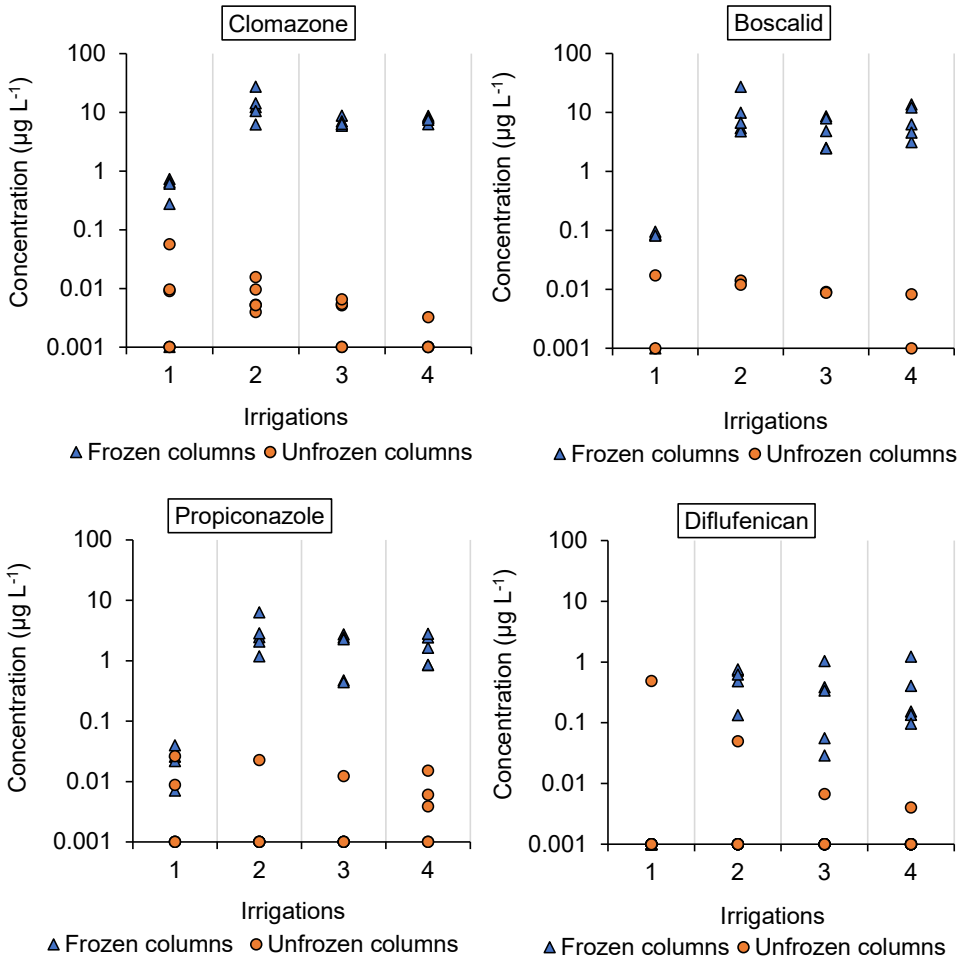

Fig. 3: Concentrations of the four studied pesticides in bulk leachate samples from frozen and unfrozen Kroer loam topsoil (0-20 cm) columns for each of four irrigation events. Concentrations are shown on log10 scale. Detections below LOQ (0.005 µg L^{-1}) are set to 0.001 in the plots.

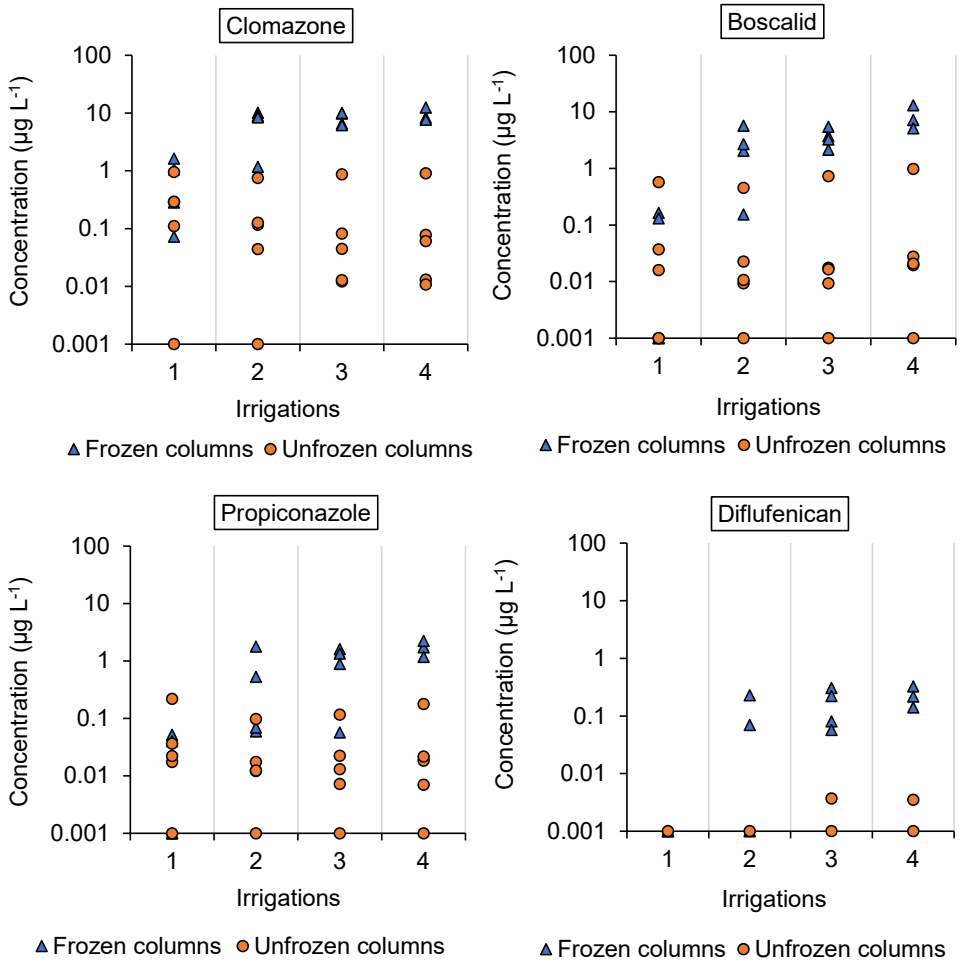

Fig. 4: Concentrations of the four studied pesticides in bulk leachate samples of leachate from frozen and unfrozen Kroer loam subsoil (20-40 cm) columns for each of four irrigations events. Concentrations are shown on log10 scale. Detections below LOQ (0.005 µg L^{-1}) are set to 0.001 in the plots.

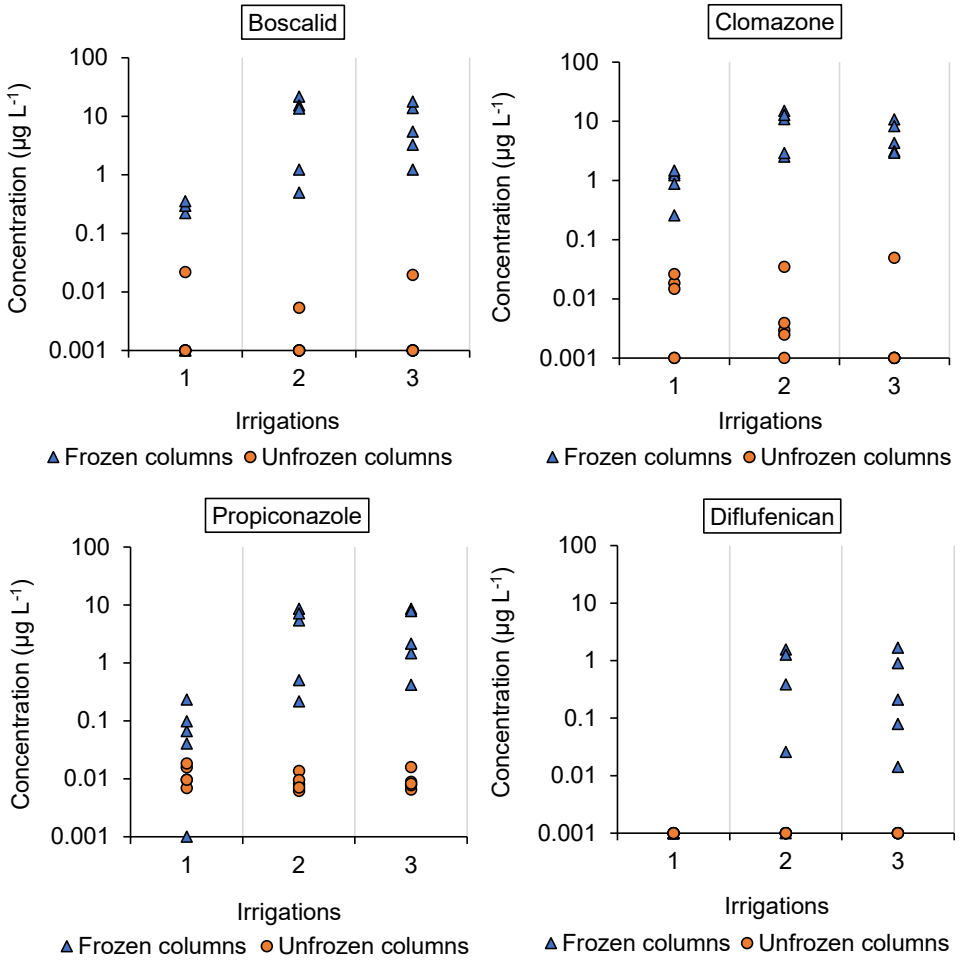

Fig. 5: Concentrations of the four studied pesticides in bulk leachate samples of leachate from frozen and unfrozen Hov silt topsoil (0-20 cm) columns for each of four irrigations events. Concentrations are shown on log10 scale. Detections below LOQ (0.005 µg L^{-1}) are set to 0.001 in the plots.

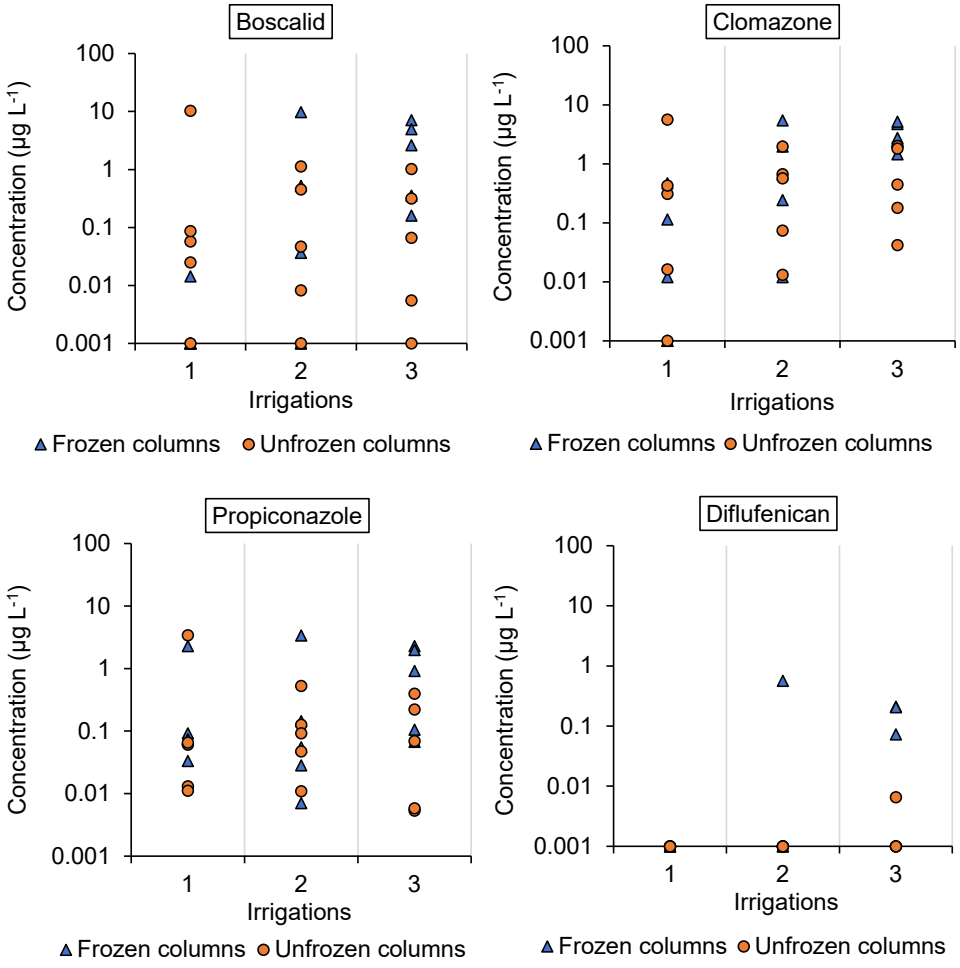

Fig. 6: Concentrations of the four studied pesticides in bulk leachate samples of leachate from frozen and unfrozen Hov silt subsoil (20-40 cm) columns for each of four irrigations events. Concentrations are shown on log10 scale. Detections below LOQ (0.005 µg L^{-1}) are set to 0.001 in the plots.

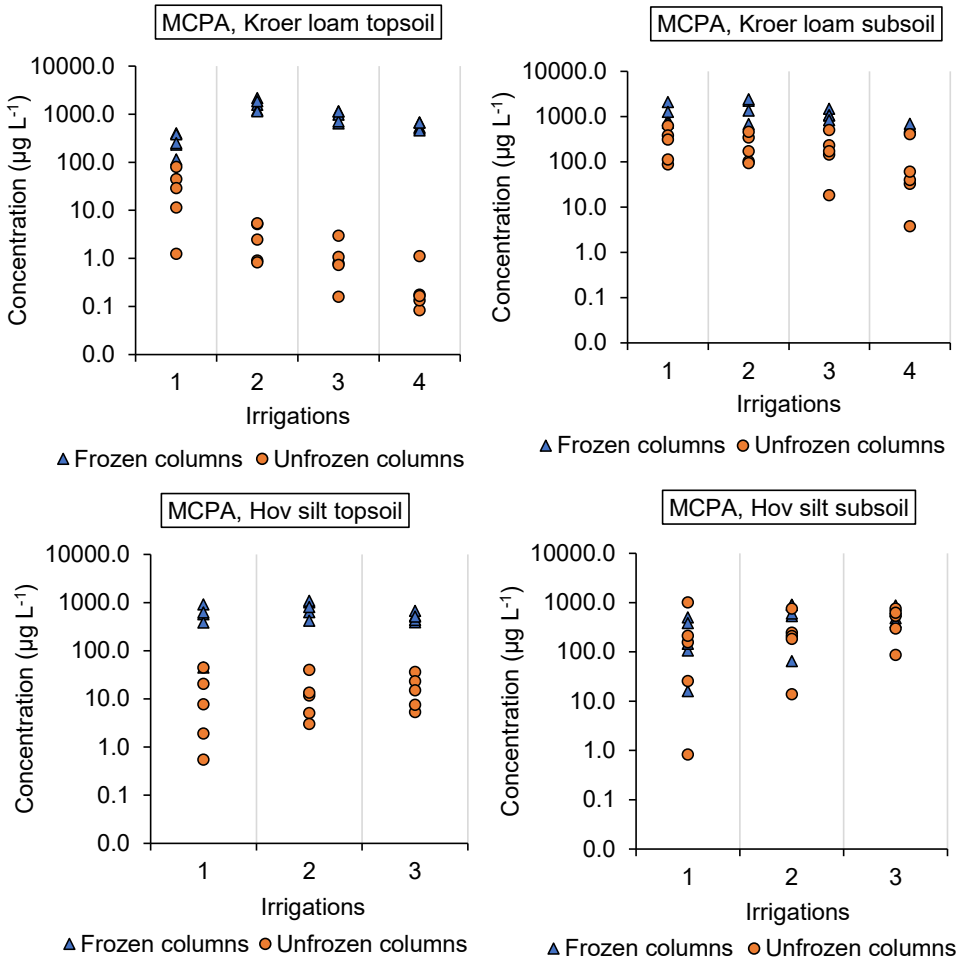

Fig. 7: Concentrations of MCPA in samples of leachate from frozen and unfrozen Kroer loam and Hov silt for each irrigation event. Concentrations were calculated as the sum of the amount of MCPA that leached from each column at each irrigation divided by the respective sum of leachate volumes. Concentrations are shown on log10 scale. Mind the different scale compared to Figures 3-6.

Table 3. Total amounts leached as percentage of applied amounts of water, bromide, MCPA, clomazone, boscalid, propiconazole and diflufenican leaching from Kroer loam soil columns during four irrigations and Hov silt soil columns during three irrigations. Different superscript letters denote significant differences, based on pairwise comparisons (ANOVA III + Tukey test) of samples from frozen and unfrozen columns of the same soil. The statistics were done on log-transformed data.

Soil	Depth (cm)	Temp. (°C)	Water[1] (% of appl.[2])	Bromide[1] (% of appl.[2])	MCPA[1] (% of appl.[2])	Clomazone (% of appl.[2])	Boscalid (% of appl.[2])	Propiconazole (% of appl.[2])	Diflufenican (% of appl.[2])
Kroer, loam	0-20	-3	60.2 ^{b}	37.4 ^{c}	24.5 ^{a}	7.7 ^{a}	1.0 ^{a}	0.60 ^{a}	0.13 ^{a}
	0-20	+4	91.2 ^{a}	57.5 ^{b}	0.4 ^{c}	7.8E^{-5} ^{c}	7.2E^{-6} ^{c}	1.9E^{-5} ^{c}	1.2E^{-4} ^{c}
	20-40	-3	47.1 ^{c}	28.2 ^{c}	24.1 ^{a}	1.0 ^{a}	0.65 ^{a}	0.15 ^{a}	0.019 ^{b}
	20-40	+4	87.1 ^{a}	72.1 ^{a}	8.6 ^{b}	0.049 ^{b}	0.026 ^{b}	8.2E^{-3} ^{b}	6.2E^{-5} ^{c}
Hov, silt	0-20	-3	75.7 ^{B}	25.2 ^{AB}	16.4 ^{A}	6.2 ^{A}	1.3 ^{A}	1.2 ^{A}	0.19 ^{A}
	0-20	+4	94.0 ^{A}	31.5 ^{A}	0.5 ^{B}	0.014 ^{C}	6.9E^{-4} ^{C}	4.8E^{-3} ^{C}	nd[3]
	20-40	-3	52.7 ^{C}	13.1 ^{B}	10.3 ^{A}	1.7 ^{AB}	0.32 ^{AB}	0.25 ^{AB}	0.03 ^{AB}
	20-40	+4	82.0 ^{AB}	30.4 ^{A}	10.6 ^{A}	1.2 ^{B}	0.19 ^{BC}	0.15 ^{BC}	0.026 ^{AB}

[1] Data from Holten et al. (2018)
[2] % of nominal applied amount.
[3] Not detected in any of the samples

Table 3 shows that the leached amounts of the pesticides, expressed as percentages of the applied amounts, were in most cases significantly larger ($p<0.05$) from the topsoil columns that were subjected to freezing than from the unfrozen topsoils. The differences between the amounts leaching from frozen and unfrozen columns were up to three to five orders of magnitude for the loam soil. The differences were less pronounced for the silt topsoil with differences of up to three orders of magnitude between the two treatments. For the loam subsoil the amount leached from frozen columns were about two orders of magnitude larger than from unfrozen columns and in all cases except diflufenican, the differences were statistically significant. For the silt subsoil, leached amounts were in the same order of magnitude in frozen and unfrozen columns and the differences were not statistically significant.

MCPA was the pesticide that leached the most in all treatments, while diflufenican leached in the smallest amounts. The rank-order in pesticide leaching was the same for most treatments, soil types and depths; MCPA > clomazone > boscalid > propiconazole > diflufenican.

While the diflufenican metabolite AE 054229 was not detected in any of the leachate samples, the metabolite AE B107137, however, was detected in leachate samples from both soil types, depths and treatments at a maximum amount of 0.15 % of the applied amount of diflufenican. The maximum amount was detected in leachate samples from unfrozen loam subsoil columns. Other detections of this metabolite were generally < 0.04 % of the applied amount of diflufenican. In comparison, the MCPA metabolite 2-MCP was found at a maximum value of 0.003 % of the applied amount of MCPA in leachate from frozen loam topsoil (Holten et al., 2018).

A general observation that was made during the experiment was that many of the leachate samples were visibly coloured due to suspended particles. This was observed in leachate from both frozen and unfrozen columns. One water sample was tested for pesticide residues in the

soil particles (after centrifugation) after extraction with acetone, but no pesticides were detected. The amount of soil particles was very low and it was not considered worthwhile to extract and analyse the soil particles as pesticide concentrations were expected to be too low to detect.

3.4 Sorption coefficients and leaching

The rank order observed for leaching follows quite closely the differences in the mean K_f values, for the five compounds (Table 2). When combining results from frozen and unfrozen columns, a highly significant ($p<0.001$) negative correlation was found between the fraction of pesticide leached and K_f in both Kroer loam and Hov silt with correlation coefficients of -0.64 and -0.69 respectively, indicating that substances with lower K_f values leached more than substances with higher K_f values (Fig. 8). This figure clearly shows that K_f has a strong effect on the leaching for both frozen and unfrozen soils, although the effect seems somewhat stronger for unfrozen subsoil than unfrozen topsoil.

Fig. 9 shows a plot of the ratio of leaching from frozen and unfrozen columns against representative substance Kf values taken from the literature. It appears that the effects of freezing in enhancing leaching are strongest for the moderately adsorbing compounds, and weaker for both weakly adsorbing (e.g. MCPA) and very strongly adsorbing compounds (e.g. diflufenican). This trend is especially apparent in the topsoil columns and somewhat weaker for the subsoils.

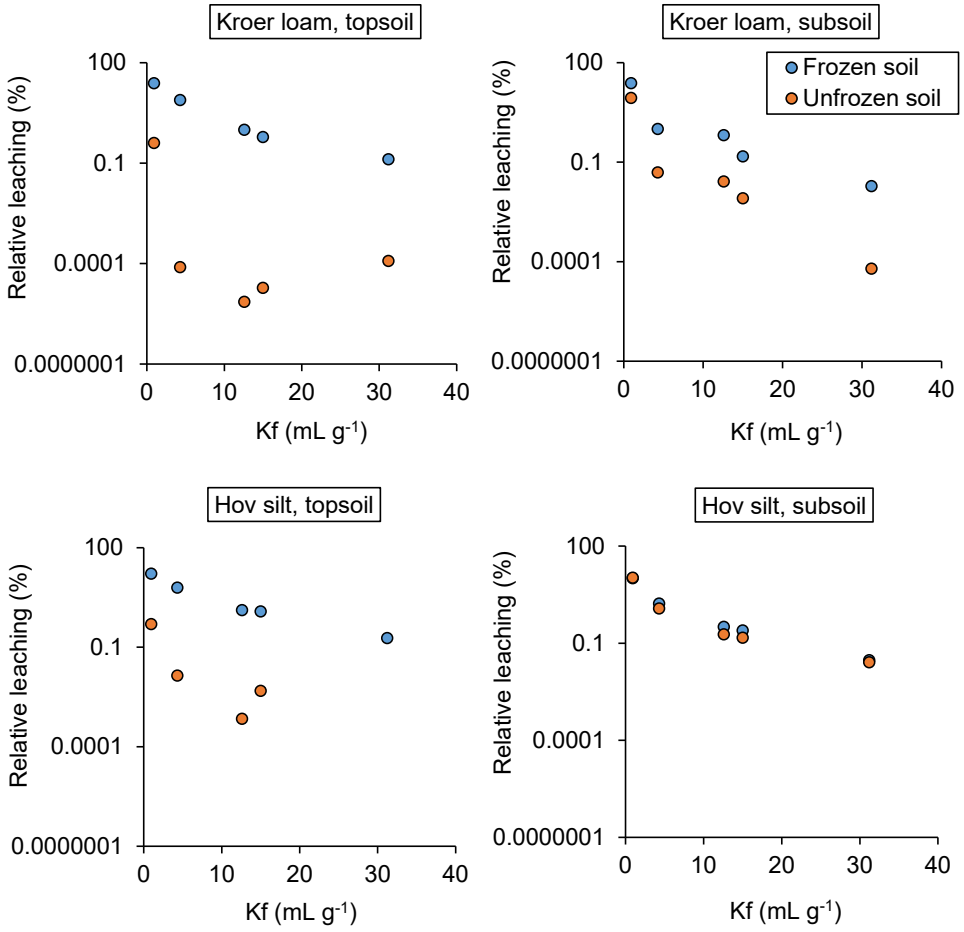

Fig. 8: Relative leaching from frozen and unfrozen soil columns plotted against mean Kf values in Kroer loam and Hov silt topsoil and subsoil. The same legend applies to all four plots.

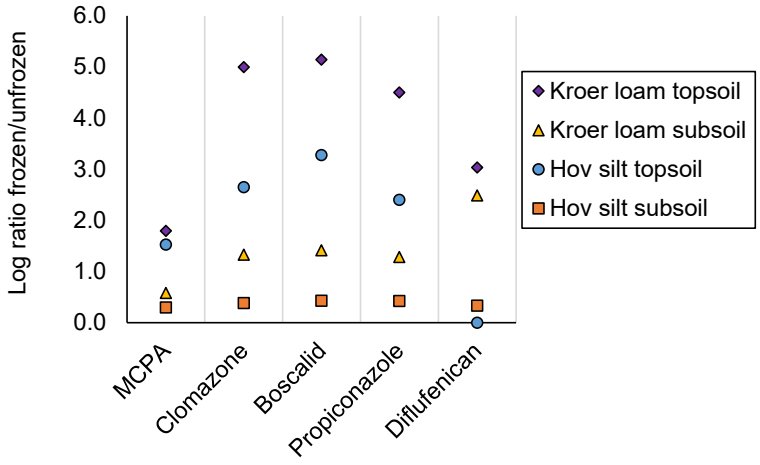

Fig. 9: The logarithm of the ratio of the percentage of the applied amount leached from frozen and unfrozen soil columns of five different pesticides.

4. Discussion

4.1 Infiltration, drainage and bromide leaching

The fact that less water drained and less bromide leached from frozen columns than unfrozen columns was unexpected since the frozen columns thawed completely during the period in the lysimeter room during irrigation events (Fig. 1), so any differences should have evened out. One likely explanation discussed in Holten et al. (2018) was that the frozen columns had not finished draining when they were returned to the freezing chamber and that some water may have been lost during the process of moving the columns. Hence, thawing seemed to be faster than drainage. Continued sampling would have been desirable to sample more water from the frozen columns, but due to time constraints, this was not possible.

Ponding was observed on all frozen columns, especially at later irrigations when the water content was higher, indicating that all pores were frozen. In these columns, infiltration started later and they continued percolating for a long time after the irrigation had stopped (Figures A1-A2 in Appendix A). As the temperature in the columns reached 0°C, infiltration could

happen quite fast with flow rates up to 35 mm h^{-1}, indicating that the ice in the macropores had, at least, partly melted. In addition, preferential flow was confirmed by bromide breakthrough curves presented in Holten et al. (2018), which in many cases showed significant concentration peaks in leachate samples during either the first or second irrigation after little water had percolated through the columns (<< 1 pore volume). The leaching pattern of bromide in unfrozen columns was very different indicating a slower and uniform flow and transport through the entire soil matrix, probably because the infiltration capacity of the unfrozen matrix was sufficient to prevent the generation of non-equilibrium preferential flow in soil macropores (Jarvis et al., 2016).

4.2 Pesticide leaching

In this study only bulk leachate samples were analysed, hence breakthrough curves such as the ones presented for MCPA and bromide by Holten et al. (2018) could not be presented. Nevertheless, significantly larger concentrations in leachate and leached amounts of these pesticides from the columns subjected to the freezing treatment indicate that the transport of all five pesticides investigated in this study was enhanced in partially frozen soil (Figures 3-7). For an advective-dispersive transport process and with the Kf values reported in Table 2, one would not expect any breakthrough until after many pore volumes had passed through the columns. The relatively rapid breakthrough of bromide, as presented in Holten et al. (2018) and the adsorbing pesticides in this case (<< 1 pore volume) indicates that the leaching process was dominated by preferential flow through soil macropores that presumably remained air-filled, hence confirming the hypothesis stated in the introduction. Conversely, the much smaller concentrations of the pesticides in leachate from unfrozen columns can probably be attributed to a more uniform transport process through the bulk of the soil, such that the pesticides were exposed to more soil surfaces and binding sites, hence resulting in stronger sorption.

The effects of freezing were much less clear in the silt subsoil (Fig. 4), where the amounts leached were not significantly different between the treatments. This can probably be attributed to a lack of connected macroporosity in the silt subsoil as shown and discussed in Holten et al. (2018).

In some samples, suspended particles were observed, but the concentration of particle-bound pesticides was not analysed in all samples due to particles being filtered out during sample preparation. This could have influenced the recovery of the more strongly adsorbing compounds like diflufenican, which may partly explain the low amounts detected in the leachate. However, a preliminary test indicated that no pesticides were adsorbed to particles extracted with acetone, although leaching losses through particle-bound transport cannot be completely ruled out.

The concentrations of the diflufenican metabolite AE B107137 and the MCPA metabolite 2-MCP detected in leachate samples were generally small. One exception was the leachate from unfrozen Kroer loam subsoil columns, where the amounts that leached of AE B107137 reached a level of 0.15 % of the applied amount of diflufenican. The amounts of diflufenican were very low in leachate from the same columns but this metabolite is very mobile, with typical K_f values of 0.11-0.42 mL g^{-1} (Agriculture & Environment Research Unit (AERU) University of Hertfordshire, 2018). This indicates that diflufenican was subject to some degradation during the course of the experiment, despite the low temperatures. Nevertheless, the amounts of the metabolite were generally low and degradation was not considered to be the reason for the differences observed between frozen and unfrozen columns.

4.3 Sorption coefficients and leaching

This study showed higher mobility for most pesticides in frozen soil columns compared to unfrozen columns. The rank order in pesticide leaching observed in this study (MCPA >

clomazone > boscalid > propiconazole > diflufenican), corresponds well to the rank-order of mean K_f values of the pesticides from a range of different soil types, both in frozen and unfrozen soils. The data in this study also show a strong negative correlation between pesticide sorption properties (K_f) and leaching (Fig. 8). This dependency has also been shown in field studies where leaching behaviour of different compounds have been compared in the presence of macropore flow (Jarvis, 2007) suggesting that compound sorption properties have a certain effect, although this will be weaker when macropore flow is present(Larsson and Jarvis, 2000). Plotting the logarithm of the ratio between the mean amounts of pesticides that leached from frozen columns and unfrozen columns (Fig. 9) indicate that MCPA and diflufenican are less influenced by macropore flow as the leaching ratios for these substances in general are lower than for substances with more intermediate sorption. This relationship seems clearer for the topsoils of both the Kroer loam and Hov silt than for subsoils, perhaps due to smaller and less well connected macropores in these subsoils (Holten et al., 2018). These results indicate, although rather indirectly, that macropores play a larger role for the transport of substances of more intermediate mobility, as argued by McGrath et al. (2010), and that this also applies to frozen soil. More mobile substances may leach regardless of the presence of macropores, while more or less immobile substances adsorb strongly to the soil in any case and are transported either particle-bound through macropores towards drains (Kjær et al., 2011, Øygarden et al., 1997) or via surface run off/erosion (Larsbo et al., 2016). The fact that diflufenican was found in very low concentrations in leachate in this study may, among other reasons (sorption, degradation), be due to loss via particle-bound transport.

The data in this study indicates higher pesticide mobility in frozen soil than unfrozen soil. This is partly in line with a study where lower K_d values were found for the mobile pesticide metribuzin at -5 °C than at +5 °C (Stenrød et al., 2008). The presence of macropore flow

however, probably explains most of the differences observed between leaching from frozen and unfrozen columns in this study.

5. Conclusion and recommendations

This study shows that air-filled and connected macropores can facilitate fast transport of high concentrations of pesticides vertically through a partially-frozen soil profile. The studied pesticides had a range of K_f values and the results suggest that sorption plays a role in determining leaching losses even in frozen soil. These relationships have to our knowledge not been investigated in detail before, at least not in frozen soils, and the findings here show that this may be worthwhile investigating further. Modelling with an appropriate model could also help to interpret some of the results (Mohammed et al., 2018). In addition, these relationships are worth considering when assessing the fate and behaviour of pesticides during the cold period of year and may be worth taking into account in pesticide monitoring programs.

Acknowledgements

This work is a part of the BIONÆR project: Innovative approaches and technologies for Integrated Pest Management (IPM) to increase sustainable food production (Smartcrop) funded by The Research Council of Norway (project no.: 244526/E50). We are grateful for the help given by Randi Bolli on the set up of the experiment and for very helpful discussion of the results. We would also like to thank Jens Kværner for valuable comments during the writing process.

References

Pesticide Properties Database (PPDB). AGRICULTURE & ENVIRONMENT RESEARCH UNIT (AERU) UNIVERSITY OF HERTFORDSHIRE. 20. September 2018. http://sitem.herts.ac.uk/aeru/ppdb/en/index.htm.

BEVEN, K. & GERMANN, P. 1982. Macropores and water flow in soils. *Water Resources Research,* 18**,** 1311-1325. DOI: 10.1029/WR018i005p01311

FLURY, M. 1996. Experimental Evidence of Transport of Pesticides through Field Soils—A Review. *Journal of Environmental Quality,* 25**,** 25-45. DOI: 10.2134/jeq1996.00472425002500010005x

GREVE, M., HELWEG, A., YLI-HALLA, M., EKLO, O. M., NYBORG, Å. A., SOLBAKKEN, E., ÖBORN, I. & STENSTRÖM, J. (eds.) 1998. *Nordic Reference Soils.* Nordic Council of Ministers. 537

HAYASHI, M. 2013. The Cold Vadose Zone: Hydrological and Ecological Significance of Frozen-Soil Processes. *Vadose Zone Journal,* 12. DOI: 10.2136/vzj2013.03.0064

HOLTEN, R., BOE, F. N., ALMVIK, M., KATUWAL, S., STENROD, M., LARSBO, M., JARVIS, N. & EKLO, O. M. 2018. The effect of freezing and thawing on water flow and MCPA leaching in partially frozen soil. *J Contam Hydrol,* 219**,** 72-85. 10.1016/j.jconhyd.2018.11.003

IRESON, A. M., VAN DER KAMP, G., FERGUSON, G., NACHSHON, U. & WEATHER, H. S. 2013. Hydrogeological processes in seasonally frozen northern latitudes: understanding, gaps and challenges. *Hydrogeology Journal***,** 53-66. DOI: 10.1007/s10040-012-0916-5

IUSS WORKING GROUP WRB 2014. World Reference Base for Soil Resources 2014. International soil classification system for naming soils and creating legends for soil maps. World Soil Resources Reports No.106. FAO, Rome.

JARVIS, N., KOESTEL, J. & LARSBO, M. 2016. Understanding Preferential Flow in the Vadose Zone: Recent Advances and Future Prospects. *Vadose Zone Journal,* 15. DOI: 10.2136/vzj2016.09.0075

JARVIS, N. J. 2007. A review of non-equilibrium water flow and solute transport in soil macropores: principles, controlling factors and consequences for water quality. *European Journal of Soil Science,* 58**,** 523-546. DOI: 10.1111/j.1365-2389.2007.00915.x

KJÆR, J., ERNSTSEN, V., JACOBSEN, O. H., HANSEN, N., DE JONGE, L. W. & OLSEN, P. 2011. Transport modes and pathways of the strongly sorbing pesticides glyphosate and pendimethalin through structured drained soils. *Chemosphere,* 84**,** 471-479. DOI: https://doi.org/10.1016/j.chemosphere.2011.03.029

LARSBO, M., SANDIN, M., JARVIS, N., ETANA, A. & KREUGER, J. 2016. Surface Runoff of Pesticides from a Clay Loam Field in Sweden. *Journal of Environmental Quality,* 45**,** 1367-1374. DOI: 10.2134/jeq2015.10.0528

LARSSON, M. H. & JARVIS, N. J. 2000. Quantifying interactions between compound properties and macropore flow effects on pesticide leaching. *Pest Management Science,* 56**,** 133-141. DOI:10.1002/(SICI)1526-4998(200002)56:2<133::AID-PS103>3.0.CO;2-N

LÖV, Å., SJÖSTEDT, C., LARSBO, M., PERSSON, I., GUSTAFSSON, J. P., CORNELIS, G. & KLEJA, D. B. 2017. Solubility and transport of Cr(III) in a historically contaminated soil – Evidence of a rapidly reacting dimeric Cr(III) organic matter complex. *Chemosphere,* 189**,** 709-716. DOI: https://doi.org/10.1016/j.chemosphere.2017.09.088

MCGRATH, G., HINZ, C. & SIVAPALAN, M. 2010. Assessing the impact of regional rainfall variability on rapid pesticide leaching potential. *Journal of Contaminant Hydrology,* 113**,** 56-65. DOI: https://doi.org/10.1016/j.jconhyd.2009.12.007

MCGRATH, G. S., HINZ, C. & SIVAPALAN, M. 2009. A preferential flow leaching index. *Water Resources Research,* 45. DOI: 10.1029/2008WR007265

MOHAMMED, A. A., KURYLYK, B. L., CEY, E. E. & HAYASHI, M. 2018. Snowmelt infiltration and macropore flow in frozen soils: overview, knowledge gaps, and a conceptual framework. *Vadose Zone Journal*. doi:10.2136/vzj2018.04.0084

R CORE TEAM 2016 R: A language and environment for statistical computing https://www.R-project.org/

RIISE, G., LUNDEKVAM, H., HAUGEN, L. E. & MULDER, J. 2006. Suspended sediments as carriers for the fungicide propiconazole in agricultural runoff. *Verhandlungen des Internationalen Verein Limnologie*, 1296–1300. DOI: https://doi.org/10.1080/03680770.2005.11902891

RIISE, G., LUNDEKVAM, H., WU, Q. L., HAUGEN, L. E. & MULDER, J. 2004. Loss of Pesticides from Agricultural Fields in SE Norway – Runoff Through Surface and Drainage Water. *Environmental Geochemistry and Health,* 26, 269-276. DOI: 10.1023/B:EGAH.0000039590.84335.d6

SIIMES, K., RÄMÖ, S., WELLING, L., NIKUNEN, U. & LAITINEN, P. 2006. Comparison of the behaviour of three herbicides in a field experiment under bare soil conditions. *Agricultural water management,* 84, 53-64. DOI: https://doi.org/10.1016/j.agwat.2006.01.007

STENRØD, M., PERCEVAL, J., BENOIT, P., ALMVIK, M., BOLLI, R. I., EKLO, O. M., SVEISTRUP, T. E. & KVÆRNER, J. 2008. Cold climatic conditions: Effects on bioavailability and leaching of the mobile pesticide metribuzin in a silt loam soil in Norway. *Cold Regions Science and Technology,* 53, 4-15. DOI: http://dx.doi.org/10.1016/j.coldregions.2007.06.007

ULÉN, B. M., LARSBO, M., KREUGER, J. K. & SVANBÄCK, A. 2013. Spatial variation in herbicide leaching from a marine clay soil via subsurface drains. *Pest Management Science,* 70, 405-414. DOI: 10.1002/ps.3574

VAN DER KAMP, G., HAYASHI, M. & GALLÉN, D. 2003. Comparing the hydrology of grassed and cultivated catchments in the semi-arid Canadian prairies. *Hydrological processes*, 559-575. DOI: 10.1002/hyp.1157

ØYGARDEN, L., KVÆRNER, J. & JENSSEN, P. D. 1997. Soil erosion via preferential flow to drainage systems in clay soils. *Geoderma,* 76, 65-86. DOI: https://doi.org/10.1016/S0016-7061(96)00099-7

Appendix A

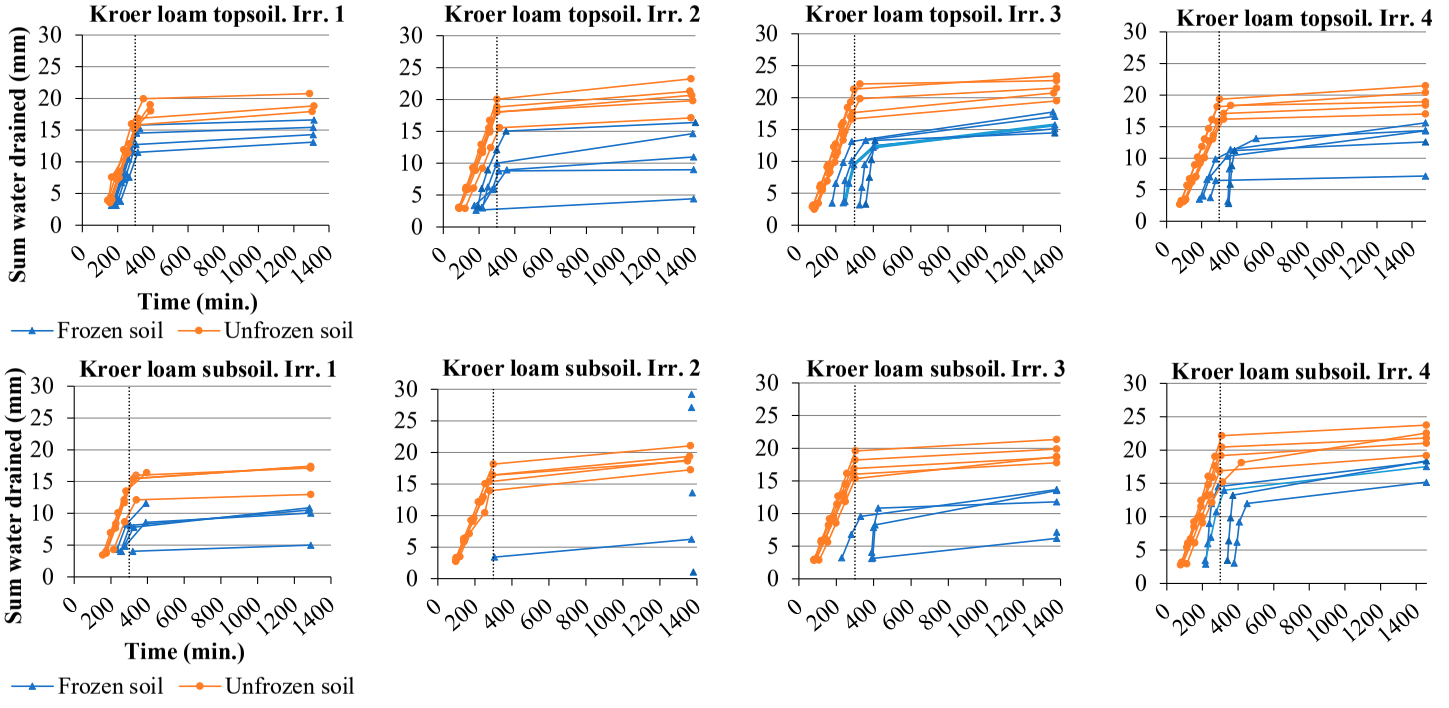

Fig. A1: The accumulated amount of water that drained from frozen and unfrozen soil columns during four irrigation events of the Kroer loam topsoil and subsoil, plotted against time. The vertical dotted line illustrates the end of the irrigations. During the second irrigation, some of the early samples from the subsoil were lost due to leakages through the thermistor holes. The same legend apply to all plots (Figure copied from Holten et al. (2018)).

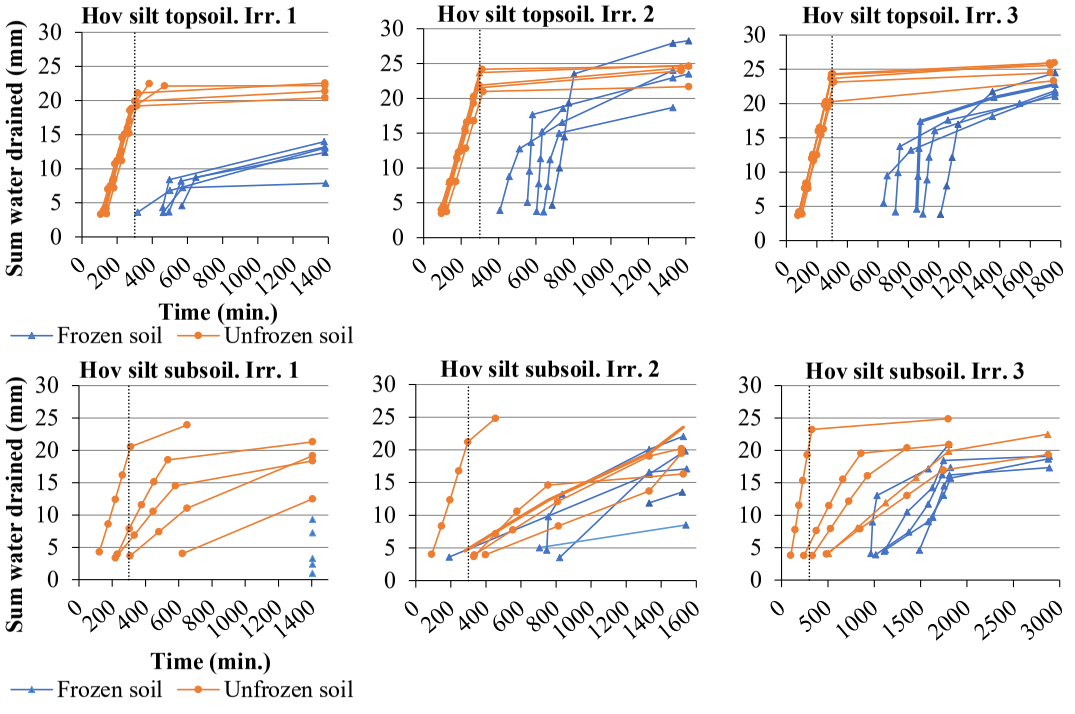

Fig. A2: The accumulated amount of water that drained from frozen and unfrozen soil columns during three irrigation events of the Hov silt topsoil and subsoil, plotted against time. The vertical dotted line illustrates the end of the irrigations. Different time scales are due to large variations in infiltration times. Only one sample was collected for each frozen subsoil column at the first irrigation due to very little percolation. The same legend apply to all plots (Figure copied from Holten et al. (2018)).

Paper III

A dual permeability approach for modelling soil water flow and heat transport during freezing and thawing

Mats Larsbo[a], Roger Holten[b,c], Marianne Stenrød[b], Ole Martin Eklo[b,c] and Nicholas Jarvis[a]

[a]Swedish University of Agricultural Sciences (SLU), Department of Soil and Environment, P.O. Box 7014 75007, Uppsala, Sweden

[b]Norwegian Institute of Bioeconomy Research (NIBIO), Division of Biotechnology and Plant Health, Department of Pesticides and Natural Products Chemistry, P.O. Box 115, NO-1431 Ås, Norway

[c]Norwegian University of Life Sciences, Faculty of Bio Sciences, Department of Plant Sciences, P.O. Box 5003, N-1432 Ås, Norway

ABSTRACT

Freezing and thawing strongly affects water flow in soil since ice may block a large part of the pore space, thereby preventing infiltration and flow through the soil. Preferential flow in soil macropores may become even more significant in frozen soils since infiltration can occurs through large, initially air-filled pores surrounded by a soil matrix with limited infiltration capacity. The objectives of this study were to develop and evaluate a dual-permeability approach for water flow and heat transport in macroporous soils undergoing freezing and thawing. This was achieved by introducing physically-based equations for soil freezing and thawing into the dual-permeability model MACRO. Richards' equation and the heat flow equation were loosely coupled using the generalized Clapeyron equation for the soil micropore domain. In accordance with the original MACRO model, we assumed that capillary forces had no influence on freezing in the macropore domain. Freezing and thawing of macropore water were governed by a first-order equation for energy transfer between the micropore and macropore domains. The model performance was evaluated for four test cases illustrating different processes, i) redistribution of water in the micropore domain during freezing, ii) a comparison between the first-order energy transfer approach and the heat conduction equation for thawing of the micropore domain, iii) infiltration and water flow in frozen soil with an initially air-filled macropore domain, and iv) thawing from the soil surface during constant rainfall. Results show that the model reproduces the limited available measured data well and that it behaves in accordance with the current understanding of water flow and heat transport in macroporous soil. To improve modelling of water and heat flow in frozen soils further, attention should be focused on providing experimental data suitable for evaluation of models accounting for macropore flow.

Key words: dual permeability, model**,** soil, water flow, heat transport, freezing and thawing

1. INTRODUCTION

Freezing and thawing strongly affects water flow in soil since ice may block a large part of the pore space, thereby preventing infiltration. At a larger scale, the reduced permeability of frozen soil layers influences the distribution of precipitation between surface runoff into rivers and lakes and infiltration into the soil that may replenish groundwater storage (e.g. Ireson et al., 2013; Lundberg et al., 2016). Effects of freezing on soil hydrology are often most significant during snowmelt when large amounts of water may reach the soil surface in a short amount of time.

Preferential flow in soil macropores has since long been recognized as an important process which influences vadose zone hydrology from the pore scale to the hillslope scale (Beven and Germann, 1982; Jones, 2010; Jarvis et al., 2016). Preferential flow may become even more significant under frozen conditions when infiltration occurs through large, initially air-filled pores surrounded by a soil matrix with limited infiltration capacity (e.g. Kane, 1980; Stadler et al., 2000, Mohammed et al., 2018). Despite its relevance in temperate and sub-polar climate zones, preferential flow in frozen soils has, to date, received little attention. Some noteworthy exceptions are van der Kamp et al. (2003) who demonstrated the importance of macropores for frozen soil infiltration rates in the Canadian prairies using single ring infiltrometers. They showed that infiltration rates were smaller for cultivated soils with few macropores compared to permanent grassland soils containing well-developed macropore networks. During snowmelt the unsaturated large macropores in the grassland soil still had substantial infiltration capacities, generally exceeding the maximum likely rate of snowmelt. The effects of macropores on water flow through frozen soil have recently also been demonstrated in column scale laboratory experiments. Watanabe and Kugisaki (2017) studied water flow through initially air-filled artificially created vertical macropores of different sizes. The exchange of energy between the frozen soil matrix and the water in the macropores resulted in freezing of the infiltrating water for macropores with a diameter of 2 mm. However, for a setup with 5-mm diameter vertical pores, the water flow rate was high enough to limit freezing of the infiltrating water, resulting in a fast drainage response at the bottom of the column.

A number of numerical models of water flow through soil that account for the effects of freezing and thawing have been developed since the 1970s. Many of these models account for freezing by coupling Richards' equation for water flow and the heat flow equation using the generalized Clapeyron equation, which relates the capillary pressure to temperature during phase change. Such physically-based modelling approaches were recently reviewed by Kuryluk and Watanabe (2013) and Mohammed et al. (2018). As far as we know, the only model that addresses the important effect of macropores on water flow and heat transport is the model by Stähli et al. (1996), which is included in the COUP model (Jansson, 2012). They developed a modelling concept, which accounted for the fact that soils often freeze when the soil is unsaturated. They argued that under such conditions, the water in the smallest pores will remain unfrozen, the water in intermediate sized pores will be frozen and the largest pores will be air-filled. If the largest pores remain air-filled during winter they will contribute to the infiltration capacity of the soil during spring snowmelt. In their model, although they make no distinction between soil macropores and the soil matrix, water infiltrating into the large (initially) air-filled pores constitutes a high water-flow domain. As water flows through the high-flow domain it may freeze due to heat transfer from the high-flow domain to the low-flow domain resulting in a shift in the boundary between the low-flow domain and the ice domain towards larger pores. This approach was shown to improve simulation results for the onset of drainage during snowmelt (Stähli et al., 1996).

Based on their review on infiltration and macropore flow in frozen soils, Mohammed et al. (2018) proposed a "matrix-macropore conceptual framework for water and heat transfer in unsaturated frozen soil". This conceptual model includes a fixed distinction between the micropore and macropore domains based on a pore size threshold. Such a distinction between pore domains has since the 1990s been used in dual-permeability models to model preferential water flow in macroporous soil, albeit without accounting for freezing (e.g. Jarvis et al., 1991; Gerke and van Genuchten, 1993). These models account for the non-equilibrium in pressure potentials between the soil matrix and larger pores, which is often encountered in soils. For frozen soils, this approach would distinguish larger, air-filled micropores, which can be blocked by ice due to redistribution of water during freezing from macropores that generally remain open during soil freezing and can only be blocked due to freezing of infiltrating water. As far as we know, there are no numerical simulation models available that can account for the effects of freezing on preferential water flow through macropores using a dual-permeability approach.

The objectives of this study were to develop and evaluate a dual-permeability approach for water flow and heat transport in macroporous soils undergoing freezing and thawing. This was achieved by introducing physically-based equations for soil freezing and thawing into the MACRO model (Larsbo et al., 2005). We tested the model for water flow in the micropore domain against available measured data on the redistribution of water during freezing. Illustrative scenario simulations were also performed to demonstrate the effects of soil macropores on water flow and heat transport in partially frozen soils.

2. MATERIALS AND METHODS

2.1. The MACRO model

MACRO is a one-dimensional dual-permeability model of variably saturated water flow and reactive solute transport in soil (Larsbo et al., 2005; Jarvis and Larsbo, 2012). It has been used since the early 1990s as a research tool to investigate the effects of macropore flow on soil hydrology and contaminant transport under transient field conditions and is one of the models used in risk assessments for pesticide leaching in the European Union (FOCUS, 2001). Here we give a very brief description of the processes that are most relevant for the further development of approaches for water flow and heat transport under winter conditions.

Rain or snowmelt is partitioned into infiltration into micropores and macropores assuming that water will only infiltrate into macropores when the infiltration capacity of the micropore domain is exceeded. Water flow in micropores is calculated with Richards' equation using soil hydraulic properties described by the Mualem-van Genuchten model (Mualem, 1976; van Genuchten, 1980). A modified kinematic wave equation is used to calculate water flow in soil macropores, q_{mac} (mm h^{-1}):

$$q_{mac} = K_{mac,sat} S_{mac}^{\ n*} \qquad \text{Eq. 1.}$$

where the subscript *mac* denotes the macropore domain, K_{mac} (mm h^{-1}) is the hydraulic conductivity, θ_{mac} (m^3 m^{-3}) is the volumetric water content, $K_{mac,sat}$ (mm h^{-1}) is the saturated macropore hydraulic conductivity, $n*$ (-) is the kinematic exponent and $S_{mac} = \theta_{mac}/\varepsilon_{mac}$ (-) is the degree of saturation where ε_{mac} (m^3 m^{-3}) is macroporosity.

First-order water exchange from macropores to the micropore domain, S_w (s^{-1}), is calculated as:

$$S_w = \frac{G_f D_w S_{mac} \gamma_w}{d^2}(\theta_b - \theta_{mic}) \quad \text{Eq. 2.}$$

where G_f (-) is a geometry factor (set internally to 3 for a rectangular slab geometry; Gerke and van Genuchten, 1996), D_w (m^2 s^{-1}) is the soil water diffusivity, γ_w (-) is a scaling factor (Jarvis, 1994), d (mm) is the diffusion pathlength (a parameter related to the geometry of the pore network), θ_b (-) and θ_{mic} (-) are the saturated and actual water contents in the micropore domain, respectively.

In previous versions of the MACRO model, soil temperatures were calculated with a heat conduction equation assuming equilibrium between pore domains and without considering freezing/thawing.

2.2. A dual-permeability approach for coupled water flow and heat transport accounting for soil freezing

Water flow in macropores is often fast and residence times in a frozen soil layer may be short compared to the time it would take to freeze the macropore water (Watanabe and Kugisaki, 2017; Mohammed et al., 2018). Under such conditions the assumptions of equilibrium in temperatures between pore domains is not valid. In the following, we describe a dual-permeability approach for water flow and heat transport in soil that accounts for the non-equilibrium in both water pressures and temperatures that often occurs in soil during freezing and thawing. Depending on temperature, water in the micropore and macropore domains may exist both in liquid form and as ice.

The porosity in each domain is given by:

$$\varepsilon_{mic/mac,tot} = \theta_{mic/mac,liq} + \theta_{mic/mac,ice} + a_{mic/mac} \quad \text{Eq. 3}$$

where the subscripts *mic* and *mac* denote the micropore and macropore domains, respectively, $\theta_{mic/mac,liq}$ (-) and $\theta_{mic/mac,ice}$ (-) are the volumetric liquid water and ice contents (assuming no change in density), respectively, and $a_{mic/mac}$ (-) is the volumetric air content.

2.2.1. Micropore domain approaches

For the micropore domain, we followed the physically based approach for combining Richards' equation and the heat flow equation (accounting for both heat conduction and convection) given by Hansson et al. (2004) with the exception that we did not include vapour flow. We used an analogy between freezing and drying to account for the effects of ice on water flow (Koopmans and Miller, 1966). This means that water flow is driven by gradients in pressure potentials corresponding to the liquid water content. The hydraulic conductivity of soils is drastically reduced in frozen soils (Kane, 1980; Seyfried and Murdock, 1997). This is naturally handled by the decrease in liquid water contents during freezing. However, to reduce further the hydraulic conductivity in frozen soils, $K_{mic,frozen}$ (m s^{-1}), we also included an empirical impedance factor, Ω (-), in accordance with Hansson et al. (2004):

$$K_{mic,frozen} = 10^{-\Omega Q} K_{mic,unfrozen} \quad \text{Eq. 4}$$

where $Q = \theta_{mic,ice}/\theta_{mic,tot}$ and $K_{mic,unfrozen}$ (m s^{-1}) is the hydraulic conductivity calculated from the Mualem-van Genuchten model. The impedance factor was included to limit the water flow towards the freezing front (Lundin, 1990), although the physical basis for doing so is not clear (Kuryluk and Watanabe, 2013).

Soil temperatures were modelled using the one-dimensional (vertical) heat flow equation:

$$\frac{\partial C_{mic,tot} T_{mic}}{\partial t} - L_f \rho_{liq/ice} \frac{\partial \theta_{mic,ice}}{\partial t} = \frac{\partial}{\partial z}\left[k_h \frac{\partial T_{mic}}{\partial z}\right] - C_{liq} T_{mic} \frac{\partial q_{mic}}{\partial z} - (EX_{cond} + EX_{conv}) \quad \text{Eq. 5.}$$

where $C_{mic,tot}$ (J m^{-3} K^{-1}) is the soil heat capacity of the soil micropore domain, T_{mic} (K) is temperature, k_h (W m^{-1} K^{-1}) is the thermal conductivity, C_{liq} (J m^{-3} K^{-1}) is the heat capacity of water, q_{mic} (m s^{-1}) is the water flow rate, L_f (J kg^{-1}) is the latent heat of freezing, $\rho_{liq/ice}$ (Mg m^{-3}) is the density of water (not accounting for the volume expansion during freezing), EX_{cond} and EX_{conv} (W m^{-3}) are the conductive and convective energy exchanges with the macropore domain, respectively. Finally, t (s) is time and z (m) is the vertical coordinate.

To solve Eq. 5, the apparent heat capacity, which accounts for the latent heat of freezing, was defined according to Hansson et al. (2004). We used the generalized Clapeyron equation to combine Richards' equation with the heat flow equation by introducing the hydraulic capacity, $C = \partial\theta/\partial h$ (m^{-1}) in the expression for the apparent heat capacity. The Crank-Nicholson numerical scheme used in previous versions of the MACRO-model was extended to include the apparent heat capacity term, convection of heat and conductive and convective exchanges between pore domains.

It is challenging to solve Richards' equation numerically for near-saturated and saturated conditions when accounting for freezing and thawing due to the large gradients in pressure potential that occur at the freezing/thawing front. For example, as a result, the freezing and thawing module of HYDRUS 1-D runs only for unsaturated conditions (Simunek et al., 2016). Here, to handle these difficulties we used the geometric mean of hydraulic conductivities or the minimum hydraulic conductivity instead of the arithmetic mean, which is otherwise used in the MACRO model. The use of geometric means or minimum hydraulic conductivities give more weight to layers with small conductivities and thereby reduces flow at the boundaries between frozen and unfrozen numerical layers.

Soil thermal properties are affected by the presence of ice in the pore system. The soil heat capacity of the soil micropore domain accounting for the contribution of ice, is given by the sum of the heat capacities of the mineral phase, the water phase and the ice phase according to:

$$C_{mic,tot} = C_{solids}(1 - \varepsilon_{mic,tot}) + C_{liq}\theta_{mic,liq} + C_{ice}\theta_{mic,ice} \quad \text{Eq. 6.}$$

where C_{water}=4.2 MJ m^{-3} K^{-1} and C_{ice}=1.9 MJ m^{-3} K^{-1} are the heat capacities of liquid water and ice, respectively. C_{solid} (MJ m^{-3} K^{-1}) is the heat capacity of the solid phase (except ice) given by:

$$C_{solids} = C_{om} f_{om} + C_{mineral}(1 - f_{om}) \quad \text{Eq. 7.}$$

where C_{om}=2.7 MJ m^{-3} K^{-1} and $C_{mineral}$=2.0 MJ m^{-3} K^{-1} are the heat capacities of organic matter and mineral soil, respectively and f_{om} (-) is the fraction of organic matter.

Thermal conductivity, k_h (W m^{-1} K^{-1}) was estimated using the modified form of the model proposed by Campbell (1985) given by Hansson et al. (2004):

$$k_h = C_1 + C_2(\theta + F\theta_{ice}) - (C_1 - C_4)\exp\{-[C_3(\theta + F\theta_{ice})]^{C_5}\} \quad \text{Eq. 8.}$$

where $F = 1 + F_1\theta_{ice}^{F_2}$. The constants C_1 to C_5, F_1 and F_2 can be estimated by fitting Eq. 8 to measured data.

2.2.2. Macropore domain approaches

In analogy with the assumption of gravity-driven water flow in the macropore domain, the freezing temperature is assumed to be unaffected by capillary forces (i.e. liquid water and ice can only exist simultaneously at T_{mac}=0 °C). We did not account for conductive heat transport in the macropores where water flow velocities usually are large. Temperatures in macropore water are, hence, only influenced by the convection of energy and energy exchange between the pore domains. This means that thawing of water in a completely frozen saturated macropore where all the water is immobile is governed solely by energy exchange between the pore domains.

The heat flow equation for the macropores is given by:

$$\frac{dC_{mac,tot}T_{mac}}{dt} - L_f\rho_i\left(\frac{\partial\theta_{mac,ice}}{\partial t}\right) = -C_{liq}T_{mac}\frac{\partial q_{mac}}{\partial z} + (EX_{cond} + EX_{conv}) \quad \text{Eq. 9}$$

where the terms on the left hand side represent changes in the energy content given by the temperature of macropore water and changes in the latent heat content, respectively. The terms on the right hand side represent convection of sensible heat with flowing water and heat exchange between the pore domains. $C_{mac,tot}$ (J m^{-3} °C^{-1}) is the volumetric heat capacity for the macropore domain (accounting for both liquid water and ice), q_{mac} (m s^{-1}) is the water flow in the macropores. Since liquid water and ice can only exist simultaneously at T_{mac}=0 °C it is straightforward to solve Eq. 9 from the known energy inputs to a numerical layer (see Supplemental information).

From the assumption that freezing in macropores is unaffected by capillary forces it follows that the smallest water-filled macropores will freeze first, as water flow rates are comparably small and the contact area between the micropore domain and the water in macropores is large in relation to the water volumes. This leads to a simple equation for the unsaturated hydraulic conductivity in partly frozen macropores (m s^{-1}):

$$K_{mac,frozen} = K(\theta_{mac,tot}) - K(\theta_{mac,ice}) \quad \text{Eq. 10}$$

where $\theta_{mac,tot} = \theta_{mac,liq} + \theta_{mac,ice}$ is the total water content in the macropore domain. From equation 1, $K(\theta_{mac,tot})$ is calculated as:

$$K(\theta_{mac,tot}) = K_{mac,sat}S_{mac,tot}^{n*} \quad \text{Eq. 11}$$

where $S_{mac,tot} = \theta_{mac,tot}/\varepsilon_{mac}$ (-). $K(\theta_{mac,ice})$ is calculated from Eq. 11 by replacing $\theta_{mac,tot}$ with $\theta_{mac,ice}$.

2.2.3. Exchange between pore domains

The first-order mass transfer approach has been shown to work well for the exchange of water and solutes between pore domains (Gerke and van Genuchten, 1993; 1996). Here we use a similar approach for the first-order energy transfer (FOET) between pore domains, EX_{cond} (J s^{-1} m^{-3}) with differences in temperature as the driver:

$$EX_{cond} = \frac{G_f S_{mac,tot} k_h}{d^2}(T_{mic} - T_{mac}) \quad \text{Eq. 12}$$

where G_f (-) is a geometry factor, $S_{mac,tot}$ (-) is the degree of saturation in the macropore domain, including both water and ice, which accounts for the contact surface area between the water in the macropores and the soil micropore domain and d (m) is the diffusion pathlength.

The convective exchange term, EX_{conv} (J s^{-1} m^{-3}) is given by:

$$EX_{conv} = S_w\left(T_{mic/mac} C_{liq}\right) \quad \text{Eq. 13}$$

where $T_{mic/mac}$ (°C) is the temperature in the micropore domain or macropore domain depending on the direction of S_w.

2.3. Test cases

2.3.1. Redistribution of water in the micropore domain during freezing (test case 1)

Large gradients in pressure potential may develop when water freezes. Despite the limited permeability this may lead to a significant redistribution of water from unfrozen soil towards the freezing front (e.g. Williams and Smith, 1989; Stähli et al, 1999). To evaluate the numerical implementation of the model for the micropore domain we used the data on water redistribution during freezing from Mizoguchi (1990). The data was extracted from Hansson et al. (2004) using WebPlotDigitizer version 3.12. This data set has become a standard for benchmarking physically-based models of water flow during freezing (e.g. Hansson et al., 2004; Dall'Amico et al., 2011; Kelleners, 2013).

A 20-cm high soil (Kanagawa sandy loam) column was frozen from the top using a circulating fluid with a temperature of -6 °C. Heat transport through the soil surface, q_h (W m^{-2}), was modelled using a variable heat flow boundary condition:

$$q_h = -h_c\left(T_{top} - T_{coolant}\right) \quad \text{Eq. 14}$$

where h_c (W m^{-2} K^{-1}) is a heat transfer coefficient and T_{top} (K) and $T_{coolant}$ (K) are the temperatures of the soil surface and of the cooling fluid, respectively. The initial water contents ($\theta_{initial}$=0.33 m^3 m^{-3}) and temperatures ($T_{initial}$=6.7 °C) were constant with depth.

We parameterized the model according to Hansson et al. (2004). The van Genuchten parameters were: θ_s=0.535 m^3 m^{-3}, θ_r=0.05 m^3 m^{-3}, α=0.0111 cm^{-1} and n=1.48. The saturated hydraulic conductivity of the micropore domain (K_{sm}=2.66 mm h^{-1}) was calculated from the measured total saturated hydraulic conductivity of 11.5 mm h^{-1} and a pressure potential defining the boundary between pore domains set to -10 cm. The hydraulic conductivity was adjusted using an impedance factor, Ω (-) set to 7 (Eq. 4). The parameter values of the model used to calculate thermal conductivity (Eq. 8) were: C_1=0.55 W m^{-1} K^{-1}, C_2= 0.80 W m^{-1} K^{-1}, C_3=3.07, C_4=0.13 W m^{-1} K^{-1}, C_5=4, F_1=13.05 and F_2=1.06. Finally, h_c and $T_{coolant}$ were set to 28 W m^{-2} K^{-1} and -6 °C.

None of the models that have previously been compared to the Mizoguchi data set is identical to our model. For comparison we also included modelling results from D'All Amico et al. (2011), again extracted using WebPlotDigitizer version 3.12. D'All Amico et al. (2011) used a different model for estimating the thermal conductivity and different numerical methods (including the spatial and temporal discretization).

2.3.2. Comparison between FOET and the heat flow equation (test case 2)

To illustrate the FOET approach we simulated thawing of an initially frozen soil micropore domain through lateral energy transfer from a saturated macropore domain with a constant temperature, T_{mac} (Fig. 1). We used the same thermal properties as for test case 1. Simulation results for the FOET approach were compared to results from a numerical solution of the 1D heat conduction equation (Eq. 5 assuming no convective heat transport and no exchange between the micropore and macropore domains). For the FOET approach, the temperature in the micropore domain, T_{mic}, is defined by one single value at each time step. For the heat flow equation the temperature in the micropore domain will vary with distance from the boundary. For this case $T_{mic}(\boldsymbol{x})$ is a vector, from which arithmetic mean values were calculated and used in the comparisons.

The boundary conditions for the heat conduction equation were given by:

$$T_{mic}(x = 0) = T_{mac} \quad \text{Eq. 15}$$

$$q_d(x = d) = 0 \quad \text{Eq. 16}$$

where q_d (W m^{-1} K^{-1}) is the heat transport at the centre of the simulated soil aggregate and d (m) is the diffusion pathlength which for this test case was set to 60 mm.

The initial condition was given by:

$$T_{mic}(\boldsymbol{x}) = T_{initial} \quad \text{Eq. 17}$$

where $T_{initial}$ (°C) is the initial temperature.

Simulations were run with and without the new soil freezing model with T_{mac} set to 5 °C and $T_{initial}$ set to -5 °C. The heat flow equation was solved using the Crank-Nicholson numerical scheme used to solve Eq. 5. The FOET approach was solved with an explicit Euler method in R (R core team, 2018). For the simulations without the freezing model, heat capacities and thermal conductivities are constant while they vary with ice content for the simulations with the freezing model.

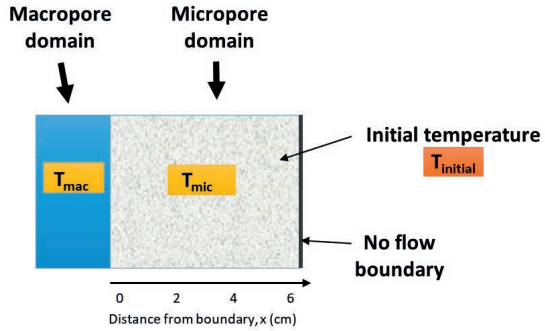

Figure 1. The simulation domain for the comparison between the FOET approach and the 1D heat conduction equation. The boundary temperature is constant at T_{mac}. For the 1D heat flow equation T_{mic} is a function of the distance from the boundary between pore domains, x (cm).

2.3.3. Infiltration into frozen soil during controlled irrigation with initially air-filled macropores (test case 3)

There are currently no suitable data available in the literature for a quantitative evaluation of the modelling approach used for the macropore domain. To illustrate the behaviour of the macropore model we simulated freezing of water infiltrating initially air-filled macropores. For these simulations, no water flow or heat transport was allowed in the micropore domain, which was saturated and kept at a constant temperature of -2 °C. The soil was irrigated for 6 minutes every 30 minutes at a rate of 1 mm h^{-1}. The irrigation water had a temperature of 1 °C. Since no water flow occurred in the micropore domain all irrigation water was directed to the macropore domain. The macroporosity was 0.015 m^3 m^{-3}, the macropore saturated hydraulic conductivity was 2 mm h^{-1} and the kinematic exponent was 2 (-). This means that at saturation the water velocity is 133 mm h^{-1}. Freezing of infiltrating water in the macropores was, for this case, governed only by the conductive energy exchange between pore domains (Eq. 9 without convective exchange). The diffusion pathlength, *d*, was set to 60 mm (Eq. 12) to represent soils with intermediate potential for non-equilibrium flow (i.e. the conductive exchange of energy between pore domains was intermediate).

2.3.4. Thawing of initially frozen soil during constant rainfall (test case 4)

To evaluate the complete model we simulated thawing from the soil surface of an initially frozen (T=-2 °C) 20-cm high soil column during constant rainfall at 1.5 mm h^{-1}. Initial total water contents (liquid water and ice) were calculated from drainage equilibrium. The conductive heat transport at the top boundary was calculated from an air temperature set to 7 °C while the conductive heat transport at the bottom boundary was set to zero. We divided the soil column into 80 equally thick numerical layers. As in test case 1, we parameterized the micropore domain according to Hansson et al. (2004). The macroporosity was set to 0.015 m^3 m^{-3}, the total saturated hydraulic conductivity was set to 20 mm h^{-1} and the kinematic exponent was set to 2. The model was run for two different values of the diffusion

pathlength to simulate intermediate (d=60 mm) and slow (d=300 mm) exchange of energy between domains (Eq. 12).

For this test case, in addition to the previously described measures taken to limit numerical artefacts (see 2.2.1), we allowed oversaturation in the micropore domain when solving Richards' equation. Any water in excess of θ_b was then redistributed to the numerical layer above and pressure potentials were updated accordingly. Finally, to smooth out the large gradients in pressure potential at the freezing front, gradients were estimated over a distance equal to three times the numerical layer thickness (i.e. the gradient between layer i and layer i+1 was estimated from the pressure potentials in layer i-1 and layer i+2). In the original MACRO-model gradients are estimated between adjacent numerical layers. We used a simulation time step of 1 s, which resulted in run times of about 3 minutes on a standard lap top computer for a 120-h simulation.

3. RESULTS AND DISCUSSION

3.1. Redistribution of water in the micropore domain during freezing (test case 1)

As soil water freezes from the soil surface the pressure potential decreases and creates a hydraulic gradient directed towards the frozen part of the soil. This gradient creates an upward flow of water, which leads to increased water content close to the surface (Figure 2). The model simulated this process well with the depth of the freezing front (i.e. where there is a large decrease in water contents with increasing depth) accurately reproduced especially at 24 and 50 h. Differences between measurements and modelling results are possibly due to uncertain estimates of the boundary heat flow and hydraulic conductivity as discussed in Hansson et al. (2004). The small differences between the simulation results for the MACRO model and the model by Dall'Amico et al. (2011) are likely due to differences in spatial and temporal discretization.

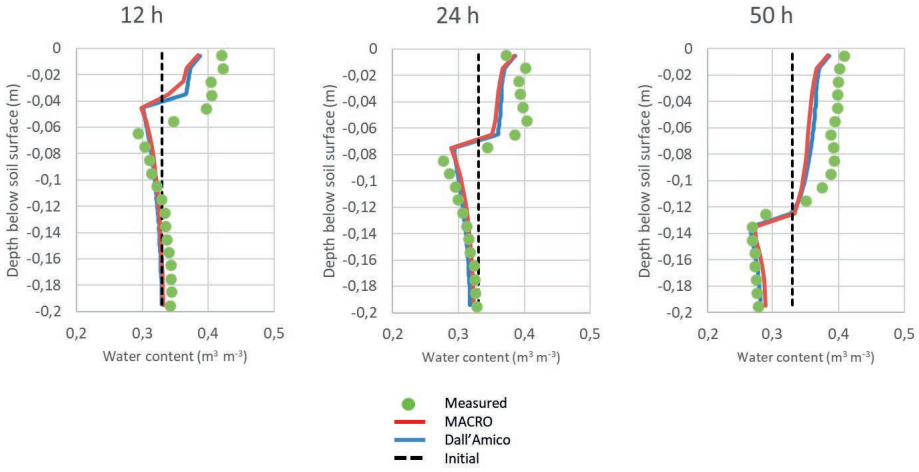

Figure 2. Measured (Mizoguchi, 1990) and modelled distribution of water (liquid and ice) in the soil micropore domain during freezing from the soil surface (test case 1) at three time points. Modelling results from Dall'Amico et al. (2011) were included for comparison.

3.2. Comparison between FOET and the heat flow equation (test case 2)

Without the freezing model, the FOET approach reproduced the energy exchange and the average temperature given by the heat conduction equation well (Fig. 3a and b). The FOET was smaller than the mean energy transfer from the heat flow equation simulations during the initial phase which resulted in an underestimation of the average temperature. Since the temperature close to the macropore wall (x=0 cm), which determines the driving force for energy transfer for the heat flow equation, increases much faster than the micropore domain temperature for the FOET approach the energy exchange also decreases faster.

For the simulations with the freezing model, both the energy exchange and the average temperature were less accurately reproduced by the FOET approach (Fig. 3c and d). The gradual increase in average temperatures during the thawing process simulated by the heat flow equation cannot be captured by the FOET approach since the temperature in the soil matrix is represented by only one value and all soil water thaws at temperatures close to 0 °C. It takes longer to completely thaw the soil for the FOET approach (about 20 h) compared to the heat flow equation (about 15 h). The much larger initial energy exchange for the simulations with the freezing model (Fig. 3a and c) is due to the larger thermal conductivity of ice (2.2 W m^{-1} $^{o}C^{-1}$) compared to liquid water (0.57 W m^{-1} $^{o}C^{-1}$).

The FOET model is an approximation to the heat flow equation and a perfect fit should, therefore, not be expected. Although it would be interesting, we did not investigate the possible consequences of the difficulties to simulate energy transfer between pore domains during thawing for different modelling scenarios.

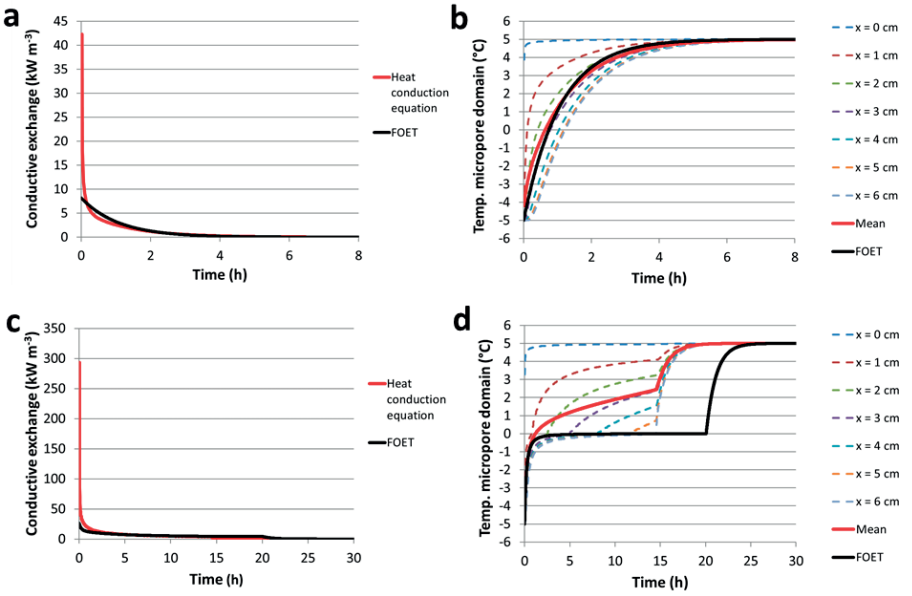

Figure 3. Comparison between first-order energy transfer (FOET) and a numerical solution to the heat conduction equation (test case 2) without the freezing model (a, b) and with the freezing model (c, d). The left column (a, c) shows the energy exchange from the macropore domain to the micropore domain while the right column (b, d) shows temperatures in the micropore domain. The solution to the heat flow equation is given for different distances (x) from the boundary and as the mean value. Note the different scales on horizontal and vertical axes.

3.3. Water flow in macropores during freezing (test case 3)

The simulation results without the freezing model show a kinematic wave moving down through the soil macropores (dotted line in fig. 5). The velocity of the wave decreases on cessation of irrigation as the degree of saturation in the wave decreases (Eq. 1). Before the start of the third irrigation the wave from the second irrigation has intercepted the first wave (Fig. 5d). At the end of the simulation the infiltrated water has reached a depth of 12 cm (Fig. 5f).

The patterns of simulated water contents are very different when the freezing model is applied, especially towards the end of the simulation. Freezing starts immediately when water infiltrates into the macropores (Fig. 5a and b). Before the onset of the second irrigation all water in the surface 1.5 cm is frozen (Fig. 5c). At this time, water exists both in liquid form and as ice below 1.5 cm depth. With consecutive irrigations a larger fraction of the macroporosity becomes blocked with ice. At the end of the simulation, the macropores are completely blocked by ice at the soil surface which prevents further infiltration (Fig. 5f).

Simulation results are in line with our perception of the processes and the limited data on water flow through macropores (Watanabe and Kugisaki, 2017). However, the model should now be evaluated and tested against measured data on the distribution of ice in macropore networks following infiltration into frozen soil for soils with contrasting macropore structure, initial conditions and

boundary conditions. Such data could be provided through X-ray imaging of frozen macroporous soils before and after infiltration events.

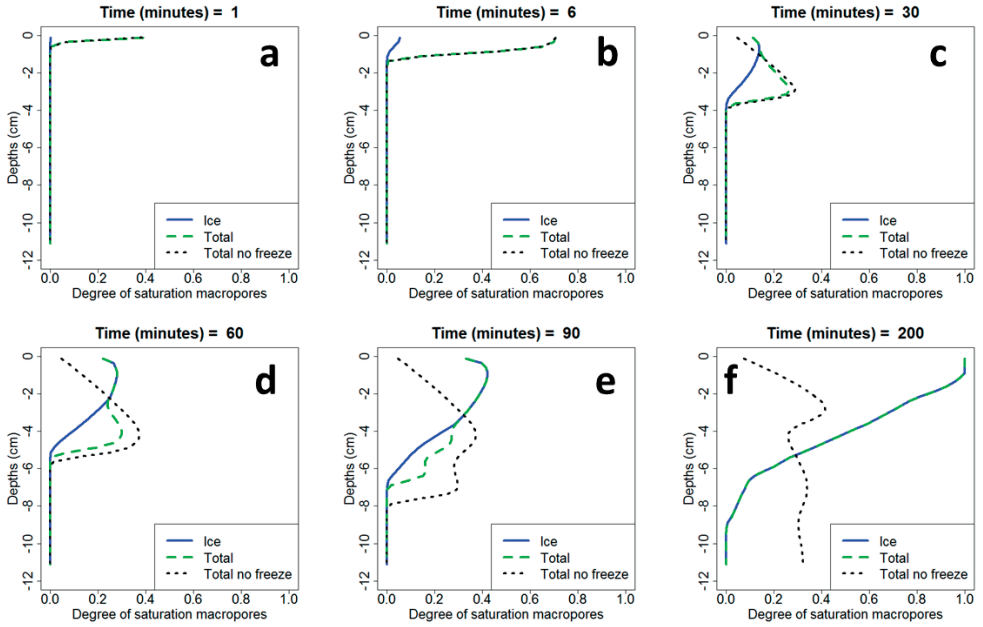

Figure 4. Simulation results for macropore infiltration (test case 3) with and without the freezing model with a) initially air-filled macropores, b) after irrigation 1, c), d) and e) before irrigation 2, 3 and 4, respectively, and f) final state.

3.4. Thawing of initially frozen soil during constant rainfall (test case 4)

The pattern of simulated soil temperatures are similar to those observed in experimental studies with similar boundary conditions (Holten et al., 2018). Soil temperatures close to the surface increase very quickly towards the air temperature (Fig. 5a, b). With increasing depth, a more pronounced plateau at temperatures just below 0 °C develops. In this temperature range, the energy supplied from the soil surface is used for the phase change from ice to liquid water rather than to increase temperatures.

The freezing and melting of water in the macropores is governed by the transfer of energy between pore domains (Eq. 12). To illustrate this process the conductive energy transfer, EX_{cond}, at 10-cm depth is shown as an example in figures 5c and 5d. During the initial phase the infiltration capacity of the frozen matrix is limited and water at an initial temperature of 7 °C enters the macropore domain. This results in an energy transfer from the macropore domain to the initially frozen micropore domain. Temperatures in the macropore domain decrease and freezing starts if temperatures reach 0 °C. Figure 5e and 5f show the degree of ice saturation in the macropores, $S_{ice} = \theta_{mac,ice}/\varepsilon_{mac,tot}$, where a value of 1 means that the macropore domain is completely blocked by ice. For the simulations with intermediate transfer the negative energy transfer stops after a few hours (Fig. 5c) when the macropore domain becomes completely blocked by ice down to a depth of 10 cm (Fig. 5e) and temperatures in

the two domains reach equilibrium. When the temperature in the micropore domain increases due to thawing from the top (Fig. 5a) energy transfer from the micropore domain to the completely frozen macropore domain starts and the ice in the macropore domain starts to melt when temperatures reach 0 °C. For the intermediate energy transfer simulations this happens at about t=27 h (Fig. 5c). When all ice in the macropore domain has melted (t=38 h) temperatures in the pore domains again reach equilibrium. For the slow energy transfer simulation the macropore domain never gets completely blocked by ice and the energy transfer from the macropore domain to the micropore domain continues until the micropore domain is completely thawed at about t=26 h (Fig. 5b, d, f). At t>26 h, energy is transferred from the micropore domain to the partly frozen macropore domain (Fig. 5d, f).

Water flow in the macropores starts as soon as there is some liquid water in the macropores (Eqs. 1, 10 and 11). As water in the macropores moves downwards it may again reach depths where the soil is frozen and the water refreezes due to energy transfer from the macropore to the micropore domain. This process can be seen in the increase in the degree of ice saturation at depth 15 cm at time=45 h and at depth 20 cm at about t=68 h (Fig. 5e).

The percolation for the simulations with intermediate energy transfer shows an initial peak where percolation equals the rain intensity of 1.5 mm h^{-1} (Fig. 5g). The rain infiltrates into the initially air-filled macropores and water continues to flow until ice completely blocks the macropore domain when percolation drops to zero. Percolation starts again when ice no longer completely blocks the macropore domain at any depth. At t=80 h the micropore domain is completely thawed (Fig. 5a) and no more refreezing of macropore water occurs. Water stored in the macropore domain above previously frozen layers can now flow unhindered and the percolation reaches a peak value of almost 5 mm h^{-1}. Finally, percolation recedes to the rainfall intensity of 1.5 mm h^{-1}.

For the slow transfer simulations, infiltration equals the rainfall intensity throughout the simulation because the macropore domain never becomes completely blocked by ice (Fig. 5d, h). Hence the infiltrating water continuously adds energy to the soil. This is not the case for the intermediate transfer simulations where infiltration is limited for a large part of the simulation due to ice blocking both pore domains. Despite an intermediate transfer of energy the total cumulative energy transfer was for this simulation smaller than for the slow transfer (not shown). These differences in total cumulative energy transfer between simulations resulted in differences in the time needed to completely thaw the 20-cm soil column (80 and 73 h for the intermediate and slow transfer, respectively).

Despite the measures taken to limit numerical artefacts (see 2.2.1 and 2.3.2) the percolation for the slow transfer simulations shows fluctuations until the micropore domain was completely thawed (Fig. 5h). These artefacts do call for further investigation. However, they did not influence the interpretation of the results and did not cause errors in the water balance (relative error less than 0.0001%).

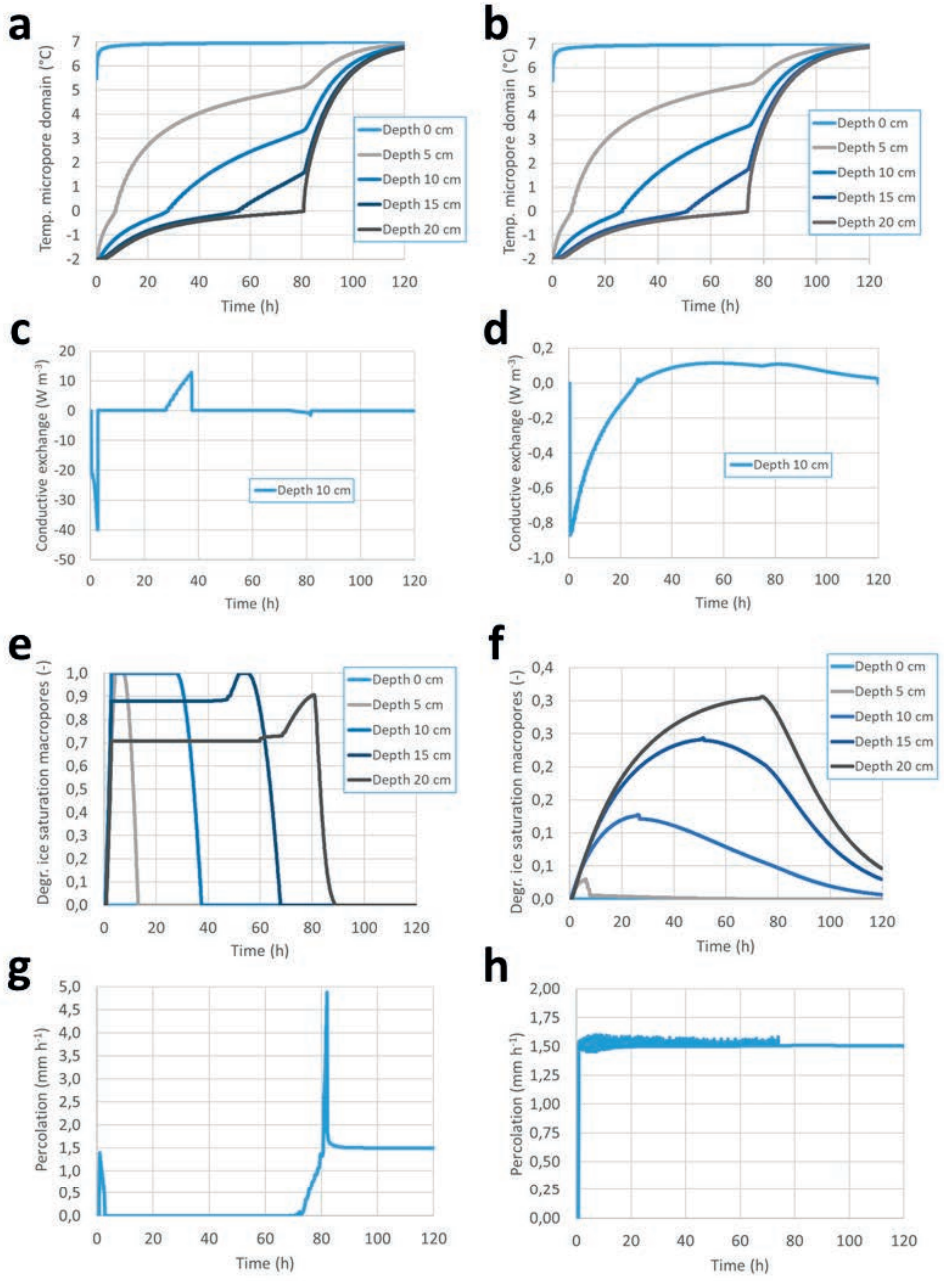

Figure 5. Simulation results for thawing during constant rainfall (test case 4). The left column (a, c, e and g) and the right column (b, d, f and h) show results from simulations with intermediate (d=60 mm) and slow (d=300 mm) energy transfer between pore domains, respectively. Panels a and b show soil temperatures at five depth below the soil surface. Panels c and d show the conductive energy transfer at 10-cm depth. Panels e and f show

the degree of ice saturation in the macropores. Panels g and h show the percolation at the bottom of the soil column. Note the different scales on the vertical axes.

4. CONCLUSIONS

We have presented a first attempt to include the effects of soil freezing in a physically based dual-permeability model for water flow and heat transport. The model enables the simulation of water infiltration into frozen soil with initially air-filled macropores, a situation which is often encountered during snowmelt. Results from the four test cases investigated here show that the model reproduces the limited available measured data well and that it behaves in accordance with the current understanding of water flow and heat transport in macroporous soil. We acknowledge that measured data for a quantitative model evaluation is largely lacking. To improve modelling of water and heat flow in frozen soils further, attention should be focused on providing experimental data suitable for evaluation of models accounting for macropore flow.

ACKNOWLEDGEMENTS

This study was funded by the Research Council of Norway (Smartcrop, project no. 244526/E50) and the Center for Chemical Pesticides at the Swedish University of Agricultural Sciences (SLU).

REFERENCES

Beven, K. and Germann, P. 1982. Macropores and water flow in soils. Water Resour. Res. 18: 1311–1325.

Campbell, G. S., Soil physics with Basic; Transport models for soil-plant systems, Elsevier, New York, 1985.

Dall'Amico, M., Endrizzi, S., Gruber S., and Rigon, R. 2011. A robust and energy-conserving model of freezing variably-saturated soil. Cryosphere 5: 469–484.

Forum for the coordination of pesticide fate models and their use. 2001. FOCUS surface water scenarios in the EU evaluation process under 91/414/EEC. Report of the FOCUS working group on surface water scenarios. EC Document Reference Sanco/4802/2001-rev.1.221. EU Commission, Brussels.

Gerke, H. H. and van Genuchten, M. T. 1993. Evaluation of a first-order water transfer term for variably saturated dual-porosity flow models. Water Resour. Res. 29: 1225–1238.

Gerke, H. H. and van Genuchten, M. T. 1996. Macroscopic representation of structural geometry for simulating water and solute movement in dual-porosity media. Adv. Water Resour. 19: 343–357.

Hansson, K., Šimůnek, J., Mizoguchi, M., Lundin, L.-C., and van Genuchten, M. T. 2004. Water flow and heat transport in frozen soil. Vadose Zone J. 3: 693–704.

Ireson, A. M., van der Kamp, G., Ferguson, G., Nachshon, U., and Wheater, H.S. 2013. Hydrogeological processes in seasonally frozen northern latitudes: understanding, gaps and challenges. Hydrogeology Journal 21: 53–66.

Jansson, P.-E. 2012. CoupModel: Model use, calibration, and validation. Trans. ASABE, 55: 1337–1346, doi:10.13031/2013.42245

Jarvis, N. J., Jansson, P-. E., Dik, P. E., and Messing, I. 1991. Modeling water and solute transport in macroporous soil. 1. Model description and sensitivity analysis. J. Soil Sci. 42: 59–70.

Jarvis, N. and Larsbo, M. 2012. MACRO (v5.2): Model use, calibration, and validation. Trans. ASABE 55: 1413–1423.

Jarvis, N., Koestel, J., and Larsbo, M. 2016. Understanding preferential flow in the vadose zone: recent advances and future prospects. Vadose Zone J. 15. doi:10.2136/vzj2016.09.0075

Jones, J. A. A. 2010. Soil piping and catchment response. Hydrol. Process. 24: 1548–1566.

Kane, D. L. 1980. Snowmelt infiltration into seasonally frozen soils. Cold Regions Sci. Technol. 3: 153–161.

Kelleners, T. J. 2013. Coupled water flow and heat transport in seasonally frozen soils with snow accumulation. Vadose Zone J. 12. doi:10.2136/vzj2012.0162.

Koopmans, R. W. R. and Miller, R. D. 1966. Soil freezing and soil water characteristic curves 1. Soil Sci. Soc. Am. J. 30: 680–685.

Kurylyk, B. L. and Watanabe, K. 2013. The mathematical representation of freezing and thawing processes in variably-saturated, non-deformable soils. Adv. Water Resour. 60: 160–177.

Larsbo, M., Roulier, S., Stenemo, F., Kasteel, R., and Jarvis, N. 2005. An improved dual-permeability model of water flow and solute transport in the vadose zone. Vadose Zone J. 4: 398–406.

Lundberg, A., Ala-Aho, P., Eklo, O. M., Klöve, B., Kværner, J., and Stumpp, C. 2016. Snow and frost: implications for spatiotemporal infiltration patterns – a review. Hydrol. Process. 30: 1230–1250.

Lundin, L.-C. 1990. Hydraulic properties in an operational model of frozen soil. J. Hydrol. 118: 289–310.

Mizoguchi, M. 1990. Water, heat and salt transport in freezing soil. PhD thesis (In Japanese), University of Tokyo.

Mohammed, A. A., Kurylyk, B. L., Cey, E. E., and Hayashi, M. 2018. Snowmelt infiltration and macropore flow in frozen soils: overview, knowledge gaps, and a conceptual framework. Vadose Zone J. 17. doi:10.2136/vzj2018.04.0084

Mualem, Y. 1976. A new model for predicting the hydraulic conductivity of unsaturated porous media. Water Resour. Res. 12: 513–522.

R Core Team, 2018. R: A language and environment for statistical computing. R Foundation for Statistical Computing, Vienna, Austria.

Seyfried, M. S. and Murdock, M. D. 1997. Use of air permeability to estimate infiltrability of frozen soil. J. Hydrol. 202: 95–107.

Simunek, J., van Genuchten, M. T., and Sejna, M. 2016. Recent developments and applications of the HYDRUS computer software packages. Vadose Zone J. 15. doi:10.2136/vzj2016.04.0033.

Stadler, D., Stähli, M., Aeby, P., and Fluhler, H. 2000. Dye tracing and image analysis for quantifying water infiltration into frozen soils. Soil Sci. Soc. Am. J. 64: 505–516.

Stähli, M., Jansson, P-. E., and Lundin, L-. C. 1996. Preferential water flow in a frozen soil - A two-domain model approach. Hydrol. Process. 10: 1305–1316.

van der Kamp, G., Hayashi, M., and Gallén, D. 2003. Comparing the hydrology of grassed and cultivated catchments in the semi-arid Canadian prairies. Hydrol. Process. 17: 559–575.

van Genuchten, M. T. 1980. A closed-form equation for predicting the hydraulic conductivity of unsaturated soils. Soil Sci. Soc. Am. J. 44: 892–898.

Watanabe, K., and Kugisaki, Y. 2017. Effect of macropores on soil freezing and thawing with infiltration. Hydrol. Process., 31, 270–278.

Williams, P. J. and Smith, M. W. 1989. The frozen earth – Fundamentals of geocryology. Cambridge University Press, Oxford.

Supporting information

A dual permeability approach for modelling soil water flow and heat transport during freezing and thawing

Mats Larsbo[a], Roger Holten[b,c], Marianne Stenrød[b], Ole Martin Eklo[b,c] and Nicholas Jarvis[a]

[a]Swedish University of Agricultural Sciences (SLU), Department of Soil and Environment, P.O. Box 7014 75007, Uppsala, Sweden

[b]Norwegian Institute of Bioeconomy Research (NIBIO), Division of Biotechnology and Plant Health, Department of Pesticides and Natural Products Chemistry, P.O. Box 115, NO-1431 Ås, Norway

[c]Norwegian University of Life Sciences, Faculty of Bio Sciences, Department of Plant Sciences, P.O. Box 5003, N-1432 Ås, Norway

Solution to the heat flow equation for the macropore domain

The heat flow equation for the macropore domain (Eq. 9 in the main article) is given by:

$$\frac{dC_{mac,tot}T_{mac}}{dt} - L_f\rho_i\left(\frac{\partial\theta_{mac,ice}}{\partial t}\right) = -C_{liq}T_{mac}\frac{\partial q_{mac}}{\partial z} + (EX_{cond} + EX_{conv}) \quad \text{[Eq. S1]}$$

The solution starts at the top numerical layer where the temperature of incoming water is known. The solution then uses temperatures at t+Δt.

The initial (i.e. at time *t*) energy (J m^{-2}) in the macropores for a numerical layer, *i*, is given by:

$$E_i^t = \Delta z\left[\left(\theta_{mac,liq,i}^t C_{liq} + \theta_{mac,ice,i}^t C_{ice}\right)T_{mac,i}^t + \rho_{liq/ice}L_f\theta_{mac,liq,i}^t\right] \quad \text{[Eq. S2]}$$

and the final energy is given by:

$$E_i^{t+\Delta t} = \Delta z\left[\left(\theta_{mac,liq,i}^{t+\Delta t} C_{liq} + \theta_{mac,ice,i}^{t+\Delta t} C_{ice}\right)T_{mac,i}^{t+\Delta t} + \rho_{liq/ice}L_f\theta_{mac,liq,i}^{t+\Delta t}\right] \quad \text{[Eq. S3]}$$

The energy added to a numerical layer (J m^{-2}) is given by:

$$E_{in} = \Delta t\left(q_{mac,in}C_{liq}T_{mac,i-1}^{t+\Delta t} + Ex_{liq,i}C_{liq}T_{mic/mac,i}^t + \left(q_{mac,in} + Ex_{liq,i}\right)\rho_{liq/ice}L_f\right) \quad \text{[Eq. S4]}$$

Where $Ex_{liq,i}$ (mm s^{-1}) is the net exchange of water between pore domains.

The energy removed from a numerical layer (J m^{-2}) is given by:

$$E_{out} = \Delta t\left(q_{mac,out}C_{liq}T_{mac,i}^{t+\Delta t} + q_{mac,out}\rho_{liq/ice}L_f\right) \quad \text{[Eq. S5]}$$

The final energy (i.e. at time t+Δt) is given by:

$$E_i^{t+\Delta t} = E_i^t + E_{in} - E_{out} \quad \text{[Eq. S6]}$$

1. Assume that $T_{mac,i}^{t+\Delta t}$= 0 °C (= -273.15 K)

Then water can exist both as ice and liquid water and $\theta_{mac,ice,i}^{t+\Delta t} = \theta_{mac,tot,i}^{t+\Delta t} - \theta_{mac,liq,i}^{t+\Delta t}$

Eq. S3 solved for $\theta_{mac,liq,i}$ gives:

$$\theta_{mac,liq,i}^{t+\Delta t} = \left(\frac{E_i^{t+\Delta t}}{\Delta z} - \theta_{mac,tot,i}^{t+\Delta t} T_{mac,i}^{t+\Delta t} C_{ice}\right) / \left(\left(C_{liq} - C_{ice}\right) T_{mac,i}^{t+\Delta t} + \rho_{liq/ice} L_f\right) \quad \text{[Eq. S7]}$$

2. If $\theta_{mac,liq,i}^{t+\Delta t} < 0$ then the macropore water is completely frozen and

$\theta_{mac,ice,i}^{t+\Delta t} = \theta_{mac,tot,i}^{t+\Delta t}$

$\theta_{mac,liq,i}^{t+\Delta t} = 0$

All energy flows except the outflow are known:

The final energy can for this case be written as:

$$E_i^{t+\Delta t} = \Delta z \left(\theta_{mac,tot,i}^{t+\Delta t} C_{ice}\right) T_{mac,i}^{t+\Delta t} \quad \text{[Eq. S8]}$$

Combining Eq. S4, S5 and S7 gives:

$$E_i^t + E_{in} - \Delta t \left(q_{mac,out} C_{liq} T_{mac,i}^{t+\Delta t} + q_{mac,out} \rho_{liq/ice} L_f\right) = \Delta z \theta_{mac,tot,i}^{t+\Delta t} C_{ice} T_{mac,i}^{t+\Delta t} \quad \text{[Eq. S9]}$$

Eq. S9 solved for $T_{mac,i}^{t+\Delta t}$ gives:

$$T_{mac,i}^{t+\Delta t} = \frac{E_i^t + E_{in} - \Delta t q_{mac,out} \rho_{liq/ice} L_f}{\Delta z \theta_{mac,tot,i}^{t+\Delta t} C_{ice} + \Delta t q_{mac,out} C_{liq}} \quad \text{[Eq. S10]}$$

3. If $\theta_{mac,liq,i}^{t+\Delta t} > \theta_{mac,tot,i}$ ***then the macropore water is completely in liquid form and***

$$\theta_{mac,ice,i}^{t+\Delta t} = 0$$

$$\theta_{mac,liq,i}^{t+\Delta t} = \theta_{mac,tot,i}^{t+\Delta t}$$

The final energy can for this case be written as:

$$E_i^{t+\Delta t} = \Delta z\left[\left(\theta_{mac,tot,i}^{t+\Delta t} C_{liq}\right) T_{mac,i}^{t+\Delta t} + \rho_{liq/ice} L_f \theta_{mac,tot,i}^{t+\Delta t}\right] \quad \text{[Eq. S11]}$$

Combining Eq. S5, S6 and S11 gives:

$$E_i^t + E_{in} - \Delta t\left(q_{mac,out} C_{liq} T_{mac,i}^{t+\Delta t} + q_{mac,out} \rho_{liq/ice} L_f\right) =$$

$$\Delta z\left[\theta_{mac,tot,i}^{t+\Delta t} C_{liq} T_{mac,i}^{t+\Delta t} + \rho_{liq/ice} L_f \theta_{mac,tot,i}^{t+\Delta t}\right] \quad \text{[Eq. S12]}$$

Eq. S12 solved for $T_{mac,i}^{t+\Delta t}$ gives:

$$T_{mac,i}^{t+\Delta t} = \frac{E_i^t + E_{in} - \rho_{liq/ice} L_f \left(\Delta t q_{mac,out} + \Delta z \theta_{mac,tot,i}^{t+\Delta t}\right)}{C_{liq}\left(\Delta z \theta_{mac,tot,i}^{t+\Delta t} + \Delta t q_{mac,out}\right)} \quad \text{[Eq. S13]}$$

Errata

Side	Line	Changed from	Changed to
Paper I	Fig. 5, caption	Bromide and MCPA (mg L^{-1}) concentrations plotted as a function of accumulated amount of percolate (mm) for a representative soil column from frozen and unfrozen topsoil and subsoil of Kroer loam and Hov silt. Dotted lines indicate the first sampling of leachate after the onset of a new irrigation.	Bromide and MCPA (mg L^{-1}) concentrations plotted as a function of accumulated amount of percolate (mm) for a representative soil column from frozen and unfrozen topsoil and subsoil of Kroer loam. Dotted lines indicate the first sampling of leachate after the onset of a new irrigation.
Paper I	Fig. 6, caption	Bromide and MCPA (mg L^{-1}) concentrations plotted as a function of accumulated amount of percolate (mm) for a representative soil column from frozen and unfrozen topsoil and subsoil of Kroer loam and Hov silt. Dotted lines indicate the first sampling of leachate after the onset of a new irrigation.	Bromide and MCPA (mg L^{-1}) concentrations plotted as a function of accumulated amount of percolate (mm) for a representative soil column from frozen and unfrozen topsoil and subsoil of Hov silt. Dotted lines indicate the first sampling of leachate after the onset of a new irrigation.
Paper I	Fig. A2, caption	MCPA (µg L^{-1}) concentrations plotted as a function of accumulated amount of percolate (mm) for all soil columns from the Kroer loam soil. Dotted lines indicate the first sampling of leachate after the start of a new irrigation. For frozen loam subsoil one of the five columns was excluded due to leakages through thermistor holes.	MCPA (mg L^{-1}) concentrations plotted as a function of accumulated amount of percolate (mm) for all soil columns from the Kroer loam soil. Dotted lines indicate the first sampling of leachate after the start of a new irrigation. For frozen loam subsoil one of the five columns was excluded due to leakages through thermistor holes.
Paper I	Fig. A4, caption	MCPA (µg L^{-1}) concentrations plotted as a function of accumulated amount of percolate (mm) for all soil columns from frozen silt soil. Dotted lines indicate the first sampling of leachate after the onset of a new irrigation.	MCPA (mg L^{-1}) concentrations plotted as a function of accumulated amount of percolate (mm) for all soil columns from frozen silt soil. Dotted lines indicate the first sampling of leachate after the onset of a new irrigation.
Paper I	Fig. A4, axis title	Two bottom plots, Axis titles are µg L^{-1}	Axis titles in all plots should be in mg L^{-1}

ISBN: 978-82-575-1584-3
ISSN: 1894-6402

NIBIO
NORWEGIAN INSTITUTE OF
BIOECONOMY RESEARCH

Norwegian University
of Life Sciences

Postboks 5003
NO-1432 Ås, Norway
+47 67 23 00 00
www.nmbu.no

102553 / ANDVORDGRAFISK.NO